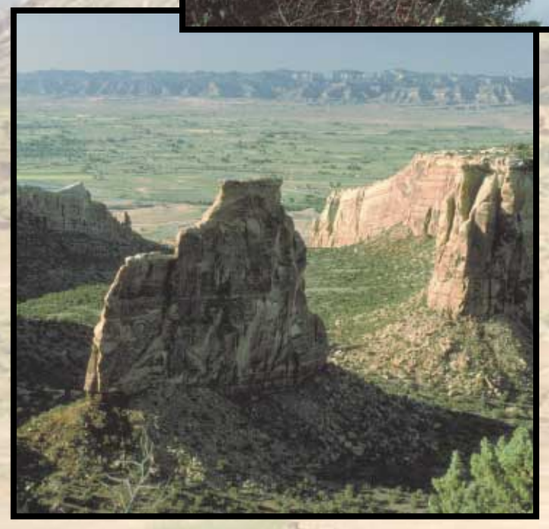

Introduction to Visibility

William C. Malm

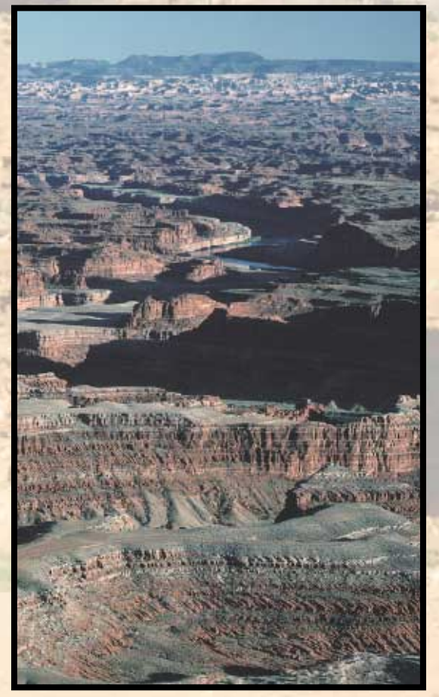

CIRA

Colorado State University

ISSN 0737-5352-40

Introduction to Visibility

William C. Malm

INTRODUCTION TO VISIBILITY

By
William C. Malm
Air Resources Division
National Park Service

Cooperative Institute for Research in the Atmosphere
(CIRA)
NPS Visibility Program
Colorado State University
Fort Collins, CO 80523

Under Cooperative Agreement
CA2350-97-001: T097-04, T098-06

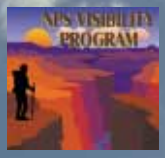

May, 1999

Table of Contents

List of Figures

Figure **Page**

Figure **Page**

Figure **Page**

List of Tables

INTRODUCTION

Visibility, as it relates to management of the many visual resources found in national parks, is a complex and difficult concept to define. Should visibility be explained in strictly technical terms that concern themselves with exact measurements of illumination, threshold contrast, and precisely measured distances? Or is visibility more closely allied with value judgments of an observer viewing a scenic vista?

Historically, "visibility" has been defined as "the greatest distance at which an observer can just see a black object viewed against the horizon sky." An object is usually referred to as at threshold contrast when the difference between the brightness of the sky and the brightness of the object is reduced to such a degree that an observer can just barely see the object. Much effort has been expended in establishing the threshold contrast for various targets under a variety of illumination and atmospheric conditions. An important result of this work is that threshold contrast for the eye, adapted to daylight, changes very little with background brightness, but it is strongly dependent upon the size of the target and the time spent looking for the target.

Nevertheless, visibility is more than being able to see a black object at a distance for which the contrast reaches a threshold value. Coming upon a mountain such as one of those shown in Figures Ia and Ib, an observer does not ask, "How far do I have to back away before the vista disappears?" Rather, the observer will comment on the color of the mountain, on whether geological features can be seen and appreciated, or on the amount of snow cover resulting from a recent storm system. Approaching landscape features such as those shown in Figures Ic and Id, the observer may comment on the contrast detail of nearby geological structures or on shadows cast by overhead clouds.

Visibility is more closely associated with conditions that allow appreciation of the inherent beauty of landscape features. It is important to recognize and appreciate the form, contrast detail, and color of near and distant features. Because visibility includes psychophysical processes and concurrent value judgments of visual impacts, as well as the physical interaction of light with particles in the atmosphere, it is of interest to understand the psychological process involved in viewing a scenic resource, the value that an observer places on visibility, and to be able to establish a link between the physical and psychological processes.

Whether we define visibility in terms of visual range or in terms of some parameter more closely related to how visitors perceive a visual resource, the preservation or improvement of visibility requires an understanding of what constituents in the atmosphere impair visibility as well as the origins of those constituents.

Scientists know that introduction of particulate matter and certain gases into the atmosphere interferes with the ability of an observer to see landscape features. Monitoring, modeling, and controlling sources of visibility-reducing particulate matter and gases depend on scientific and technical understanding of how these pollutants interact with light, transform from a gas into par-

(a) The farthest scenic feature is the 130 km distant Navajo Mountain, as seen from Bryce Canyon National Park.

(b) The La Sal Mountains, as seen from the Colorado River, are a dominant form on the distant horizon.

(c) This view in Canyonlands National Park shows the highly textured foreground canyon walls against the backdrop of the La Sal Mountains. The La Sals are 50 km away from the observation.

(d) Bryce Canyon as seen from Sunset Point. Notice the highly textured and brightly colored foreground features.

Fig. I. Photographs (a) through (d) show that, from a visual resource point of view, visibility is not how far a person can see, but rather the ability of an observer to clearly see and appreciate the many and varied scenic elements in each vista.

ticles that impair visibility, and are dispersed across land masses and into local canyons and valleys.

Scientific understanding of some of these issues is more complete than of others. The goal of this publication is to assist the reader in developing basic knowledge of those concepts for which there is an understanding and to indicate the areas that need further research.

SECTION 1

ON THE NATURE OF LIGHT

One of our principal contacts with the world around us is through light. Not only are we personally dependent on light to carry visual information, but also much of what we know about the stars and the solar system is derived from light waves registering on our eyes and on optical instruments.

Light can be thought of as waves, and to a certain extent they are analogous to water and sound waves. Figure 1.1 is a schematic representation of water waves with the distance from crest to crest denoted as one wavelength.

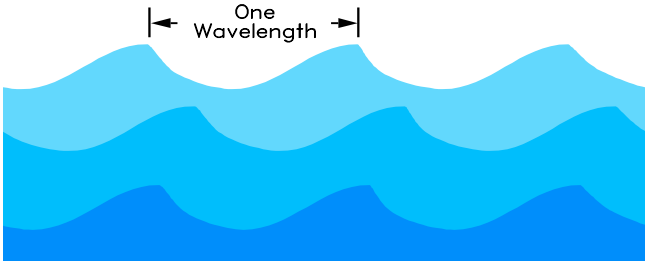

Fig. 1.1 Water waves illustrate the concept of wavelengths. A wavelength is defined as the distance from one crest to the next.

Similar oscillations of electric and magnetic fields are called electromagnetic radiation. Ordinary light is a form of electromagnetic radiation, as are x-rays, ultraviolet, infrared, radar, and radio waves. All of these travel at approximately 300,000 km/sec (186,000 mi/sec) and only differ from one another in wavelength.

Figure 1.2 is a schematic representation of the electromagnetic spectrum with the visible portion shown in color to emphasize the portion of the spectrum to which the human eye is sensitive. The visible spectrum is white light separated into its component wavelengths or colors. The wavelength of light, typically measured in terms of millionths of a meter (microns, or μm), extends from about 0.4 to 0.7 microns.

Waves of all kinds, including light waves, carry energy. Electromagnetic energy is unique in that energy is carried in small, discrete parcels called photons. Schematic representations of a blue, green, and red photon are shown in Figure 1.3. Blue, green, and red photons have wavelengths of around 0.45, 0.55, and 0.65 microns, respectively. The color properties of light depend on its behavior both as waves and as particles.

Colors, created from white light by passing it through a prism, are a result of the wave-like

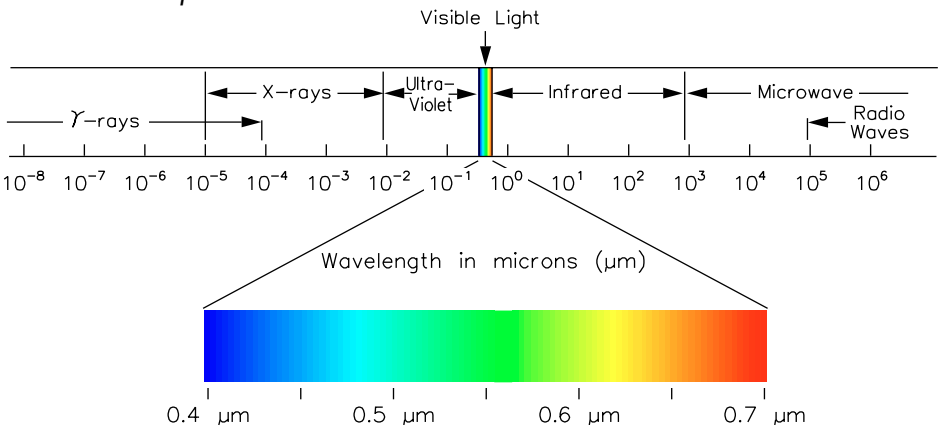

Fig. 1.2 Vibrations of electric and magnetic fields are referred to as electromagnetic radiation. This diagram shows the wavelengths of various types of electromagnetic radiation including visible light. The wavelength of the visible spectrum varies from 0.4 microns (blue) to 0.7 microns (red). One micron equals one millionth of a meter.

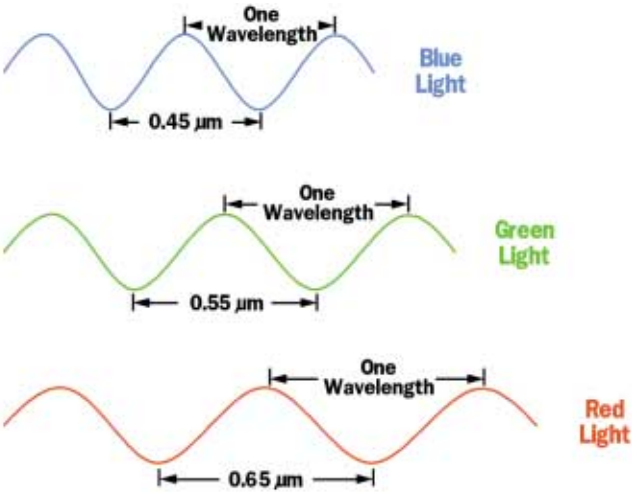

Fig. 1.3 At times light can exhibit either wave-like or particle-like characteristics. Light can be thought of as consisting of bundles of vibrating electric and magnetic waves. These bundles of energy are called photons, and the wavelengths of radiant energy making up the photon determine its "color." (a), (b), and (c) schematically show a blue, green and red photon, respectively.

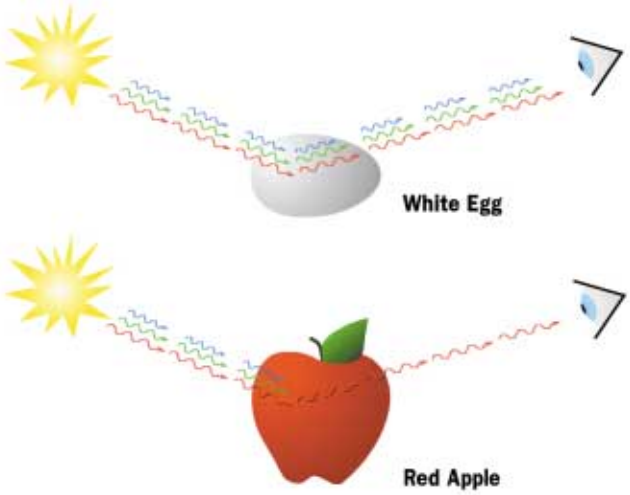

Fig. 1.4 Why some objects appear white while others appear colored. White light, which is composed of all "colors" of photons, strikes an object. If the object is white, photons of every color are reflected. However, if some photons are absorbed while others are reflected, the object will appear to be colored; a red apple, for instance, reflects red photons and absorbs all others.

nature of light. A prism separates the colors of light by bending (refracting) each color to a different degree. Colors in a rainbow are the result of water droplets, acting like small prisms, dispersed through the atmosphere. Each water droplet refracts light into the component colors of the visible spectrum.

More commonly, the colors of light are separated in other ways. When light strikes an object, certain color photons are captured by molecules in that object. Different types of molecules capture photons of different colors. The only colors we see are those photons that the surface reflects. For instance, chlorophyll in leaves captures photons of red and blue light and allows green photons to bounce back, thus providing the green appearance of leaves. Nitrogen dioxide, a gas emitted into the atmosphere by combustion sources, captures blue photons. Consequently, nitrogen dioxide gas tends to look reddish brown. Figure 1.4 is an example of an eggshell reflecting all wavelengths of light. The eye perceives the eggshell to be white. An apple, on the other hand, reflects mostly red light while absorbing all others, so the apple, to an eye-brain system, appears to be red.

For all practical purposes, in visibility, it is most convenient to think of light as being made of small colored particles. The following sections of this document will discuss more specifically how these "light" particles interact with atmospheric particulate matter and gases.

Visibility involves more than specifying how light is absorbed and scattered by the atmosphere. Visibility is a psychophysical process of perceiving the environment through the use of the eye-brain system.

Important factors involved in seeing an object are outlined in Figure 1.5 and summarized here.

- Illumination of the overall scene by the sun, including illumination resulting from sunlight scattered by clouds and atmosphere as well as reflections by ground and vegetation.

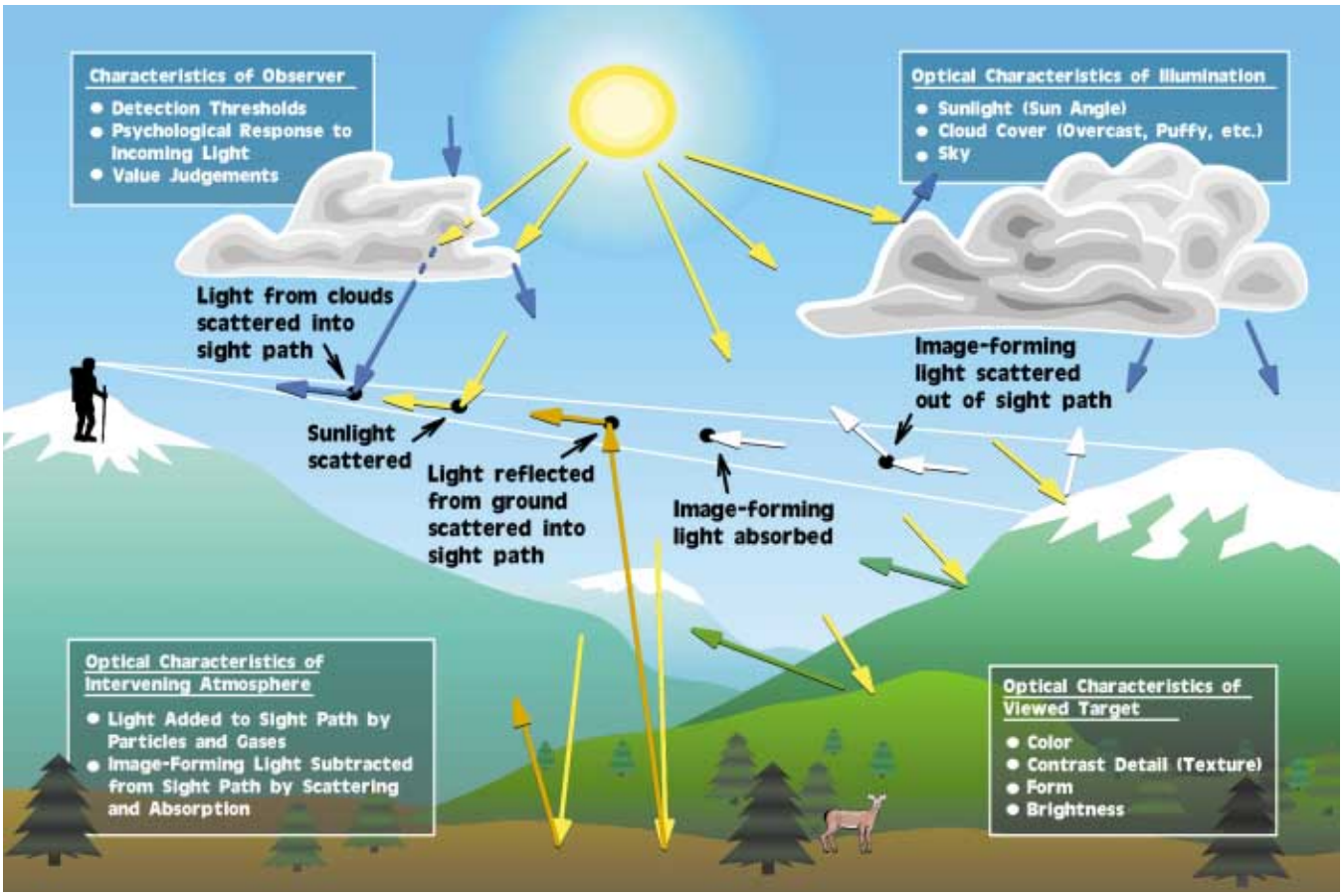

Fig. 1.5 Important factors involved in seeing a scenic vista are outlined. Image-forming information from an object is reduced (scattered and absorbed) as it passes through the atmosphere to the human observer. Air light is also added to the sight path by scattering processes. Sunlight, light from clouds, and ground-reflected light all impinge on and scatter from particulates located in the sight path. Some of this scattered light remains in the sight path, and at times it can become so bright that the image essentially disappears. A final important factor in seeing and appreciating a scenic vista are the characteristics of the human observer.

- Target characteristics that include color, texture, form, and brightness.
- Optical characteristics of intervening atmosphere:
  i. image-forming information (radiation) originating from landscape features is scattered and absorbed (attenuated) as it passes through the atmosphere toward the observer, and
  ii. sunlight, ground reflected light, and light reflected by other objects are scattered by the intervening atmosphere into the sight path.
- Psychophysical response of the eye-brain system to incoming radiation.

It is important to understand the significance of the light that is scattered in the sight path toward the observer. The amount of light scattered by the atmosphere and particles between the object and observer can be so bright and dominant that the light reflected by the landscape features becomes insignificant. This is somewhat analogous to viewing a candle in a brightly lit room and in a room that would otherwise be in total darkness. In the first case, the candle can hardly be seen, while in the other it becomes the dominant feature in the room.

SECTION 2

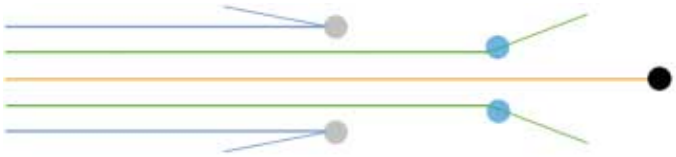

INTERACTION OF LIGHT AND PARTICLES

A photon (light "particle") is said to be scattered when it is received by a particle and re-radiated at the same wavelength in any direction. Visibility degradation results from light scattering and absorption by atmospheric particles and gases that are nearly the same size as the wavelength of the light. Particles somewhat larger than the wavelength of light can scatter light as a result of a combination of the first three phenomena shown schematically in Figures 2.1a, 2.1b, and 2.1c. Figure 2.1a shows diffraction, a phenomenon whereby radiation is bent to "fill in the shadow" behind the particle. Figure 2.1b depicts light being bent (refracted) as it passes through the particle. A third effect resulting from slowing a photon is a little difficult to understand. Consider two photons approaching a particle, each vibrating "in phase" with one another. One passes by the particle, retaining its original speed, while the other, passing through the particle, has its speed altered. When this photon emerges from the particle, it will be vibrating "out of phase" with its neighbor photon; when it vibrates up, its neighbor will vibrate down. As a consequence, they interfere with each other's ability to propagate in certain directions (Figure 2.1c).

Figure 2.1d indicates how a photon can be absorbed by the particle. The radiant energy of the photon is transferred to internal molecular energy or heat energy. In the absorption process, the photon is not redistributed into space; the photon ceases to exist.

The efficiency with which a particle can scatter light and the direction in which the incident light is redistributed are dependent on all four of these effects. Photons can be scattered equally in all directions (isotropic scattering), but in most instances photons are scattered in a forward direction.

Figures 2.2 and 2.3 show the distribution of scattered light for particles that are respectively much smaller and much larger than the wavelength of light. If the particles are small (such as the air molecules themselves) the amount of light

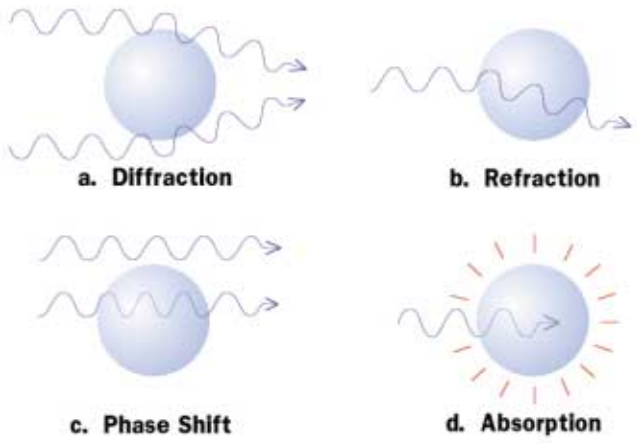

Fig. 2.1 Large particle light scattering and absorption. Diffraction (a) and refraction (b) combine to "bend" light to "fill in the shadow" behind the particle. Diffraction, an edge effect, causes photons passing very close to a particle to bend into the shadow area; refraction is a result of the light wavefront slowing down as it enters the particle. While the photon is within the particle, its wavelength is also shortened. Thus, when it emerges from the particle, it may vibrate out of phase with adjacent photons and interfere with their ability to propagate in a pre-prescribed direction. This effect (phase shift) is shown in (c). As a fourth possibility, the photon may be absorbed by the particle (d). In this case, the internal energy of the particle is increased. The particle may rotate faster or its molecules may vibrate with greater amplitude.

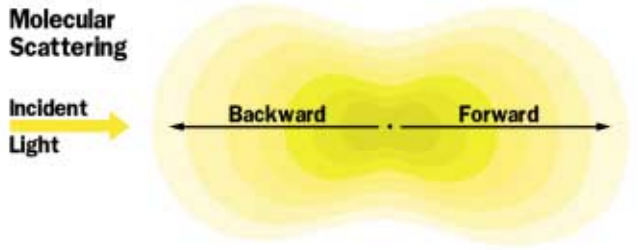

Fig. 2.2 Light interacts with a particle through the processes shown in Fig. 2.1. If the particle is very small (the size of a molecule) the net result of the interaction process is to redistribute incident light in a way shown in the above diagram. Equal numbers of photons are scattered in the forward and backward directions and about one-half of the number of forward scattered photons are directed to the sides (90 degree scattering).

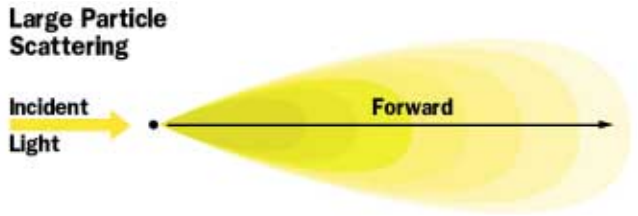

Fig. 2.3 If the particle is large (greater than 10 microns), most of the incident light is scattered in the forward direction.

scattered in the forward and backward directions are nearly the same. This type of scattering is referred to as Rayleigh scattering. As the particle increases in size, more light tends to scatter in the forward direction until for large particles nearly 100% of the incident photons end up being scattered in the forward direction.

The fact that light scatters preferentially in different directions as a function of particle size is extremely important in determining the effects that atmospheric particulates have on a visual resource. The angular relationship between the sun and observer in conjunction with the size of particulates determines how much of the sunlight is redistributed into the observer's eye.

The effect of particulates on visibility is further complicated by the fact that particulates of different sizes are able to scatter light with varying degrees of efficiency. It is of interest to investigate the efficiency with which an individual particle can scatter light. The efficiency factor is expressed as a ratio of a particle's effective cross section to its actual cross section. Figure 2.4 shows how this efficiency varies as a function of particle size. Very small particles and molecules are very inefficient at scattering light. As a particle increases in size, it becomes a more efficient light scatterer until, at a size that is close to the wavelength of the incident light, it can scatter more light than a particle five times its size. Even particles that are very large scatter light as if they were twice as big as they actually measure. These particles remove twice the amount of light intercepted by its geometric cross-sectional area.

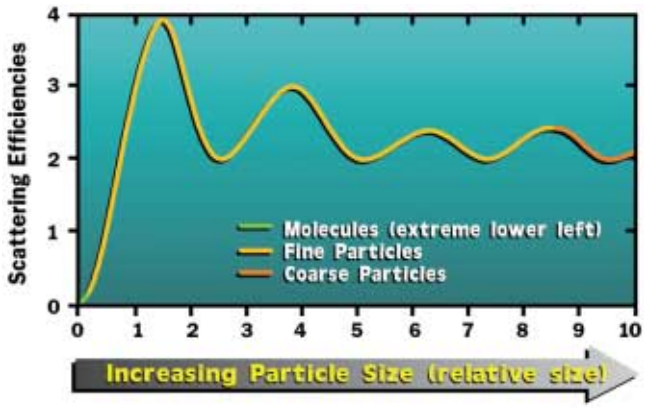

Fig. 2.4 The relative efficiency with which particles of various sizes scatter light. The green line corresponds to the scattering efficiency of molecules. The orange and red lines show the efficiency with which fine and coarse particles scatter light. Note that fine particles (0.1 microns to 1.0 microns) can be more efficient at scattering light than are either molecules or coarse particles.

Figure 2.5 shows the relative amounts of small and large particles found in the atmosphere. The blue line is a typical mass size distribution of particles. The y-axis is the amount of mass in a given

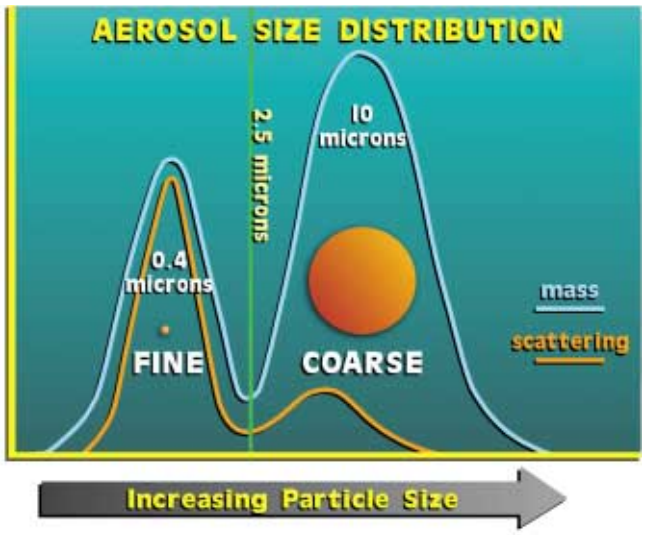

Fig. 2.5 The blue line shows the relative amount of mass typically found in a given particle size range. The orange line shows the relative amount of particle scattering associated with that mass. Note that even though mass is associated with coarse particles, it is the fine particles that are primarily responsible for scattering light.

size range; the x-axis is particle size measured in microns. Notice the two-humped, or bi-modal curve. Those particles less than about 2.5 microns are referred to as fine particles and particles larger than 2.5 microns are called coarse particles.

The orange curve is the corresponding amount of light scattering that can be associated with each size range. Even though there is less mass concentrated in the fine mode, it is the fine particulates that are the most responsible for scattering light. This is because fine particles are more efficient light scatterers than large particles, and because there are more of them, even though their total mass is less than the coarse mode. Consequently, it is the origin and transport of fine particles that is of greatest concern when assessing visibility impacts.

It is this scattering phenomenon that is responsible for the colors of haze in the sky. The sky is blue because blue photons, with their shorter wavelengths, are nearer the size of the molecules that make up the atmosphere than are their green and red counterparts. Thus blue photons are scattered more efficiently by air molecules than red photons, and as a consequence, the sky looks blue.

Figure 2.6 schematically shows what happens when the red, blue, and green photons of white light strike small particles. Only the blue photons are scattered because scattering efficiency is greatest when the size relationship of photon wavelength to particle is close to 1:1. The red and green photons pass on through the particles. To an observer standing to the side of the particle concentration, the haze would appear to be blue. Figure 2.7 shows what happens when the particles are about the same size as the incoming radiation. All photons are scattered equally, and the haze appears to be white or gray.

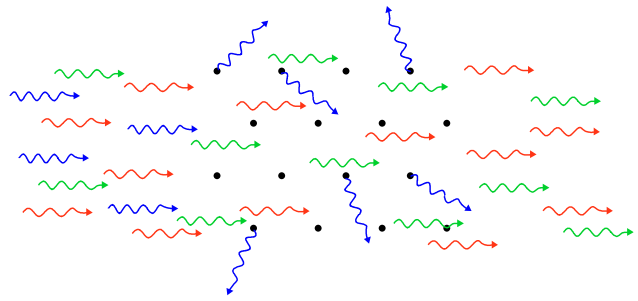

Fig. 2.6 As a beam of white light (consisting of all "colored" photons) passes through a haze made up of small particles, it is predominantly the blue photons, which are scattered in various directions.

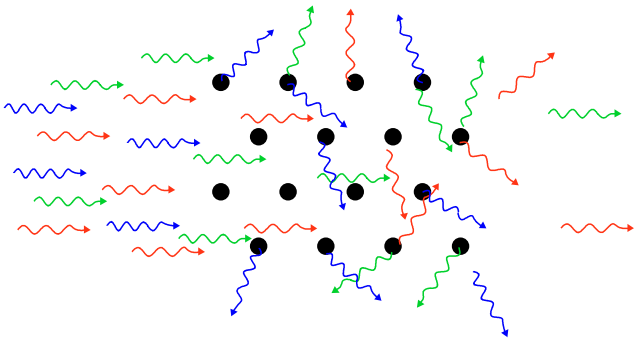

Fig. 2.7 When particles are near or larger than the wavelength of the incident light, photons of all colors are scattered out of the beam path.

Figure 2.8 is a similar diagram of white light passing through a concentration of nitrogen dioxide (NO_2) molecules. Blue photons are absorbed, so a person viewing a NO_2 haze would see it as being reddish brown (i.e. without blue) rather than white.

Figures 2.9a and 2.9b further exemplify the relationship of particle size and the color of scattered light. Figure 2.9a shows a lighted cigarette held in a strong beam of white light. Notice that the smoke appears to have a bluish tinge to it. One can conclude that these particles must be quite small because they are scattering more blue than green or red photons. Figure 2.9b is smoke from the same cigarette. However, the smoke in Figure 2.9b has been held in the mouth for a few seconds. The inside of a person's mouth is humid, and smoke particles have a high affinity for water vapor. These hygroscopic particles tend to grow to sizes that are near the wavelengths of light and thus scatter all wavelengths of light equally. Scattered photons having wavelengths that extend over the whole visible spectrum are, of course, perceived to be white or gray.

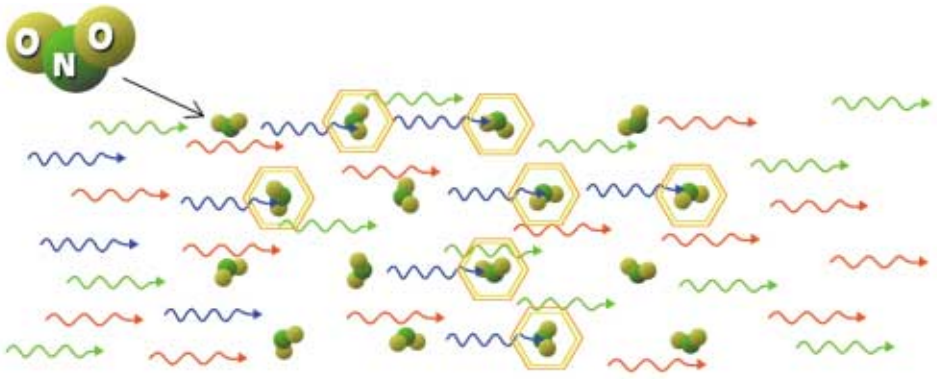

Fig. 2.8 An atmosphere containing nitrogen dioxide (NO_2) will tend to deplete the number of blue photons through the absorption process. As a result, white light will tend to look reddish or brownish in color after passing through a nitrogen dioxide haze.

(a)

(b)

Fig. 2.9 (a) This photograph shows the color of small particles that have been illuminated by white light. Because the smoke appears blue it can be concluded that the scattering particles must be quite small, less than the wavelength of visible light. (b) A photograph of similar particles after they have been allowed to grow in a humid environment. Note that as a result of equal scattering of all photon colors, these larger particles appear white instead of blue.

SECTION 3

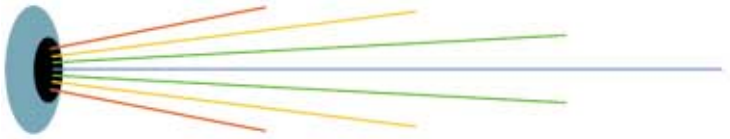

VISION THROUGH THE ATMOSPHERE

The eye, shown in Figure 3.1, is much like a camera in that it has a lens, an aperture to control the amount of light entering the eye (iris), and a detector, called the retina. The eye, whether it is looking at a vista or a candle in the room, detects relative differences in brightness rather than the overall brightness level. That is to say, the eye measures contrast between adjacent objects or between an object and its background. Contrast of an object is simply the percent difference between object luminance and its background luminance.

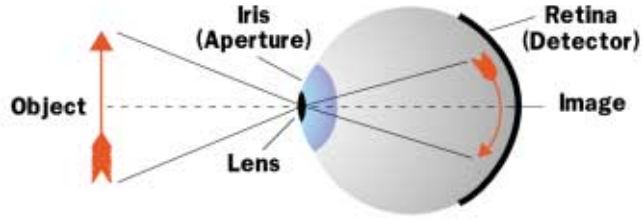

Fig. 3.1 The human eye operates much like a photographic camera. It has a lens to focus an image on a very sensitive detector called the retina. Also, the amount of light entering the eye is controlled by an aperture called the iris. The iris is the colored portion of the eye.

(a)

(b)

(c)

(d)

Fig. 3.2 The effect of regional or uniform haze on a Glacier National Park vista. The view is of the Garden Wall from across Lake McDonald. Atmospheric particulate concentrations associated with photographs (a), (b), (c), and (d) correspond to 7.6, 12.0, 21.7, and 65.3 μg/m^3.

Fig. 3.3 Effects of uniform haze on the Chuska Mountains as seen from Mesa Verde National Park. The atmospheric particulate concentration on the day this photograph was taken corresponded to 1 μg/m³.

The camera can be an effective tool in capturing the visual impact that pollutants have on a visual resource. In the following paragraphs, pictures are presented that show the visual impact that haze has on scenic vistas under different lighting and air quality conditions.

Figure 3.2a,b,c, and d show the effect that different levels of uniform haze have on Glacier National Park in Montana. These photographs were taken near Apgar on the southwestern end of Lake McDonald. Sky-mountain contrasts are -0.18, -0.14, -0.04, and greater than -0.02, while the associated atmospheric fine particulate concentrations in each case are 7.6, 12.0, 21.7, and 65.3 μg/m^3, respectively. Figures 3.3 and 3.4 show similar hazes of vistas at Mesa Verde and Bryce Canyon National Parks. The Chuska Mountains in Figure 3.3 are 95 km away, with the contrast at -0.26. Navajo Mountain is 130 km distant (Figure 3.4) and in this photograph the sky-mountain contrast is -0.08. This photograph should be compared with Figure Ia, a photograph of Navajo Mountain taken on a day in which the particulate concentration in the atmosphere was near zero.

Under stagnant air mass conditions, aerosols can be "trapped" and produce a visibility condition usually referred to as layered haze. Figure 3.5 shows Navajo Mountain viewed from Bryce Canyon National Park with a bright layer of haze that extends from the ground to about halfway up the mountain. Figure 3.6 is a similar example of layered haze but with the top portion of the mountain obscured. Figure 3.7 is a classic example of plume blight. In plume blight instances, specific sources such as those shown in Figure 3.8 emit pollutants into a stable atmosphere. The pollutants are then transported in some direction with little or no vertical mixing.

Fig. 3.4 Uniform haze degrades visual air quality at Bryce Canyon National Park. The 130 km distant landscape feature is Navajo Mountain. Atmospheric particulate concentration on the day this photograph was taken is 3 μg/m³.

Fig. 3.5 Navajo Mountain as seen from Bryce Canyon National Park, showing the appearance of layered haze. The pollutants are trapped in a stable air mass that extends from the ground to about halfway up the mountain side.

Fig. 3.6 Photograph of Navajo Mountain similar to Figure 3.5 but with a suspended haze layer that obscures the top portion of the mountain.

Fig. 3.7 Classic example of "plume blight." The thin, dark plume on Navajo Mountain results from a point source emitting particulate matter into a stable atmosphere.

Fig. 3.8 An example of one kind of point source that emits pollutants into the atmosphere.

Figures 3.9, 3.10, 3.11, and 3.12 show other layered haze conditions that frequently occur at Grand Canyon and Mesa Verde National Parks. At the Grand Canyon layered hazes are usually associated with smoke and nearby coal-fired power plants, while at Mesa Verde, much of the pollution comes from urban areas and the Four Corners and San Juan Power Plants.

Figures 3.13 and 3.14 show the appearance of plumes containing carbon. In both of these cases the pollutants are being emitted from forest fires. However, Figure 3.13 shows the appearance of a specific forest fire plume, while Figure 3.14 shows the effect of viewing a vista through a concentration of particles containing carbon. In this instance, the vista is the north wall of the Grand Canyon as seen from the top of San Francisco Peaks in northern Arizona. Notice the overall "graying" and reduction of contrast of the distant

Fig. 3.9 Smoke trapped by an inversion layer in the Grand Canyon. During the winter months inversions are quite common in almost all parts of the United States.

scenic features. Remember that carbon absorbs all wavelengths of light and scatters very little. Thus the scene will always tend to be darkened.

Figure 3.15 shows the effects of illumination on the appearance of power plant plumes. The two plumes on the left are particulate plumes, while the two plumes on the right consist of water droplets. The plume on the far right, which is illuminated by direct sunlight, appears to be white. The second identical water droplet plume, which is shaded, appears dark. The amount of illumination can have a significant effect on how particulate concentrations appear.

Figure 3.16 demonstrates how the effect of nitrogen dioxide gas (NO_2), in combination with varied background illumination, can combine to yield a very brown atmospheric discoloration. If a volume of atmosphere containing NO_2 is shaded and if light passes through this shaded portion of the atmosphere, the light reaching the eye will be deficient in photons

Fig. 3.10 An example of power plant emissions trapped in an air inversion layer in the Grand Canyon.

Fig. 3.11 Effects of an inversion layer in the Grand Canyon. In this case, a cloud has formed within the canyon walls.

Fig. 3.12 Effects of layered haze trapped in front of the Chuska Mountains as viewed from Mesa Verde National Park. This condition occurs 30 to 40% of the time during winter months.

Fig. 3.13 Forest fire plume exemplifying the appearance of carbon particles and demonstrating the effect of lighting. Where the plume is illuminated it appears gray, but identical particles in the shadow of the plume appear dark or almost black.

Fig. 3.14 Example of how light-absorbing particles (in this case carbon) affect the ability to see a vista. Carbon absorbs all wavelengths of light and generally causes a "graying" of the overall scene. Shown here is the north wall of the Grand Canyon as seen from the top of the San Francisco Peaks in northern Arizona.

Fig. 3.15 The effect of illumination on the appearance of plumes. The two plumes on the right are identical in terms of their chemical make-up, in that they are primarily water droplets. However, the far right plume is directly illuminated by the sun and the plume second from the right is shaded. The first plume appears white and the second appears almost black. The two plumes on the left are fly-ash plumes.

in the blue part of the spectrum. As a consequence, the light will appear brown or reddish in color. However, if light is allowed to shine on, but not through, that same portion of the atmosphere, scattered light reaches the observer's eye and the light can appear to be gray in nature. Both of these conditions are shown in Figure 3.16. On the right side of the photo the mixture of NO_2 and particulates is shaded by clouds. The same atmosphere, illuminated because the cloud cover has disappeared, appears almost gray in the middle portion of the photograph.

Figure 3.17 is an easterly view of the La Sal Mountains in southeastern Utah as seen from an elevated point that is some 100 kilometers distant. The photograph shown in Figure 3.17a was taken at 9:00 a.m., while the photograph shown in 3.17b was taken later in the

Fig. 3.16 The brown discoloration resulting from an atmosphere containing nitrogen dioxide (NO_2) being shaded by clouds but viewed against a clear blue sky. Light scattered by particulate matter in that atmosphere can dominate light absorbed by NO_2, causing a gray or blue appearing haze (left side of photograph).

(a)

(b)

Fig. 3.17 Photographs showing how the vistas appeared on a day when pollutants were trapped under an inversion layer. In (a) the haze appears white; in (b) the identical haze is dark or gray. Because most of the light energy is scattered in the forward direction (white haze), it can be concluded that the particles must be quite large in comparison to the wavelength of light.

day. These photographs show how these views, or vistas, appear when obscured by a layer of haze. In the first view the haze layer appears white, but the same air mass viewed later in the day has a dark gray appearance. This effect is entirely due to the geometry involved with the observer and the sun. In the first view the sun is low in the eastern sky. Consequently, the photons reaching the observer have been scattered in the forward direction. Because the haze appears white, we can conclude that the particles must be quite large in comparison to the wavelength of light. The assumption that particles are large is further reinforced by their appearance when the sun is behind the observer as shown in 3.17b. In order for scattered photons to reach the observer, they would have to be back scattered from the particles. Because the haze appears dark, we can conclude that there is very little back scattering, which is consistent with the large particle hypothesis.

The angle at which the sun illuminates a vista or landscape feature (sun angle) plays another important role. Figures 3.18a-d exemplify this effect. The view is from Island in the Sky, Canyonlands National Park, looking out over Canyonlands with its many colorful features toward the 50 km distant La Sal Mountains. Figure 3.18a shows how the canyon appears when it is in total shadow (6:00 a.m.). Figures 3.18a, b, and c show a progressively higher sun angle until in Figure 3.18d the scene is entirely illuminated. In each case, the air quality is the same. The only change is in the angle at which the sun illuminated the vista. There are primarily two reasons for the apparent change in visual air quality. First, at higher sun angles, there is less scattering of light by the intervening atmosphere

(a)

(b)

(c)

(d)

Fig. 3.18 Four photographs showing the effect of a progressively shifting sun angle on the appearance of a vista as seen from Island in the Sky, Canyonlands National Park. In each photograph, the air quality is the same. In (a) (6:00 a.m.) the sun angle-observer-vista geometry results in a large amount of scattered air light (forward scattering) added to the sight path, but minimal amount of imaging light reflected from the vista. (d) (12 noon) shows just the opposite case. Scattered light is minimized and reflected imaging light is at a maximum.

in the direction of the observer. Second, the vista reflects more light; consequently, more image-forming information (reflected photons from the vista) reaches the eye. The contrast detail and scene are enhanced.

SECTION 4

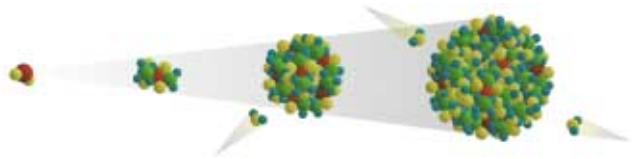

TRANSPORT AND TRANSFORMATION OF ATMOSPHERIC PARTICULATES AND GASES AFFECTING VISIBILITY

Understanding how air moves across the oceans and land masses is key to understanding how pollutants are transported and transformed as they move from their source to locations where they impair visibility.

4.1 Meteorology

Meteorological factors, such as wind, cloud cover, rain, and temperature are interesting in that they are affected by pollution, and they in turn affect pollution. The rate at which pollutants are converted to other pollutants—sulfur dioxide gas to sulfate particles or nitrogen oxides and hydrocarbons to ozone—is determined by the availability of sunlight and the presence or absence of clouds. The vertical temperature profile of the atmosphere determines whether the pollutants are mixed and diluted throughout the atmosphere or whether they are "clamped" under a lid (inversion) and become trapped and thus accumulate in the communities that produce the pollution.

Figure 4.1 schematically illustrates the temperature change above the earth's surface. The red depicts warm air, while the shading to blue is meant to show the decrease in temperature as the distance above ground increases. The sun heats the earth's surface, and the surface in turn heats the air that comes in contact with it. The warm air rises, while at the same time cooler air sinks and the cycle goes on. When these processes are in equilibrium, there is about a 5.5°F change per 1000 feet change in elevation. For instance, at Grand Canyon National Park, where the rim is 5000 feet higher than the Colorado River, one would expect about a 25-30°F difference between the top and bottom of the canyon. A temperature of 80°F at the top translates into 105-110°F on the river.

The rate at which temperature changes above the earth's surface determines the stability of the atmosphere. Consider air masses labeled A and B in Figure 4.1. Air mass A is warmer (redder) than its surrounding air and will therefore rise through the atmosphere, while air mass B, which is cooler than its surroundings, will sink. As air mass A rises, it will expand and therefore cool. Even though air mass A cools, as long as it stays warmer than its surroundings, it will continue to rise. If this happens, the atmosphere is said to be unstable.

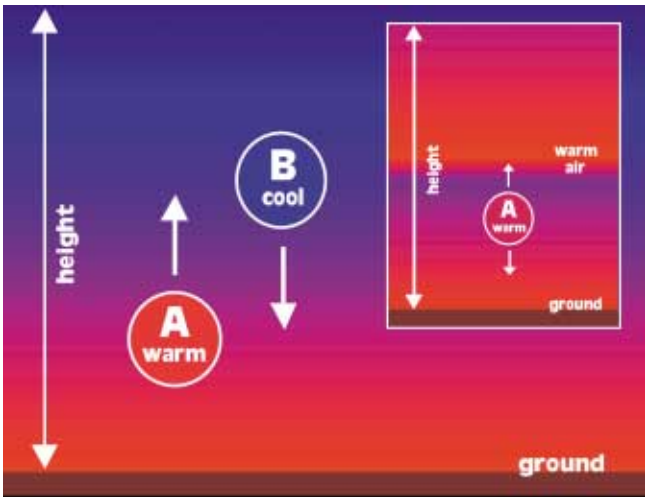

Fig. 4.1 Warm air rises through the earth's atmosphere, while cool air sinks. Atmospheric resistance to these vertical disturbances (stability) depends on the temperature distribution of the atmosphere.

Conversely, if its cooling process causes air mass A to become cooler than its surroundings, then it will stop rising and either sink or stay at some height above the earth's surface. When this happens, the atmosphere is said to be stable.

The inset in Figure 4.1 shows an example of where a layer of warmer air has developed at some height above the surface. This layer is schematically depicted by the red ridge line labeled warm air on the inset. Air mass A on the inset is just below the warm layer. It is depicted to be warmer (redder) than its immediate surroundings but cooler (bluer) than the layer. Thus, the air mass will rise until it comes in contact with the layer but will not rise above it. This phenomenon is known as an inversion. Pollutants become trapped below this layer and can only escape after sunlight penetrates the inversion and heats the earth's surface sufficiently to break up the inversion.

The heating of the earth's surface and the resultant vertical temperature profile determine whether pollutants are dispersed or mixed vertically. A second and important process for mixing of the earth's atmosphere is wind and the resultant mechanical mixing when wind passes over surface structures such as tall buildings or mountainous terrain. Some of the cleanest and clearest air is found on the windiest days.

Pollutants emitted that are well mixed will appear as a uniform haze. This condition is shown schematically in Figure 4.2a. When pollutants are emitted into a stable atmosphere, usually one of two things will happen, depending on whether there is surface wind or not. If a wind is present, the emitted pollutants usually form a plume, as indicated in Figure 4.2b. If there are no surface winds or if pollutants are emitted into a stagnant air mass over periods of days, a condition schematically shown in Figure 4.2c can occur. A layer of haze forms near the ground and continues to build as long as the stagnation condition persists. Layered hazes are usually associated with emissions that are local in nature as opposed to pollutants that are transported over hundreds of kilometers.

4.2 Atmospheric Chemistry

Particulates and gases in the atmosphere can originate from natural or man-made sources. Table 4.1 includes the terms that are usually used to describe airborne particles; Table 4.2 shows the size range of typical atmospheric aerosols.

The ability to see and appreciate a visual resource is limited, in the unpolluted atmosphere, by light scattering of the molecules that make up the atmosphere. These molecules are primarily nitrogen and oxygen along with some trace gases such as argon and hydrogen. Other forms of natural aerosol that limit our ability to see are condensed water vapor (water droplets), wind-blown dust, and organic aerosols such as pollen and smoke from wild fires.

Aerosols, whether they are man-made or natural, are said to be primary or secondary in nature. Primary refers to gases or particles emitted from a source directly, while secondary refers to airborne dispersions of gases and particles formed by atmospheric reactions of precursor or primary emissions. Examples of primary particles are smoke from forest and prescribed fires, soot from diesels, fly ash from the burning of coal, and wind-blown dust. Primary gaseous emissions of concern are sulfur dioxides emitted from coal burning, nitrogen oxides that are the result of any type of combustion such as coal-fired power plants and automobiles, and hydrocarbons, usually associated with automobiles but are also emitted by vegetation, especially conifers.

These gases can be converted into secondary particles through complex chemical reactions. Furthermore, primary gases can combine to form other secondary gases. Atoms and molecules of special interest along with their relative sizes are shown in Figure 4.3. Five atoms, in order of their size, that play significant roles in determining air

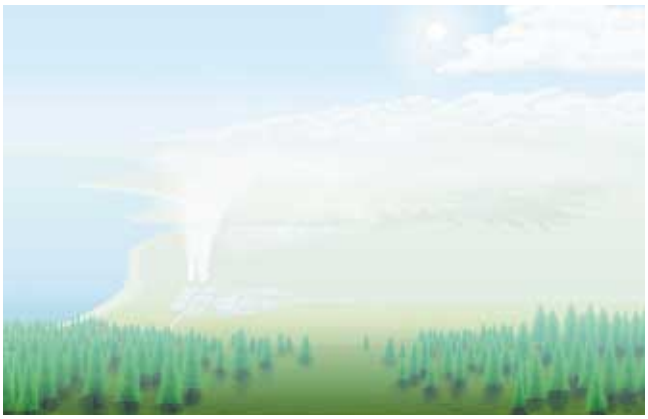

(a)

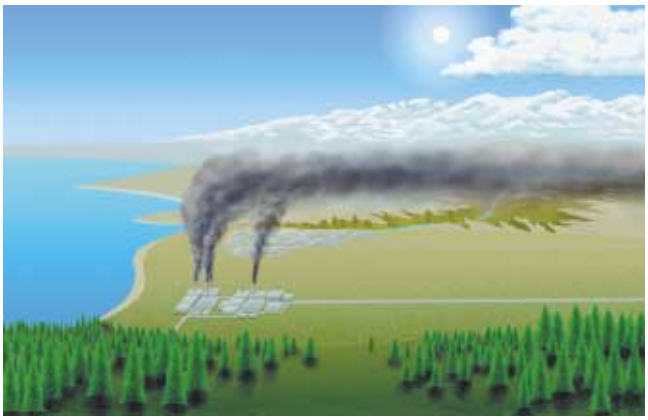

(b)

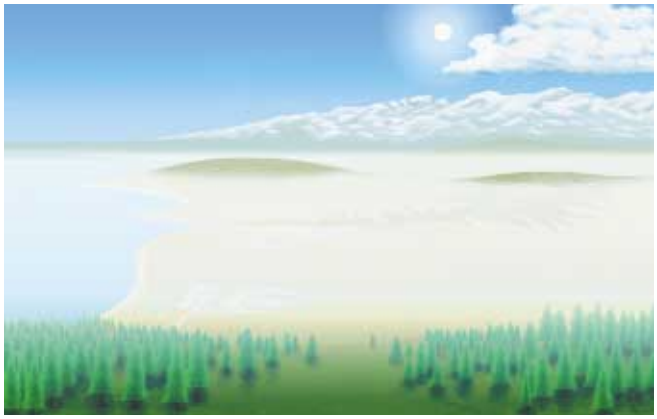

(c)

Fig. 4.2 The three ways that air pollution can visually degrade a scenic vista. When there is sufficient sunlight to cause the atmosphere to become turbulent, pollutants emitted into the atmosphere become well mixed and appear as a uniform haze. This condition is shown in (a). On the other hand, during cold winter months the atmosphere becomes stagnant. Pollutants emitted during these periods will appear either as a coherent plume (b) or as a layered haze (c).

Table 4.1. Definitions of terms that describe airborne particulate matter.

Term	**Definition**
Particulate matter	Any material, except uncombined water, that exists in the solid or liquid state in the atmosphere or gas stream at standard condition.
Aerosol	A dispersion of microscopic solid or liquid particles in gaseous media.
Dust	Solid particles larger than colloidal size capable of temporary suspension in air.
Fly ash	Finely divided particles of ash entrained in flue gas. Particles may contain unburned fuel.
Fog	Visible aerosol.
Fume	Particles formed by condensation, sublimation, or chemical reaction, predominantly smaller than 1 micron (tobacco smoke).
Mist	Dispersion of small liquid droplets of sufficient size to fall from the air.
Particle	Discrete mass of solid or liquid matter.
Smoke	Small gasborne particles resulting from combustion.
Soot	An agglomeration of carbon particles.

Table 4.2 Typical size ranges of a number of aerosols commonly found in the atmosphere.

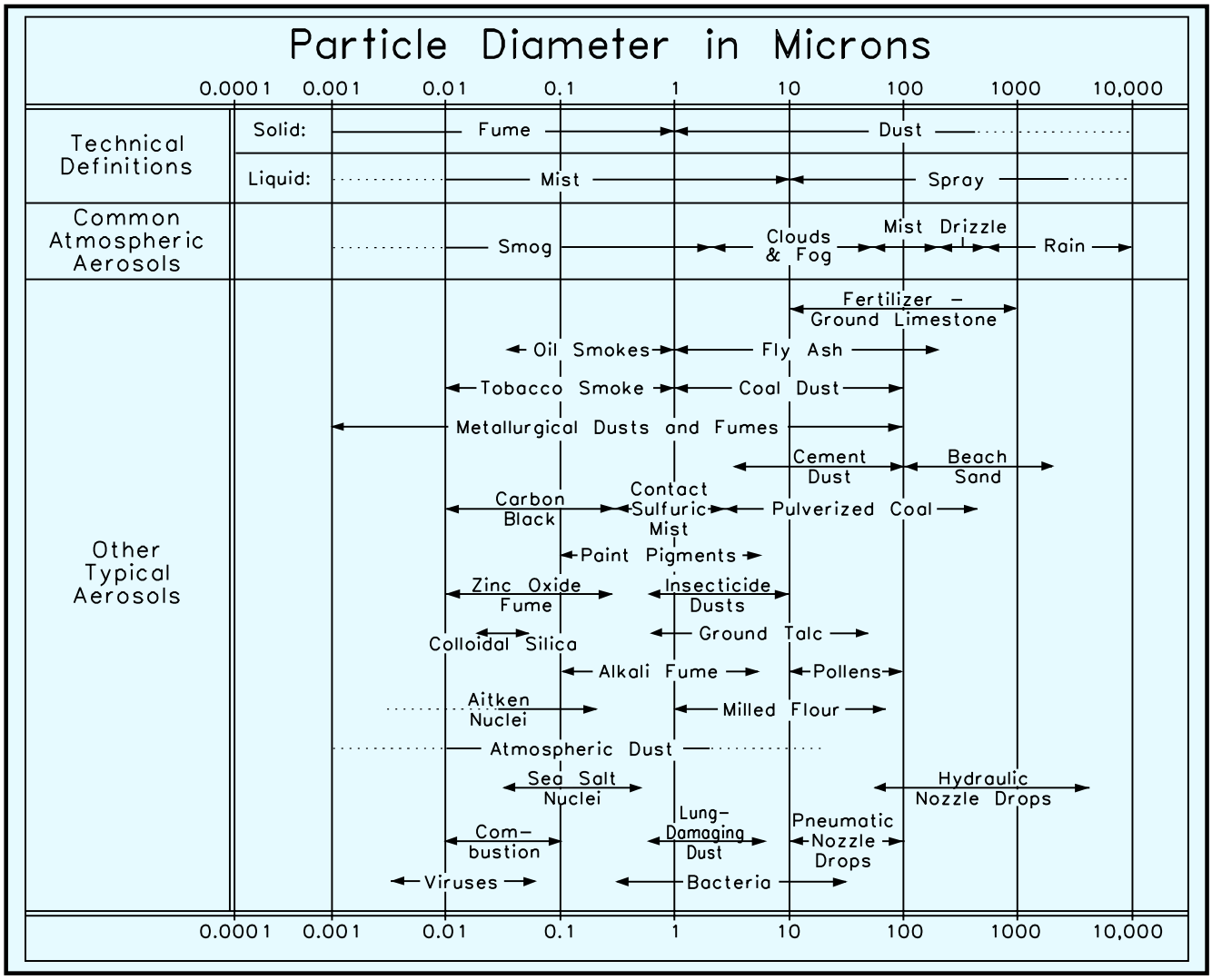

quality are hydrogen (H), oxygen (O), nitrogen (N), carbon (C), and sulfur (S). Sulfur dioxide (SO_2) is ultimately converted to sulfates, such as ammonium sulfate ($(NH_4)_2SO_4$), nitrogen oxides (NO_x) convert to nitrates such as nitric acid or ammonium nitrate (NH_4NO_3), hydrocarbons convert to larger organic or hydrocarbon molecules, and hydrocarbon gases interfere with a naturally occurring cycle between hydrocarbon and NO_2 to yield ozone (O_3).

The gas-to-particle conversion process takes place by essentially three processes: condensation, nucleation, and coagulation. Condensation involves gaseous vapors condensing on or combining with existing small nuclei, usually called condensation nuclei. Small condensation nuclei may have their origin in sea salts or combustion processes. Gases may also interact and combine with droplets of their own kind and form larger aerosols. This process is called homogeneous nucleation. Heterogeneous nucleation occurs when gases nucleate on particles of a different nature than themselves. Once aerosols are formed, they can grow in size by a process called coagulation, in which particles essentially bump into each other and "stick" together.

Figure 4.4 schematically shows the conversion of sulfur dioxide to sulfate, the growth of sulfate

molecules into sulfate particles and the very important process of water absorption by the sulfate particle. Some inorganic salts, such as ammonium sulfate and nitrate, undergo sudden phase transitions from solid particles to solution droplets when the relative humidity (RH) rises above a threshold level. Thus, under higher RH (>70%) levels, these salts become disproportionately responsible for visibility impairment as compared with other particles that do not uptake water molecules.

The size of most secondary particles ranges between 0.1 and 1.0 microns. For reference, the relative size of beach sand, a grain of flour, and a secondary particle is shown in Figure 4.5.

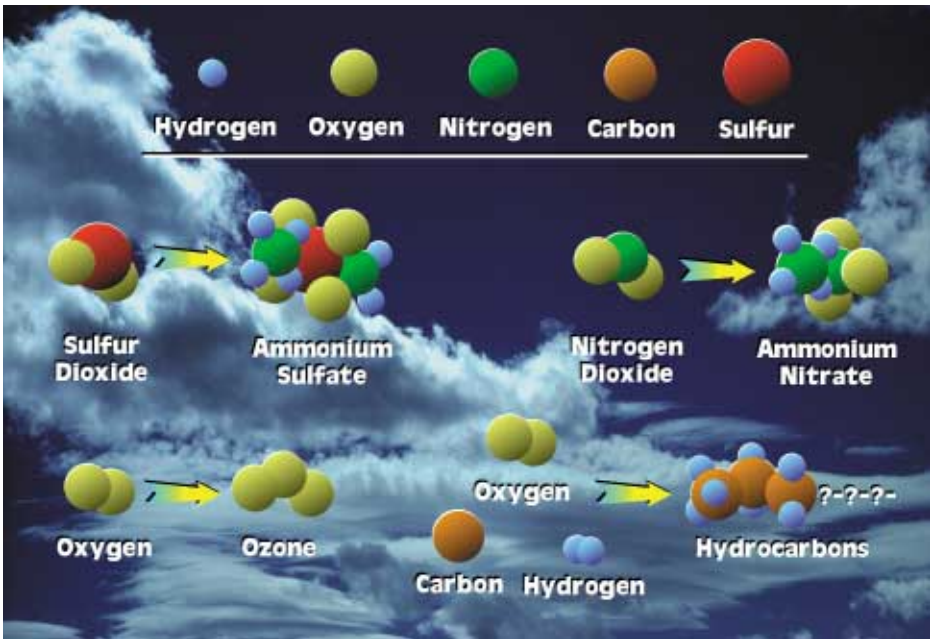

Fig. 4.3 The top row shows five atoms, in order of size, that play a significant role in determining air quality. They are hydrogen, oxygen, nitrogen, carbon, and sulfur. Through complex sets of chemical reactions, gases are formed that, in some cases, react to form visibility reducing particles. Sulfur dioxide reacts to form ammonium sulfate, nitrogen oxide forms ammonium nitrate, oxygen is converted to ozone, and carbon, hydrogen, and oxygen form hydrocarbon particles.

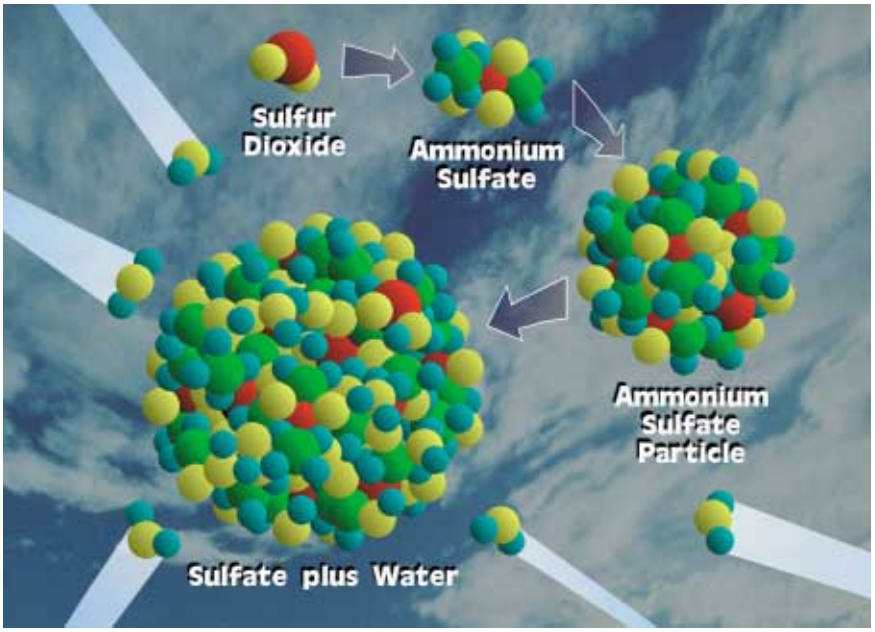

Fig. 4.4 Sulfur dioxide gas converts in the atmosphere to ammonium sulfate particles. These particles are hygroscopic, meaning they grow rapidly in the presence of water to reach a size that is disproportionately responsible for visibility impairment.

Figure 4.6 shows a typical mass size distribution for particles found in the atmosphere. Those particles less than about 2.5 microns are usually secondary in nature and are referred to as fine particles. Fine particles tend to be man-made, while particles larger than 2.5 microns, referred to as coarse particles, tend to have a natural origin. It is the fine particles that cause most of the visibility impairment and have the greatest adverse health effects. The formation mechanisms are also schematically shown in Figure 4.6.

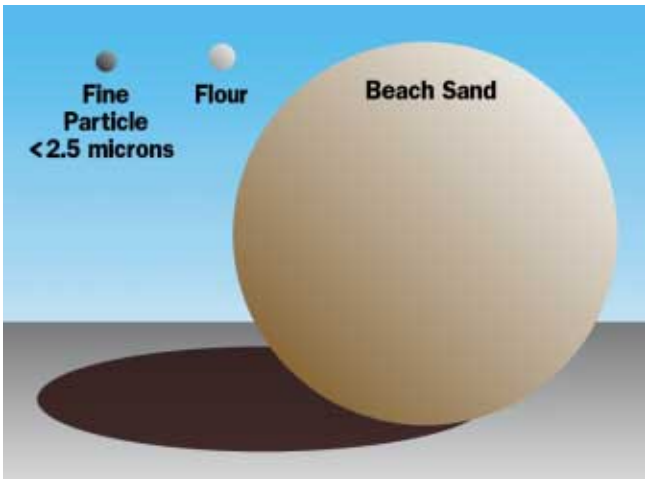

Fig. 4.5 Relative size of beach sand, a grain of flour, and a secondary fine particle.

Near a source (within 0-100 km), such as an urban center, power plant, or other industrial facilities, haze is usually a mixture of gases and secondary and primary aerosols. After these pollutants have been transported hundreds of kilometers, gaseous emissions have either deposited to aquatic or terrestrial surfaces or converted to secondary aerosols. Thus, in remote areas of the United States, man-made components of haze are usually composed of secondary particles. However, in some parts of the forested United States, fire emissions can contribute significantly to primary carbon particles.

4.3 Transport and Transformation

These concepts are summarized in Figures 4.7 and 4.8. Emissions are transported (or accumulated depending on inversion characteristics), transformed into other gaseous or particle species, and deposited to the terrestrial ecosystem. In Figure 4.7, SO_2 emissions and $(NH_4)_2SO_4$ are characterized as red and green dots, respectively. In Section A, SO_2 is emitted and immediately dispersed downwind. SO_2 begins to convert to SO_4 and both SO_2 and SO_4 are deposited to the terrestrial ecosystem (this includes water and ground surfaces as well as plants and animals) as the material is carried by air movement. This process of depositing the material to the ground is known as dry deposition. Once SO_2 enters the cloud environment, the conversion of SO_2 to SO_4 begins in earnest. The cloud droplets act as tiny reactors and the chemistry of SO_2 to SO_4 conversion goes on very rapidly as long as the chemical components necessary for conversion are present. The cloud can evaporate leaving behind SO_4 particles that affect visibility or the SO_4 can deposit out of the cloud as acid

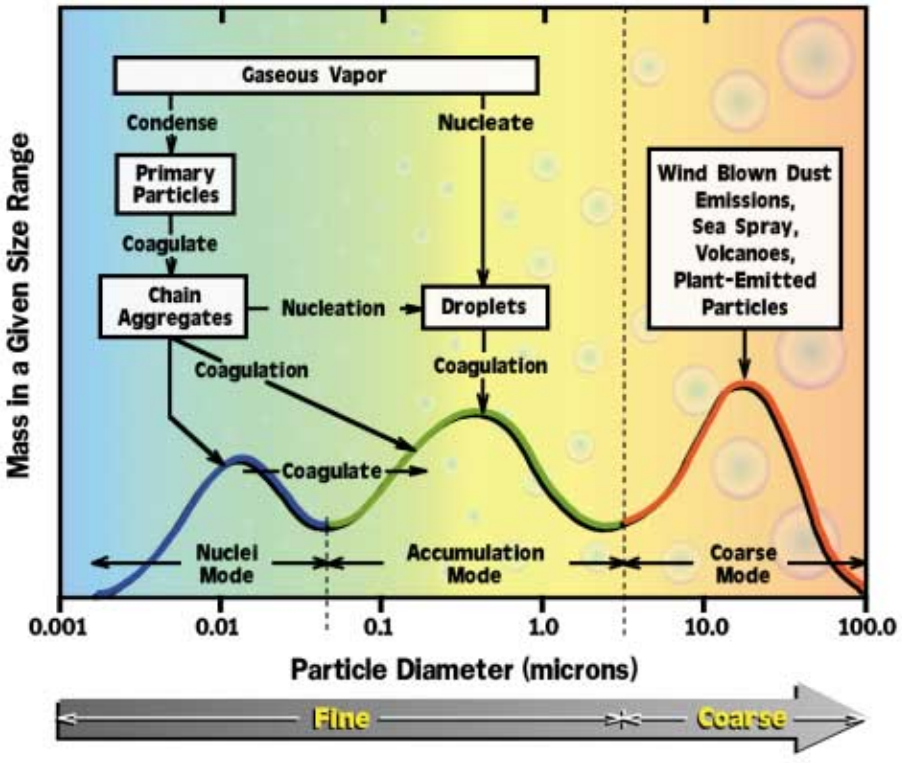

Fig. 4.6 The particles are arranged by their typical mass/size distribution in the atmosphere. Coarse particles tend to have natural origins and deposit out close to the source. Fine particles are usually man-made, can transport great distances, and cause the greatest visibility impairment.

rain (wet deposition). Figure 3.10 shows a case where SO_2 was transported into the Grand Canyon inside clouds. After the clouds evaporate, only the $(NH_4)_2SO_4$ particles are left and the walls and depths of the Grand Canyon have disappeared.

Section B of Figure 4.7 shows a similar process of SO_2 to SO_4 conversion but under stable meteorological conditions. Again, SO_2 is shown to enter the cloud reactor where it is converted to SO_4. Clouds evaporate leaving behind sulfate particles in the form of regional haze. Also, phytoplankton, shown under the magnifying glass, emit natural sulfur as dimethyl sulfide that is converted to SO_2.

Figure 4.8 shows the interrelationships between NO_x, hydrocarbons, and organic particle emissions. These reactions are very complex and Figure 4.8 is meant to show only some of the main features of the process. Gaseous hydrocarbons (labeled as volatile organic carbon or VOCs) and NO_x emissions are in the form of red and purple dots. The subscript x is meant to suggest that the emissions may be in the form of NO or NO_2. NO_x is converted into nitric acid

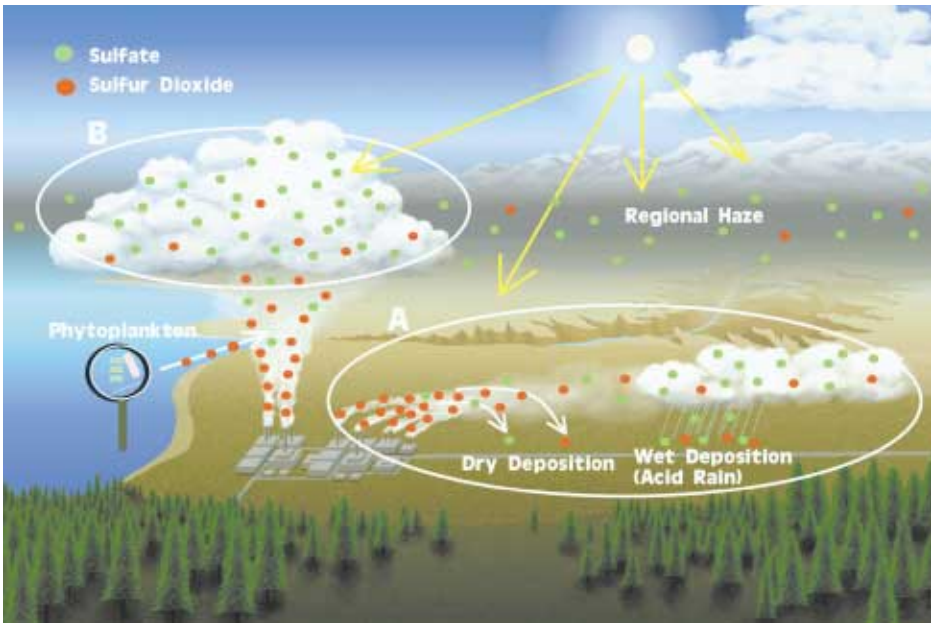

Fig. 4.7 Sulfur dioxide emissions can deposit directly to the earth's surface or biological system or they can cause rain water to acidify. Sulfur dioxide can also chemically convert to sulfate particles and deposit to the earth's surface. Together these modes of deposition are known as "acid rain." The sulfate particles that remain in the atmosphere cause visibility impairment.

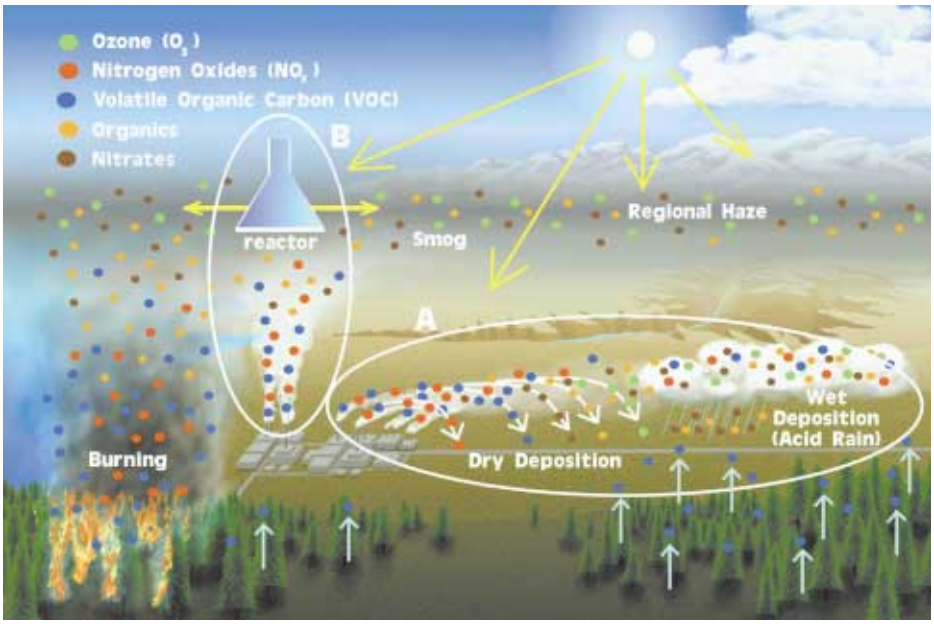

Fig. 4.8 Nitrogen oxide and hydrocarbon (VOC) gases emitted into the atmosphere cause the formation of ozone and other photochemical oxidizing agents that cause eyes to burn and stunt or kill vegetation. Nitrogen dioxide can cause acidification of cloud water and form nitric acid vapor or can change into nitrate particles. The deposition of these species is a large part of the acid rain problem. Furthermore, particulate nitrate can cause visibility impairment. Hydrocarbon gases can convert into carbon particles and carbon particulate can be emitted directly from natural sources such as fire or from the diesel engine. These carbon particles contribute significantly to visibility impairment.

vapor and NH_4NO_3 molecules that in turn form NH_4NO_3 particles with similar characteristics as $(NH_4)_2SO_4$. Nitrates are represented as brown dots. The reactor shown in Figure 4.8 represents those reactions discussed above and those that involve NO_x and VOCs and the production of O_3. O_3 is shown as green dots. Also produced in the reactor are secondary organic particles shown as yellow dots. Secondary organic particles and nitrates contribute to regional haze, while O_3 is important in the production of secondary particles and gases and has adverse effects on biological and terrestrial systems. Section A of Figure 4.8 is meant to show an unstable "windy" meteorological scheme and to explicitly show the deposition process. NO_x and VOCs are emitted, which in turn convert to nitrate and organic particles and O_3 gas. All of these species deposit to the terrestrial ecosystem as they come in contact with it. Secondly, the gases and particles can enter clouds where they continue to react and eventually rain out as acid deposition. Nitrates are important contributors to acid rain although there can be some weak organic acids.

Figure 4.8 further shows hydrocarbon emissions from forests and the emissions from fire-related activity. Fire emissions not only include NO_x and VOC gases, but also primary organic particles in the form of uncombusted material.

Figure 4.9 schematically shows the five particle types that make up nearly all of the fine particle mass found in the atmosphere. They are, in order of their relative contribution to visibility impairment, sulfates, organics, soil, elemental carbon, and nitrates. In some parts of the United States, the relative order of importance can change. For instance, in areas in southern California, nitrates can cause most of the visibility impairment.

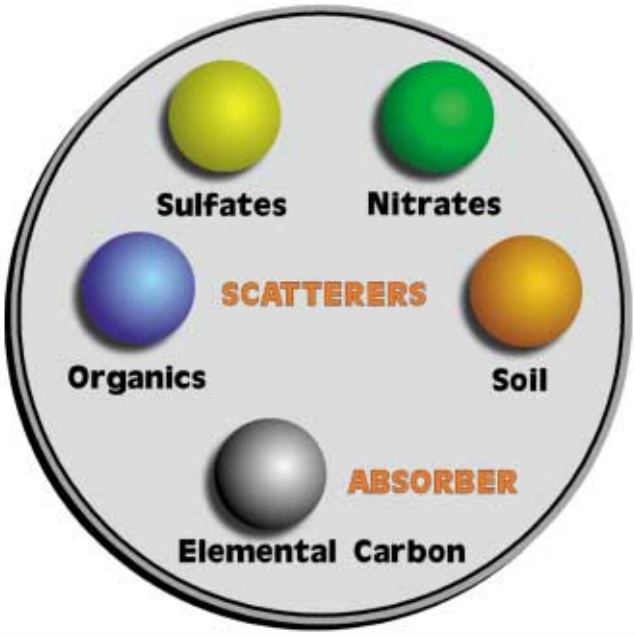

Fig. 4.9 The five particle types that make up the fine particle mass: sulfates, organics, elemental carbon, soil, and nitrates.

SECTION 5

VISIBILITY MEASUREMENTS

Developing the links between visibility and particles that scatter and absorb light requires extensive monitoring programs in which both atmospheric optical variables and particulate concentrations that cause visibility impairment are measured. Since visibility cannot be defined by a single parameter, it follows that a well-defined monitoring methodology does not exist. However, monitoring methods can be subdivided into three classes: view, optical, and aerosol monitoring.

Visibility, in the most general sense, reduces to understanding the effect that various types of aerosol and lighting conditions have on the appearance of landscape features. Many visibility indices have been proposed to quantify the appearance of a scene; however, a photograph relating the effects particles have on the appearance of landscape features is the most simple and direct form of communicating visibility impairment. Therefore, a systematic photography program (view monitoring) that records the appearance of the scene under a variety of lighting conditions and aerosol concentrations is a key part of most visibility monitoring programs. The camera in its simplest form is shown in Figure 5.1. It consists of a lens to focus the image on a strip of photographic film, and an aperture and shutter to control the amount of light entering the camera.

However, because it is difficult to extract quantitative information from color slides or pictures, some direct measure of a fundamental optical property of the atmosphere is desirable. Therefore, most visibility programs include some measure of either atmospheric extinction or scattering.

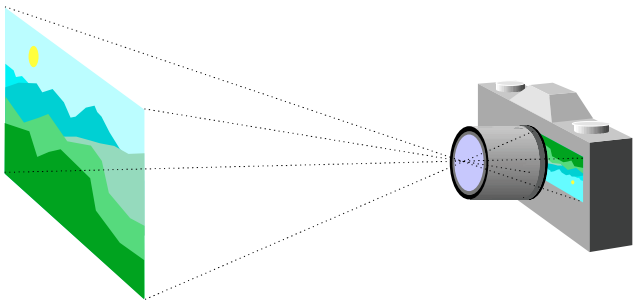

Fig. 5.1 A camera is the simplest way to monitor visibility. Much like the eye, it has a lens to focus the image onto the film, and an aperture and shutter to control the amount of light entering the camera.

5.1 Measurements of Scattering and Extinction

The scattering coefficient is a measure of the ability of particles to scatter photons out of a beam of light, while the absorption coefficient is a measure of how many photons are absorbed. Each parameter is expressed as a number proportional to the amount of photons scattered or absorbed per distance. The sum of scattering and absorption is referred to as extinction or attenuation.

Figure 5.2 is a schematic diagram showing a beam of light made up of photons with varying wavelengths that is incident on a concentration of particles and absorbing gas. Knowing the number of photons incident on a concentration of particles and measuring the number of photons successfully passing through the particulate concentration, it is possible to calculate the number of photons scattered and absorbed. The instrument that measures extinction (sum of scattering and absorption) is known as a transmissometer.

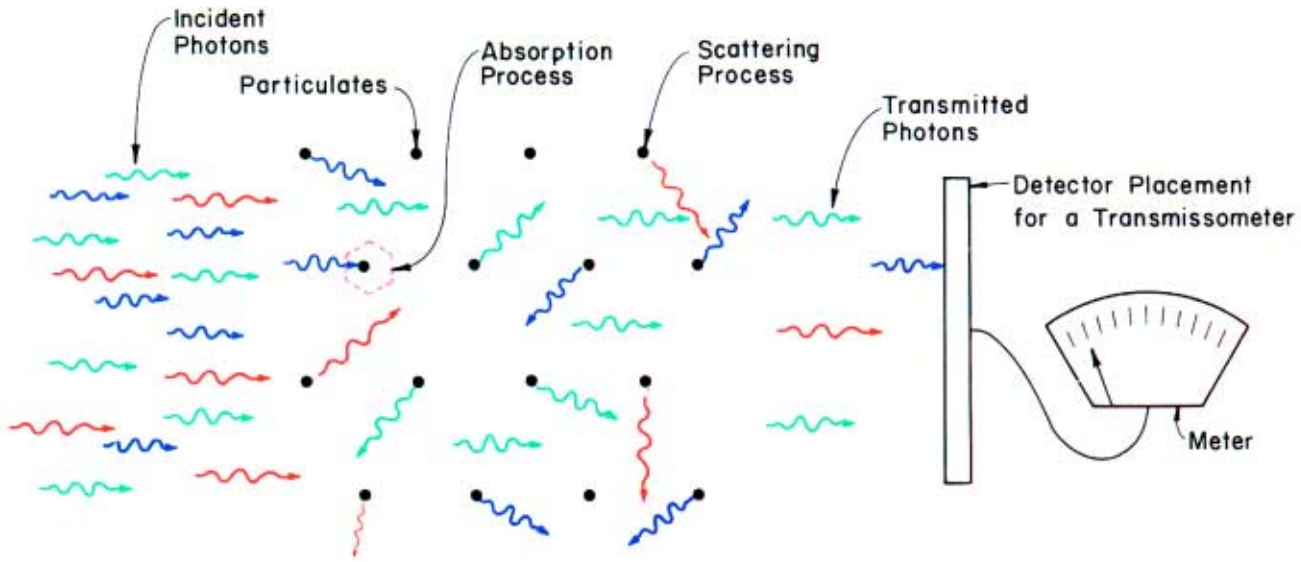

Fig. 5.2 Placement of a light source and detector as shown here is known as a transmissometer. As photons pass through a concentration of particles and gases, they are either scattered out of the light path or they are absorbed. Thus a detector placed as indicated measures only those photons that are transmitted the length of the light path. Because this instrument is sensitive to both scattering and absorption, it can be calibrated to measure the extinction coefficient.

The light source is usually an incandescent lamp, and the receiver is a telescope fitted with an appropriate detector. The light source and detector can be placed 1-10 kilometers apart, and the measurement is usually referred to as long-path measurement.

A similar light source-detector configuration can be used to measure just the scattering ability of particles and gases. If the detector is placed parallel to the incident photons, only those photons that are scattered will be detected. This type of instrument is called a nephelometer (Figure 5.3). If the detector is so aligned as to measure scattering in only one direction it is referred to as a polar nephelometer. On the other hand, if all photons scattered in forward, side, and back directions are allowed to hit the detector, the instrument is referred to as an integrating (summing) nephelometer. The instrument is usually constructed in such a way as to have the sampling chamber and light source confined to a small volume so that the instrument makes a "point" or localized measurement of scattering.

Most monitoring programs use combinations of transmissometers and integrating nephelometers to measure extinction and scattering. Historically, the National Weather Service (NWS) program estimated visual range (from which atmospheric extinction can be approximated) by viewing a series of landscape features at a variety of distances and recording the most distant feature that can be seen. While this program has been discontinued, the database, which goes back to the 1940s, is still useful for tracking visibility changes that have occurred over decades.

5.2 Measurements of Particles in the Atmosphere

Finally, particle measurements are generally made in conjunction with optical measurements to help infer the cause of visibility impairment, and to estimate the source of visibility reducing aerosols. Size and composition are the two dimensions of particle characterization most often used in visibility monitoring programs. Particles between 0.1 to

1.0 microns are most effective on a per mass basis in reducing visibility and tend to be associated with man-made emissions. Figure 5.4 shows a diagram of a cyclone-type particle monitor that separates all those particles less than a specified size (usually 2.5 μm) and collects them on a filter substrate for additional analysis. The air is caused to spin in much the same way as a merry-go-round. The heavier particles, those larger than 2.5 μm, fall off the merry-go-round and impact on the side of the sampler to be discarded to the bottom of the sampler. Those particles staying in the air stream pass through a filter where they are extracted for further analysis. Particles are speciated into sulfates, nitrates, organic material, elemental carbon (soot), and soil. The speciation of particles helps determine the chemical-optical characteristics and the ability of the particle to absorb water (RH effects) and is important to separate out the origin of the aerosol.

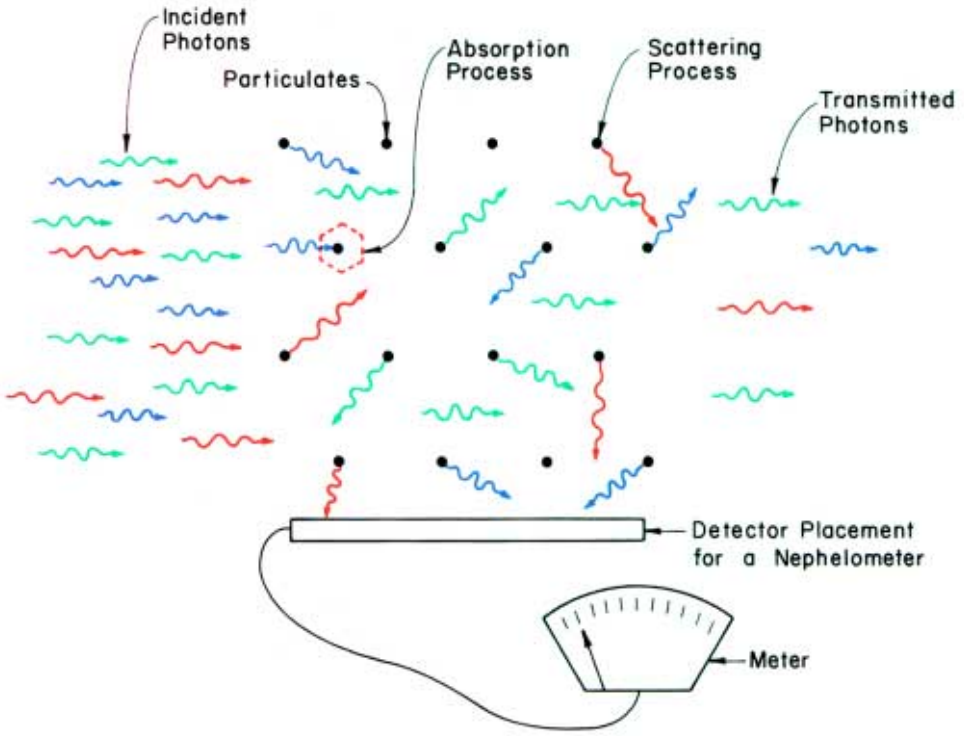

Fig. 5.3 Placement of a detector for the measurement of the number of photons scattered by a concentration of particles and gas.

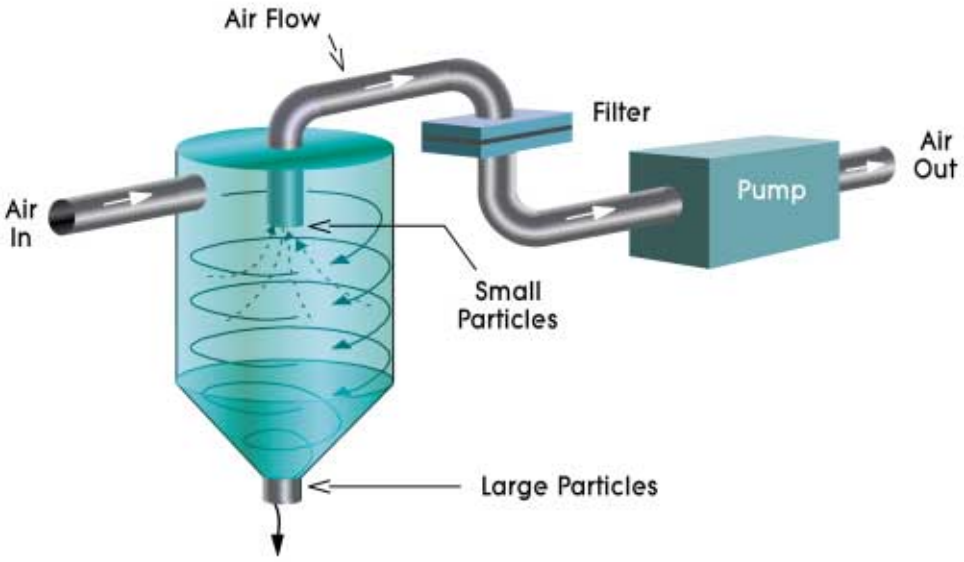

Fig. 5.4 Diagram of a cyclone-type particle monitor. The air inside the cyclone spins in such a way as to cause larger particles to deposit on the inside of the monitor and fall to the bottom, while smaller particles continue in the air stream and are collected on a filter substrate for analysis.

SECTION 6

PARTICLE CONCENTRATION AND VISIBILITY TRENDS

There are and have been a number of particle and visibility monitoring programs implemented in the United States, most notably the Interagency Monitoring of Protected Visual Environments (IMPROVE) and the National Weather Service (NWS) program. The IMPROVE program, by design, has its focus on nonurban environments, while the NWS program was carried out at airports across the United States. In the next sections, a brief summary from results of these programs will be presented. Figure 6.1 shows the locations of the monitoring sites used in the IMPROVE program.

6.1 Natural Conditions

Best estimates of average natural background particle concentrations for east and west of the Mississippi River have been developed. Neglecting effects of rain and clouds, it is possi-

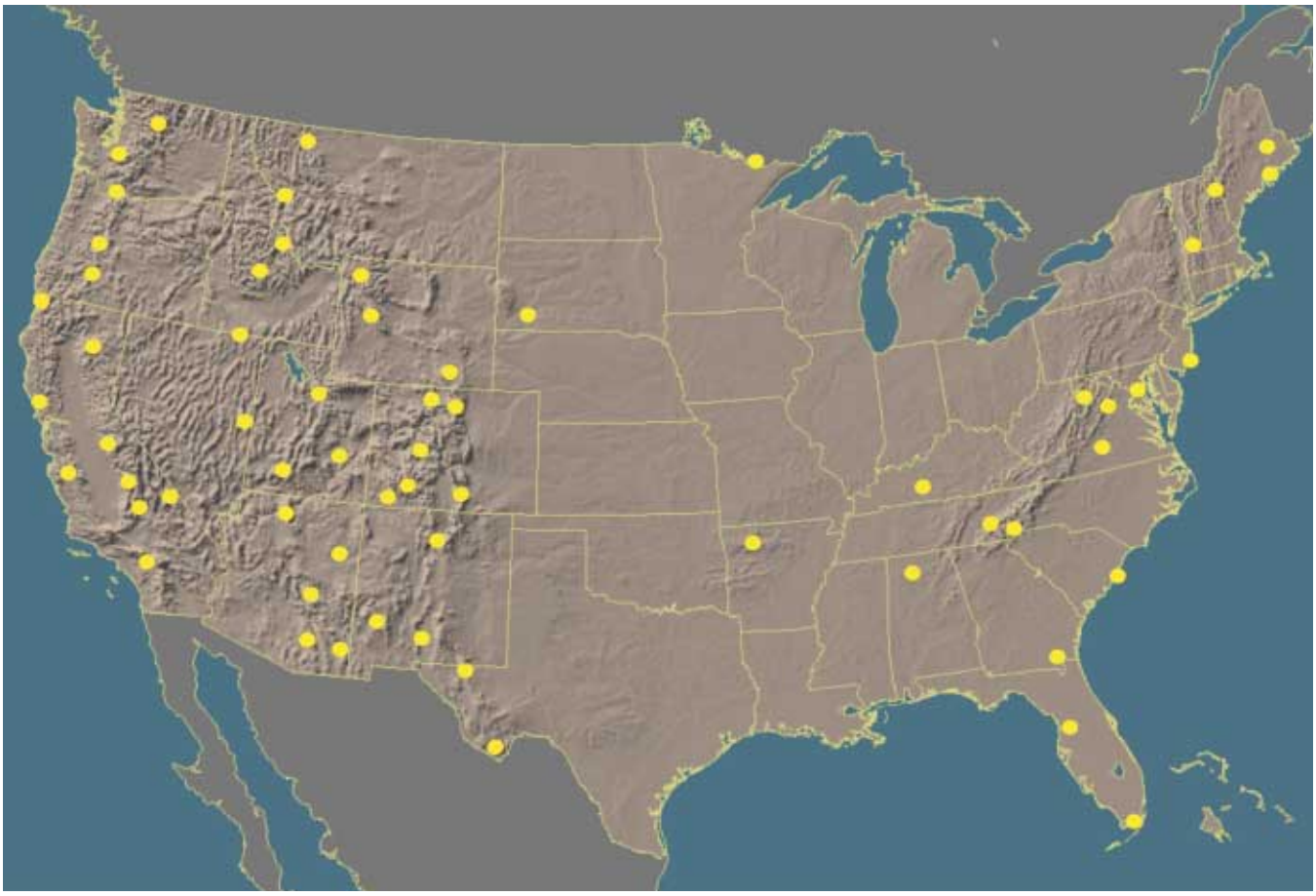

Fig. 6.1 Location of the monitoring sites used in IMPROVE. (1999)

ble to use particle concentrations, listed in Table 6.1, to estimate natural visibility conditions. The extinction efficiencies (efficiency with which the particles scatter and absorb light) assumed for each particle species, also listed in Table 6.1, are multiplied by the particle concentration to estimate dry particle extinction. The extinction efficiencies used for sulfates, nitrates, and organics are based on theoretical calculations assuming typical particle size distributions and chemical characterics as well as a literature review.

assumption that 0 to 0.5 of the organics are water soluble reflects the uncertain nature of the chemical characteristics of organic particles.

From these extinctions, and due to the scattering associated with clear sky (Rayleigh atmosphere), it is possible to estimate natural median visibilities. These calculations are summarized graphically in Figure 6.2. In the East visual ranges are estimated to be 60 to 80 miles, while in the West they are between 110-115 miles. Under

Table 6.1. Estimated natural background particulate concentrations and extinction. Assuming the dry extinction efficiencies listed in the table, and sulfates, nitrates, and half the organics are hygroscopic, average natural visual ranges, along with the percent contribution of each aerosol species to natural visibility impairment was estimated.

	Average Mass Concentrations		Dry Extinction Efficiencies	% Contribution to Visibility Reduction	
	EAST	***WEST***		***EAST***	***WEST***
FINE PARTICLES					
Sulfates ($(NH_4)_2 SO_4$)	0.23 $\mu g/m^3$	0.115 $\mu g/m^3$	3.0 m^2/gm	9-12%	5-5%
Organics	1.5 $\mu g/m^3$	0.5 $\mu g/m^3$	3.0 m^2/gm	19-38%	10-15%
Elemental Carbon	0.02 $\mu g/m^3$	0.02 $\mu g/m^3$	10.0 m^2/gm	0.5-1%	1-1%
Nitrates (NH_4NO_3)	0.1 $\mu g/m^3$	0.1 $\mu g/m^3$	3.0 m^2/gm	4-5%	4-4%
Soil Dust	0.5 $\mu g/m^3$	0.5 $\mu g/m^3$	1.25 m^2/gm	2-3%	4-4%
COARSE PARTICLES	3.0 $\mu g/m^3$	3.0 $\mu g/m^3$	0.6 m^2/gm	6-8%	11-12%
CLEAN AIR	NA	NA	NA	33-43%	61-64%
VISUAL RANGE	NA	NA	NA	100-130 km	182-193 km

Additionally, it is also necessary to estimate the effect of high relative humidity on scattering by water soluble particles, such as sulfates and nitrates. Therefore, in the East, soluble particles' extinctions are multiplied by an additional factor of 4.1, while in the West the factor used was 2.2. These factors correspond to effective relative humidity of 87% and 70%, respectively. Lower and upper bounds on natural visibility are calculated by first assuming only sulfates and nitrates are hygroscopic, and secondly assuming that 0.5 of the organics are also water soluble. The

natural conditions, carbon-based particles are responsible for most of the non-Rayleigh particle-associated visibility reduction, with all other particle species contributing significantly less. Scattering by air molecules is the largest contributing factor to the reduction of visual range, at about 40-60%.

It is expected that coastlines and highly vegetated areas may be lower than these averages, while some elevated areas could exceed these background estimates. Furthermore, it was not

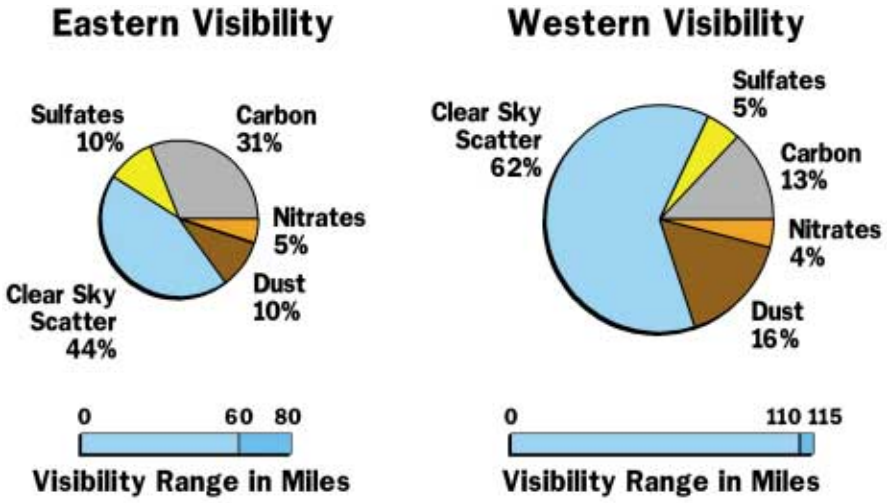

Fig. 6.2 Natural visibility in the East is estimated to be between 60 and 80 miles, while in the West it is between 110-115 miles. Under natural conditions, sulfur is only 10 and 5% of the visibility impairment in the East and West, respectively. Currently, sulfur is 60 to 90% of the visibility reduction in the East and about 30% in the West. Dust is the sum of soil dust and coarse particles.

attempted to estimate a frequency distribution of background particle concentrations and therefore a distribution of visibilities cannot be calculated. It is expected that natural or background visibility, on some days, approached the Rayleigh limit because current monitoring data show that even today there are some time periods where the atmosphere is essentially free of visibility reducing particles.

6.2 Current Conditions

Current conditions of the particle concentrations that affect visibility degradation will be explored first and their effect on visibility will be presented second.

6.2.1 Seasonal Patterns of Particle Concentrations

Sulfate and carbon species are the single largest contributors to visibility reduction at all monitoring sites. In the East, sulfate species make up over 70% of the measured visibility impacts, while in the West they are responsible for about 30%. Figure 6.3 shows time plots of sulfur concentrations measured at Shenandoah, Mount Rainier, Rocky Mountain, Grand Canyon, Acadia, and Big Bend National Parks. If the sulfur is in the form of ammonium sulfate $(NH_4)_2SO_4$, then the sulfur concentrations are multiplied by 4.125 to estimate ammonium sulfate mass. These sites were selected to show typical temporal variability of sulfate concentrations that are measured across the nonurban United States. Shenandoah shows the strongest seasonal trends with summer months having the highest concentrations, and winter the lowest. Similar trends for sulfur concentrations are observed at Grand Canyon, Rocky Mountain and Mount Rainier but not at Acadia and Big Bend. Many of the monitoring sites show seasonal trends; however, the strength of the seasonal signal diminishes as overall sulfur concentrations decrease. Elevated summer sulfate levels are a result of SO_2 to SO_4 conversion that is associated with a photochemical process involving the increase in summertime sunlight. In the East, similar trends are observed for organics, while in other parts of the United States the seasonal trend is much less pronounced and in most cases nonexistent. Nitrates, on the other hand, at almost all locations tend to be the highest during the winter and lowest during the summer months.

The average major seasonal trends are presented as seasonal fine mass budgets for four large geographic areas in Figure 6.4. The Northwest summary is a combined average of the Cascade Mountains, central Rocky Mountains, Great Basin, northern Great Plains, northern Rocky Mountains, Sierra Nevada, and Sierra-Humboldt regions. The Southwest summary combines the

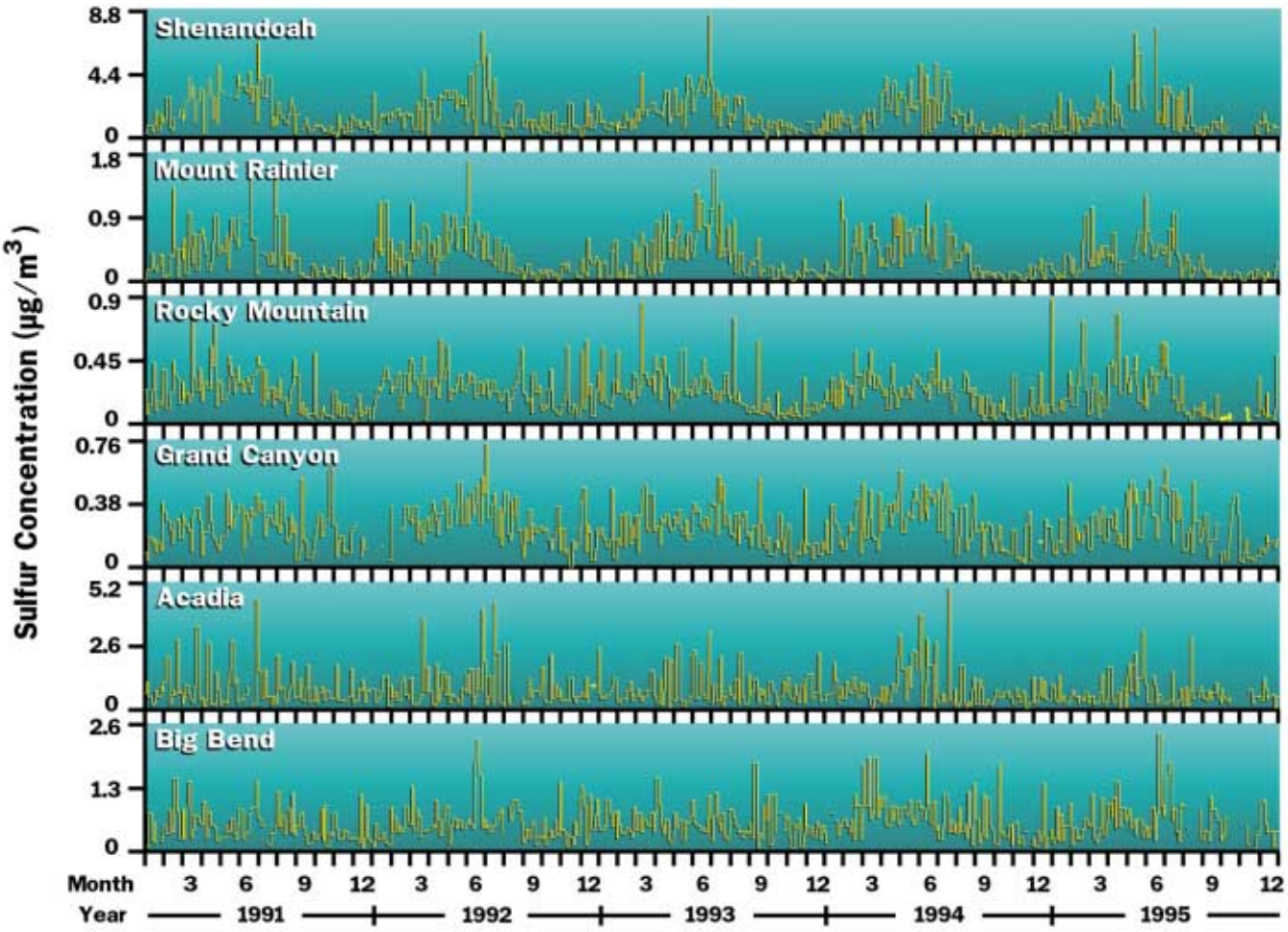

Fig. 6.3 Sulfate trends at Shenandoah, Mount Rainier, Rocky Mountain, Grand Canyon, Acadia, and Big Bend National Parks. Sulfate is usually highest during the summer months and lowest in winter. However, at some national parks, such as Acadia and Big Bend, seasonal trends are not very pronounced with more amounts of sulfur found throughout the year.

Colorado Plateau and Sonoran Desert regions, while Pinnacles National Monument, and San Gorgonio Wilderness Area make up the California summary. The Appalachian Mountains region is presented as the eastern summary.

The single outstanding feature of all four geographic areas is a similar seasonal trend in the total fine mass concentration represented as the sum of the aerosol species and in the concentration of each individual species. The highest fine mass concentration occurs in the summer, while winter has the lowest. Concentrations of sulfates and organics have a similar trend in all four areas. Nitrates tend to be higher in winter and spring than in summer and fall. Trends in soil are variable, while elemental carbon (EC) shows little variation from season to season. Sulfates are by far the single largest contributer to fine mass in the eastern United States, while in the Northwest organics contribute most to fine mass. Nitrates edge out organics and sulfates in southern California, while in the Southwest sulfates, organics, and soil all contribute about equally to fine mass.

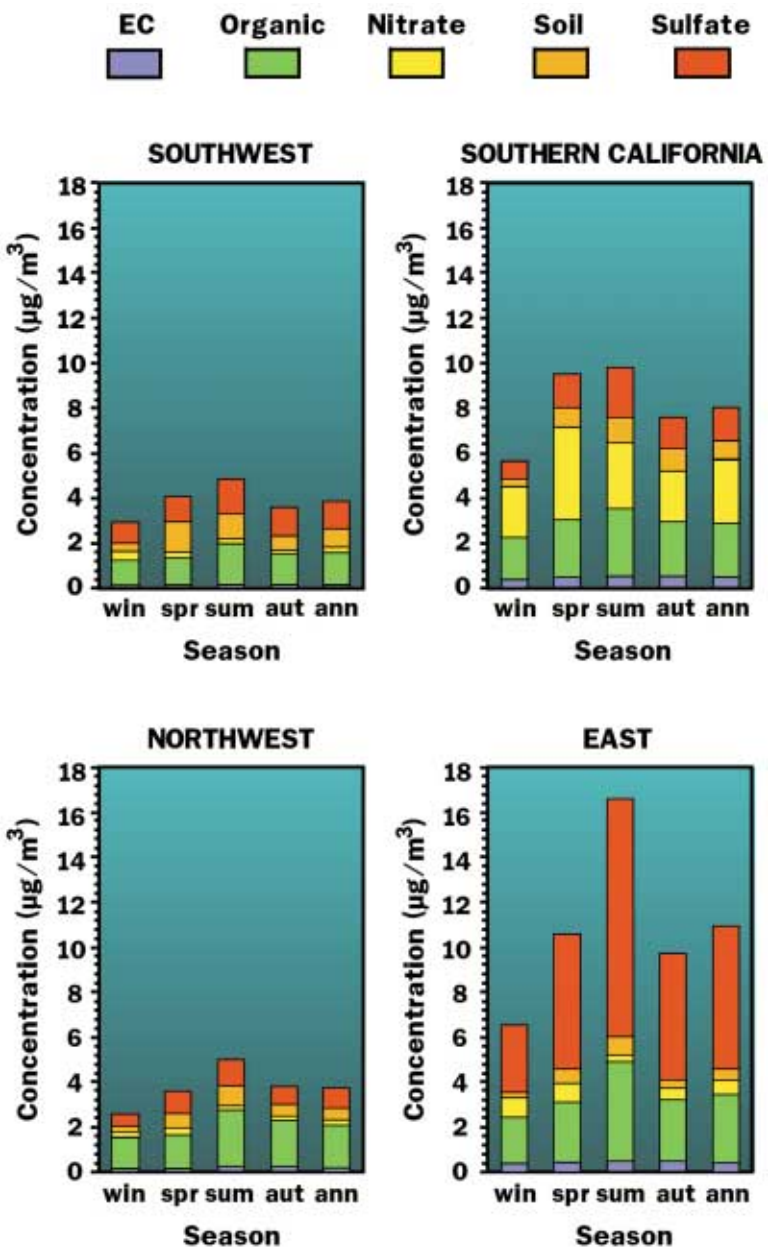

Fig. 6.4 Summary of seasonal trends in fine mass concentration for four geographic regions of the United States. The height of the bar is the fine mass in µg/m^3 and the shaded patterns are proportional to the contribution of various particle species.

6.2.2 Spatial Trends in Visibility

While there is no one definition of visibility that meets all the criteria of "seeing" of landscape features, a number of visibility indices have evolved. Extinction, in the form of inverse megameters (Mm^{-1}), is proportional to the amount of light lost as it travels over a million meters and is most useful for relating visibility directly to particle species concentrations, while deciviews are related to extinction but scaled in such a way that it is perceptually correct. For example, a one deciview change on a 20 deciview day will be perceived to be the same as on a 5 deciview day. This is not the case for extinction or visual range. For reference, Figure 6.5 compares extinction in Mm^{-1}, deciviews (dv), which are unitless, and visual range in km. For instance, 10 Mm^{-1} corresponds to about 400 km visual range and 0.0 dv, while 1000 Mm^{-1} is about 4 km visual range and 46 dv.

Since light extinction of sulfates and nitrates, on a relative basis, is larger than that of other fine particles due to associated water, and since light-absorbing carbon absorbs light very efficiently on a per mass basis, extinction budgets are different from mass budgets. However, for the sake of brevity, because spatial trends in particle mass concentration and visibility are similar, only visibility data will be presented here.

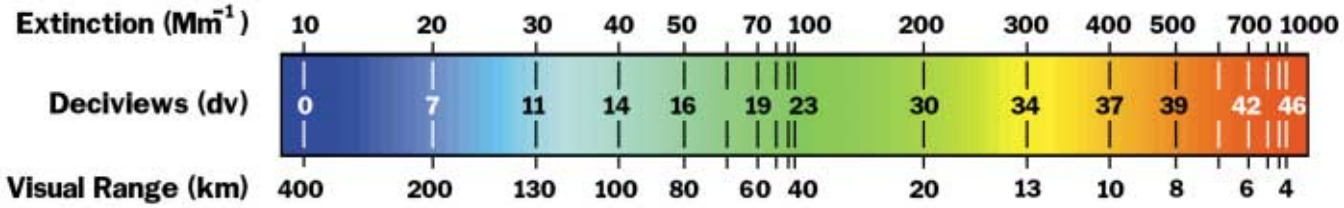

Fig. 6.5 Comparison of extinction (Mm^{-1}), deciview (dv), and visual range (km).

Figure 6.6 shows isopleths of the aerosol-only light extinction coefficient for the United States and Figure 6.7 shows the same plot but in terms of deciviews. Because there are only a few sites in the eastern United States, isopleths cannot be drawn with a high degree of accuracy. There is a strong east-west dichotomy. The highest light extinction (more than 120 Mm^{-1}) occurs in the eastern United States, while the lowest light extinction (less than 15 Mm^{-1}) occurs in the Great Basin, central Rocky Mountains, and nonurban southwest. Extinctions are also relatively high near the Los Angeles and San Francisco metropolitan areas of California, and to a lesser extent, in the Pacific Northwest. Notably, the monitoring site in southern California is not in the Los Angeles basin but in the San Gorgonio Wilderness Area, well outside the population centers of southern California.

Figures 6.8 through 6.12 are composite figures that present isopleths of extinction associated with the aerosol species on the first half of the graph and the fraction of total extinction on the second half. Figure 6.8 shows the contribution of coarse mass plus fine soil to total extinction and in most cases would be considered mostly natural, primarily wind-blown dust.

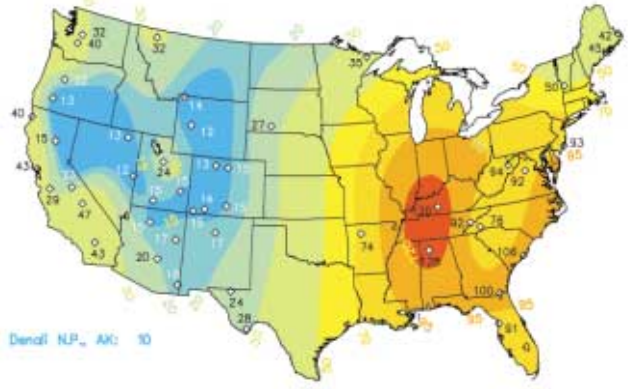

Fig. 6.6 Average reconstructed light extinction coefficient (Mm^{-1}) calculated from the aerosol concentrations measured during IMPROVE.

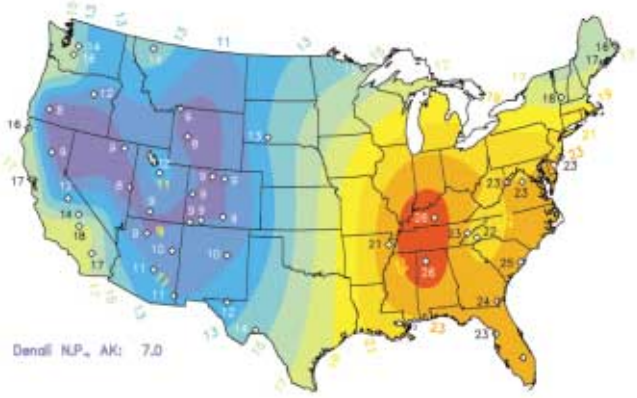

Fig. 6.7 Average visibility, expressed as deciviews, calculated from aerosol concentrations measured in the IMPROVE monitoring program.

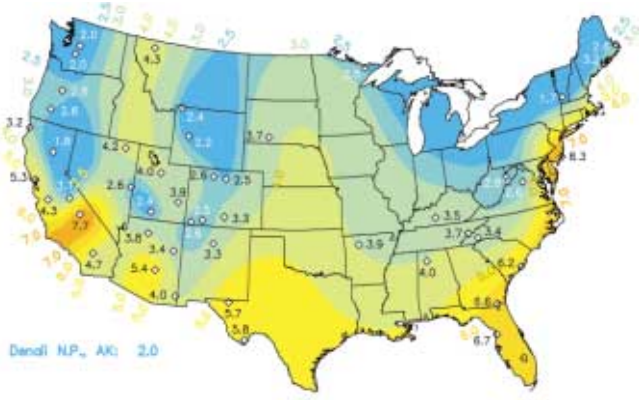

(a)

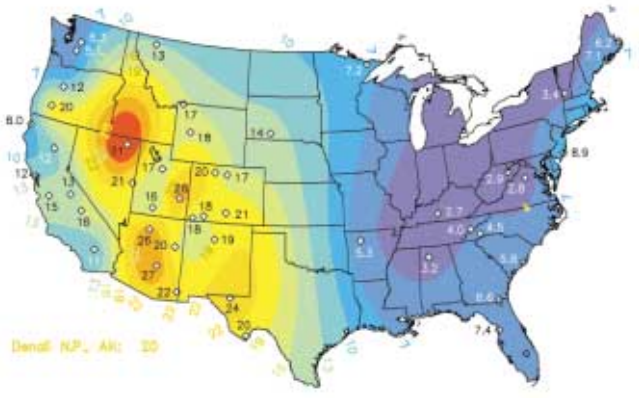

(b)

Fig. 6.8 Map (a) shows extinction, expressed in terms of inverse megameters, attributed to coarse mass and fine soil, while (b) shows the percent contribution of coarse mass and fine soil to total extinction.

Extinction associated with coarse mass/fine soil does not show strong spatial trends. It tends to be highest in the desert southwest and lowest in forested areas. The fraction that coarse mass/fine soil contributes to total extinction indicates large spatial trends primarily because in some parts of the country, especially the eastern United States, the overall extinction is so high that coarse mass/fine soil is almost negligible. However, in the west, coarse mass/fine soil is 15-20% of estimated extinction.

Figure 6.9 shows isopleths of ammonium sulfate extinction and the fraction of extinction attributed to ammonium sulfate. Note that the ammonium sulfate extinction in the eastern United States is about a factor of 25 to 30 higher than in the Great Basin area and a factor of 10 higher than the desert Southwest, central Rocky Mountains, and Sierra Mountains. There is also a gradient from the San Francisco Bay area and from the Pacific Northwest to the central West. Generally, the lowest ammonium sulfate extinction occurs in northern California and Nevada, southern Oregon, Idaho, and Wyoming. Sulfates account for roughly 60-75% of the extinction in the eastern United States, with the fractional contribution of ammonium sulfate to extinction decreasing the farther west one goes. The geographic region where sulfates contribute least to visibility impairment, about 25%, occurs in an area extending from western California, Nevada, southern Oregon, and Idaho. Sulfates account for approximately 30-40% of the visibility impairment in much of the remaining western United States.

Figure 6.10 shows isopleths of the organic carbon light extinction throughout the United States. Note that extinction fraction caused by organic carbon is largest in the Great Basin area of the United States, and is lowest in the eastern United States. In most areas of the western United States, organics contribute about 20-40% of the extinction. In the eastern United States they contribute between 10 and 15% of estimated extinction.

Figure 6.11 shows the nitrate light extinction. There is a small overall gradient from the east to west. The strongest gradient is from the urban areas of California, especially the Los Angeles metropolitan area to the California desert. Nitrate extinction is 20 times higher at monitoring sites in southern and coastal areas of California than in the Great Basin, Colorado Plateau, and Rocky Mountains. In southern California its contribution to extinction is highest at about 40%, and interestingly, only a few hundred kilometers away to the

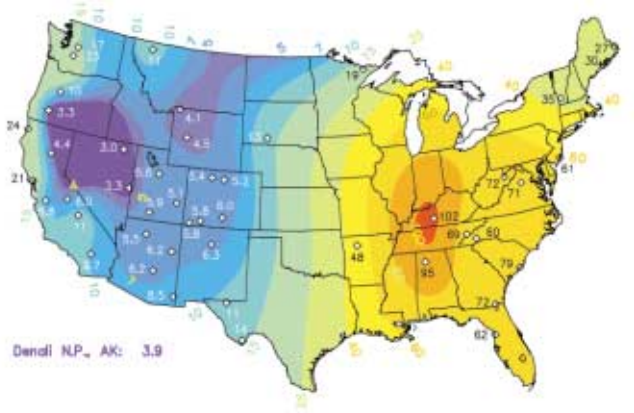

(a)

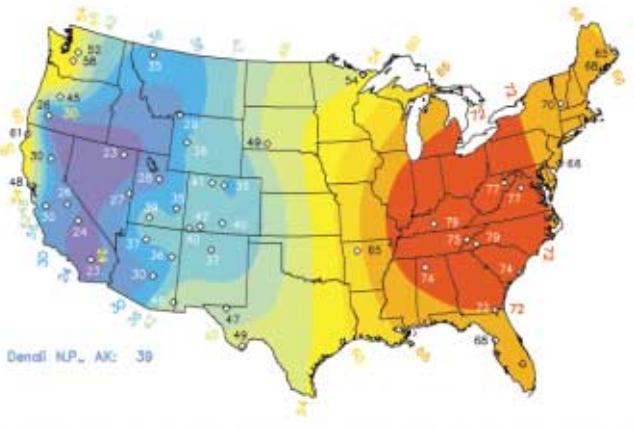

(b)

Fig. 6.9 Map (a) shows extinction, expressed in terms of inverse megameters, attributed to sulfates, while (b) shows the percent contribution of sulfates to total extinction.

north and west, its fractional contribution is about 1/6 as much. In the East, nitrates contribute between 3 and 10% of the extinction.

Figure 6.12 shows isopleths of the extinction caused by elemental and other light-absorbing carbon (LAC). It is highest in southern California and in the southeastern United States, and lowest in the nonurban west. LAC contributes about 7 to 15% to extinction in the western United States, and about 4-6% in the eastern United States.

6.3 Long-Term Trends

6.3.1 Eastern United States

Shown in Figure 6.13 are isopleths of eastern United States median visual range, derived from airport data, for 1948-1982. Winter includes January, February, and March, spring includes April, May, and June, and so on. First, the current eastern seasonal visibility trends are quite evident. Summer corresponds to the lowest visibility, while the winter months have better visibility.

Second, long-term trends are also quite evident. In the winter season, there has been some improvement in visibility in New England and the

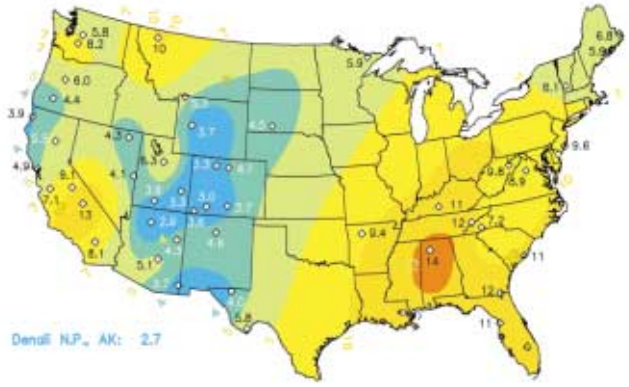

(a)

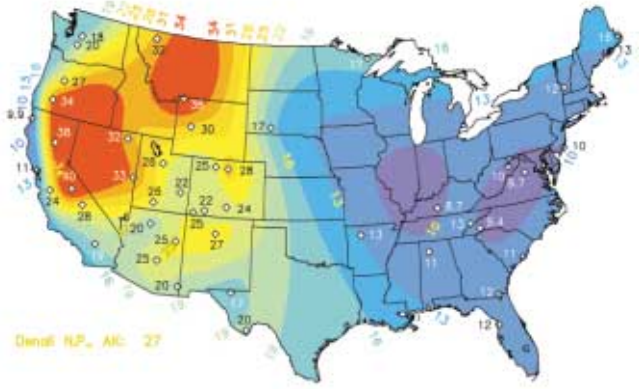

(b)

Fig. 6.10 Map (a) shows extinction, expressed in terms of inverse megameters, attributed to organic carbon, while (b) shows the percent contribution of organic carbon to total extinction.

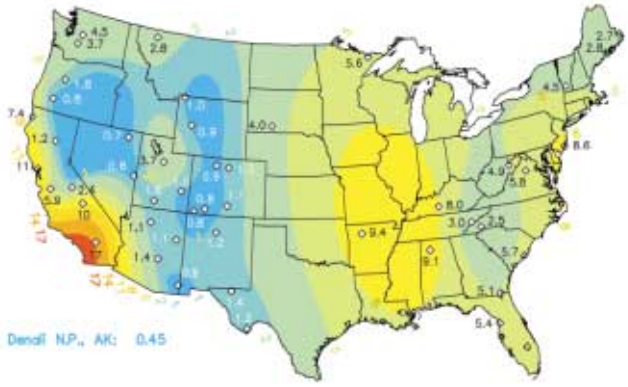

(a)

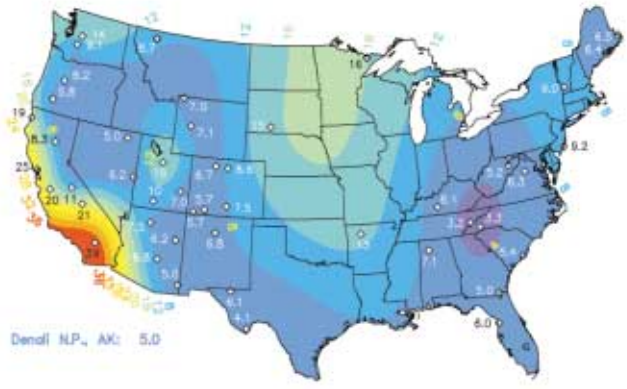

(b)

Fig. 6.11 Map (a) shows extinction, expressed in terms of inverse megameters, attributed to nitrates, while (b) shows the percent contribution of nitrates to total extinction.

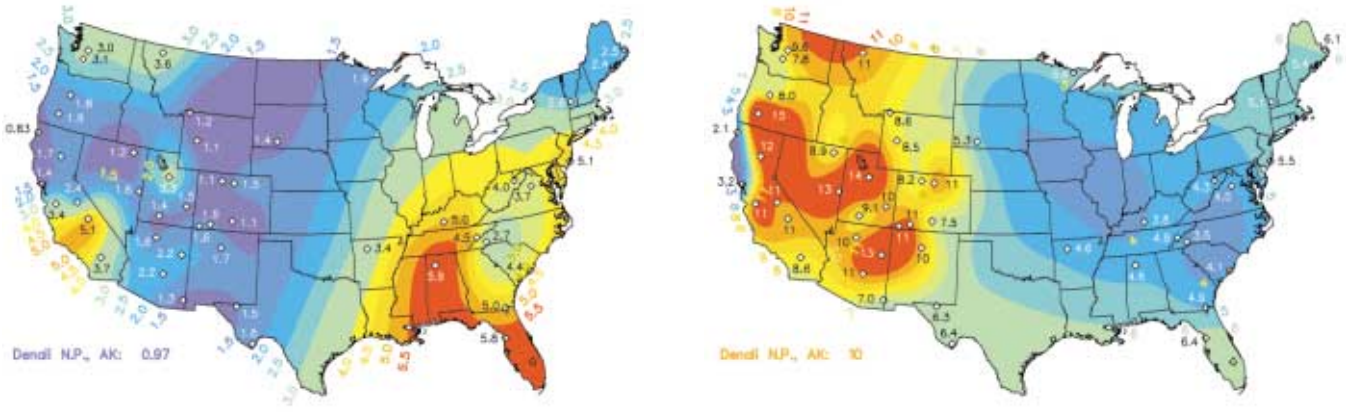

(a) *(b)*

Fig. 6.12 Map (a) shows extinction, expressed in terms of inverse megameters, attributed to light-absorbing carbon, while (b) shows the percent contribution of light-absorbing carbon to total extinction.

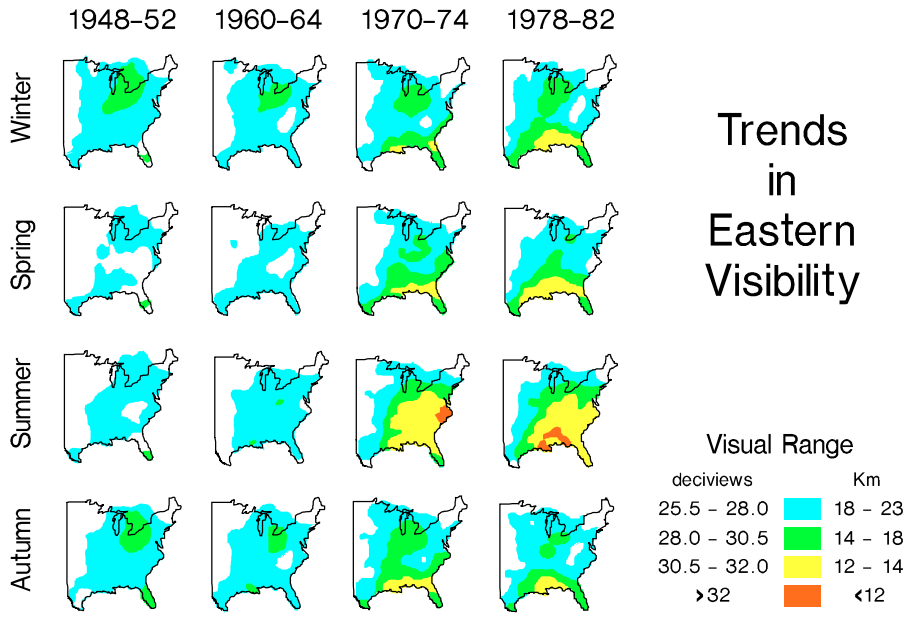

Fig. 6.13 Trends in median visual range over the eastern United States from 1948 through 1982.

north central United States from 1948-1952 and 1960-1964. However, since 1970 the winter season has shown decreased visibility, especially in the Southeast. The spring season shows a degradation of visibility in the entire eastern United States, especially along the gulf coast and the south and central east coast. The most dramatic changes, however, are evident during the summer months. A region of modest visibility in the eastern United States during 1948-1952 steadily expanded and became worse until the entire eastern United States and southeastern Canada were significantly degraded. The fall season shows significant improvement in the north central industrial areas from 1970-1974 and 1978-1982.

6.3.2 Western United States

Airport visibility data have also been examined for trends in visual air quality in the Rocky Mountains southwest over the time period from 1948 to 1976. Results suggest that in the late 1940's to the early/mid 1950's, visibility trends were mixed, with some geographic areas showing a slight improvement, and a lesser number of areas showing a slight deterioration. From the early/mid 1950's (1953-1955) to the early 1970's (1970-1972), most areas indicated a drop in visibility of approximately 10 to 30%. From the early 1970's (1970-1972) to the middle 1970's (1974-1976),

visibility generally tended to increase by about 5-10%, especially at those sites in or near Arizona.

Airport data at 67 sites in California were also examined. Plots of long-term trends in median visibility (for all data with no sorting for meteorology) at the study sites reveal that visibility trends in California tend to split into two general sub-periods, divided at approximately 1966. Before 1966, nearly all locations exhibited deteriorating visibility, with especially large visibility decreases occurring in and near central California (Central Valley). After 1966, nearly all locations have displayed improving visibility.

Other trend analyses using California airport data centered on "adverse" and "superior" visibility. "Adverse" visibility refers to those days that have concentrations of visibility-reducing particles sufficient to reduce prevailing visibility to less than 10 miles when the relative humidity is less than 70%. Visibilities that are 30 miles or more are termed "superior." The trend of the composite superior visibility for two pristine stations, Mount Shasta and Bishop, California, shows a gradual (about 1% per decade) decrease in average superior visibility occurrences.

6.4 Historical Relationships Between SO_2 Emissions and Visibility

Dominant relationships between smelter SO_2 emissions and visibility have been shown to exist in the southwestern United States. Figure 6.14 shows time plots from 1949 to 1976 of the percent of hours in one year that Phoenix and Tucson, Arizona, have visibility below 40 and 60 miles, respectively, and Arizona smelter SO_2 emissions in tons per day. The correlation between these two variables is 0.81 at Phoenix and 0.88 at Tucson.

Trends between smelter SO_2 emissions and elemental sulfur concentrations (presumably

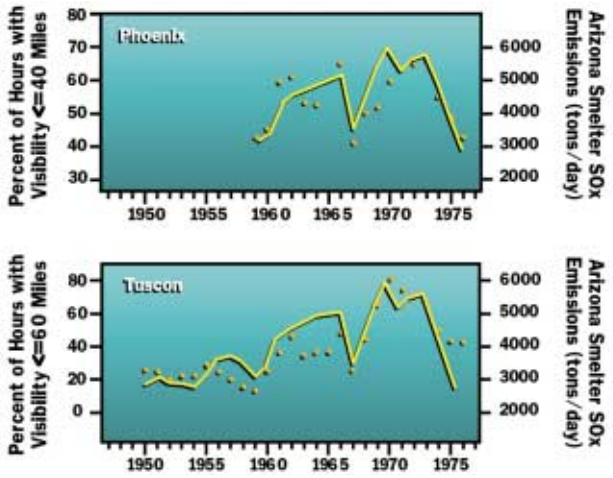

Fig. 6.14 Historical trends in percent of hours of reduced visibility at Phoenix and Tucson, compared to trends in SO_2 emissions from Arizona copper smelters.

ammonium sulfate) were examined in seven national park units: Chiricahua National Monument, Tonto National Monument, Grand Canyon National Park, Chaco Culture National Historic Park, Mesa Verde National Park, Bryce Canyon National Park, and Canyonlands National Park.

Figure 6.15 shows a scatter plot of 1980-1981 smelter sulfur dioxide emissions and sulfur concentrations for Grand Canyon and Chiricahua. There is a clear relationship between sulfur dioxide emissions and sulfur concentrations at both parks with the relationship being strongest at Chiricahua, which is located in the smelter country of southern Arizona and weaker at Grand Canyon, which is 300 km distant.

Furthermore, SO_2 emission data and visibility trend data were compiled for the eastern United States. The emissions are expressed as million tons of sulfur/year, and visibility is expressed as deciviews. Figures 6.16a and 6.16b show the sulfur emission trends for the southeastern United States for winter and summer months. Figures 6.16c and 6.16d show the same trends for the

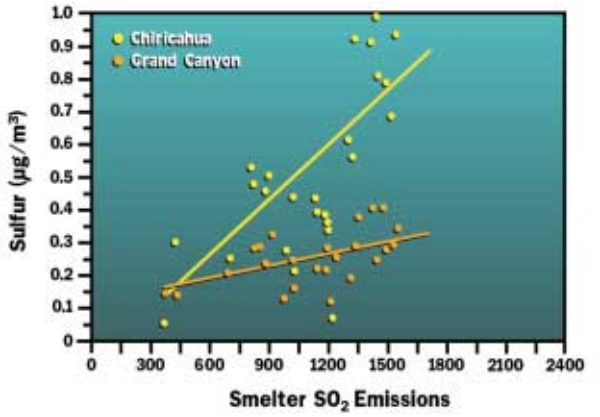

Fig. 6.15 Scatter plot of de-seasonalized sulfur concentrations ($\mu g/m^3$) vs. smelter emissions (tons/day) for monthly data at Hopi Point in Grand Canyon National Park and Chiricahua National Monument.

northeastern United States. The collinearity between SO_2 emissions and visibility reduction is impressive. However, it is apparent that the deciview change per incremental change in SO_2 emissions is significantly higher in the Southeast than Northeast. Possible explanations may be that the Southeast has higher SO_2 oxidation rates, higher humidity, and more stagnant air masses, or other emissions may be collinear with SO_2 emissions.

These data show that trends in sulfur dioxide emissions provide a plausible explanation for variability observed in regional visibility and sulfate concentration variations.

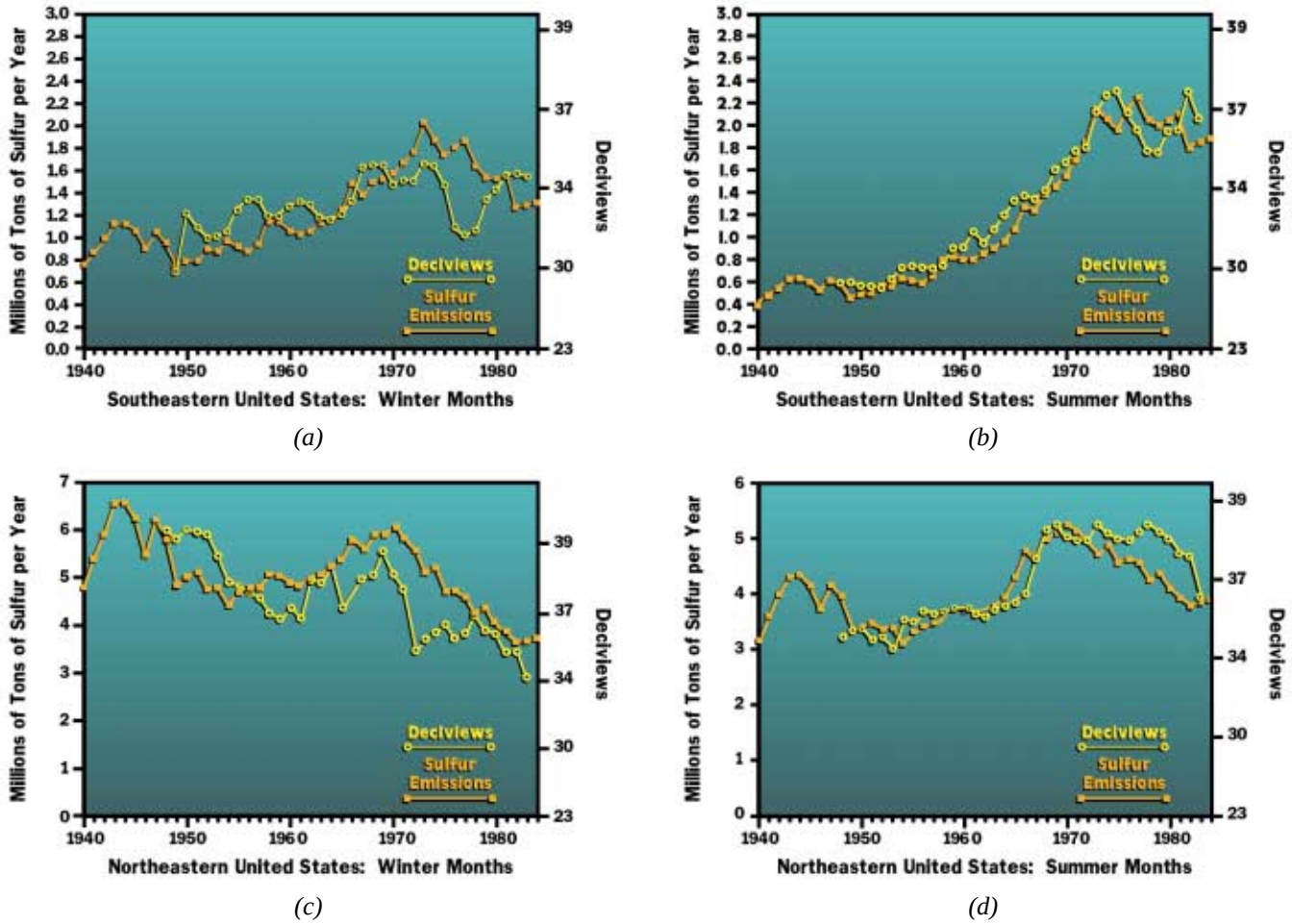

Fig. 6.16 (a) Comparison of sulfur emission trends and deciviews for the southeastern United States during the winter months. (b) Comparison of sulfur emission trends and deciviews for the southeastern United States during the summer months. (c) Comparison of sulfur emission trends and deciviews for the northeastern United States during the winter months. (d) Comparison of sulfur emission trends and deciviews for the northeastern United States during the summer months.

SECTION 7

IDENTIFICATION OF SOURCES CONTRIBUTING TO VISIBILITY IMPAIRMENT

Because the goal of identifying the particles affecting visibility is to reduce their concentration and thereby improve the seeing of landscape features, it becomes necessary to identify the sources emitting the precursor pollutants that form visibility reducing particles. There are generally two ways to go about this. One can formulate a model that mimics all those processes outlined in Figures 4.7 and 4.8. The model must predict transport of gases such as sulfur dioxide, nitrogen dioxide, and reactive hydrocarbons, convert them into secondary particles, deposit them as wet and dry deposition, and form estimates of size and composition of concentrations that affect visibility. Since the model will only be as accurate as the emission estimates that are input into the model, it is crucial to develop an accurate emission inventory. These types of models are referred to as deterministic or first-principle source-oriented models. They tend to capture only broad-scale temporal and spatial characteristics of haze formation and are computer intensive.

Diagnostic receptor-oriented models have evolved as a clear alternative to source-oriented dispersion models. Receptor models start with the measurement of specific features of the aerosol at the receptor, and use these features to develop estimates of aerosol contributions of specific source types and/or source location.

In the most general sense, geographic regions with high emissions will have high particle loadings. For instance, high sulfur dioxide emissions will be associated with high ambient sulfate concentrations and sulfate deposition, and conversely low emissions will correlate with low ambient concentrations. In North America, about 27% of emitted sulfur dioxide is dry deposited, 34% wet deposited, and 39% remains in the atmosphere and is eventually exported from the continent primarily to the Atlantic Ocean. Figure 7.1 shows the emission rates, in millions of tons per year, for sulfur dioxide, nitrogen oxides, and volatile hydrocarbon gases for five major source categories for the United States, and for comparison, Canada. Notice that the single largest source of sulfur dioxide is the electric utility industry (coal-fired power plants), while sources of nitrogen oxides are nearly evenly split between the electric utility industry and transportation. Most hydrocarbon gases are emitted by transportation sources.

The geographical distribution of those emissions is summarized in Figure 7.2 for ten different regions of the country. It is worth noting that the worst visibility occurs in the East. It is associated primarily with sulfate particles since 84% of the sulfur dioxide emissions are in the East. Nitrogen oxide and hydrocarbon emissions are more evenly split between the East and West with about a 60-40 split, with the East having the highest emissions.

The exercising of models helps to further identify or fine tune source-receptor relationships. A discussion or review of the many modeling activities that have been carried out over just the last ten or so years is beyond the scope of this discussion. However, some general and insightful relationships have been established using statistical treatments of back trajectory models.

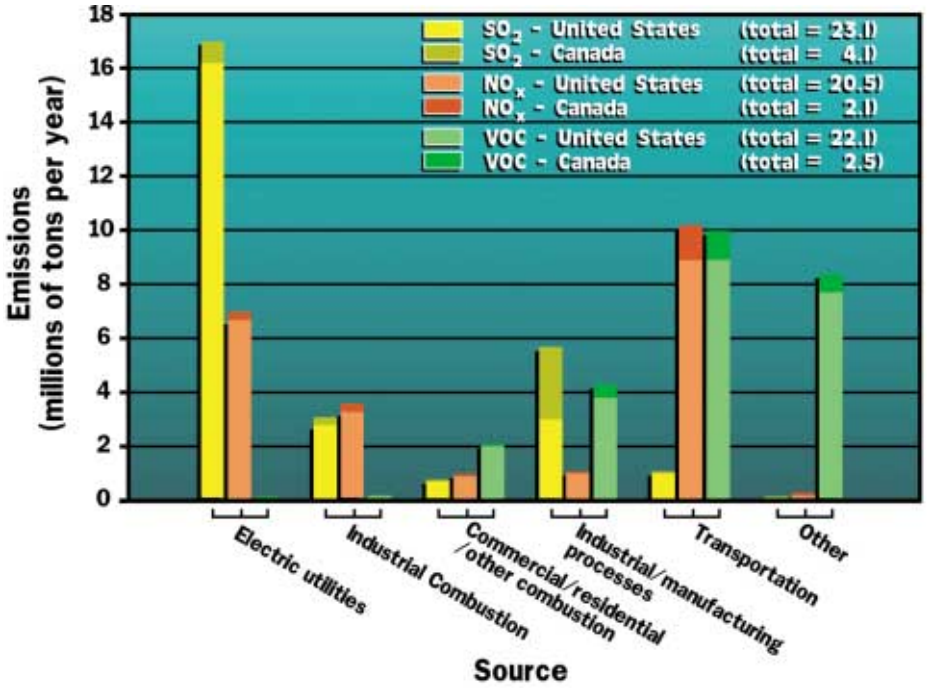

Fig. 7.1 Emission rates, in millions of tons per year, for sulfur dioxide (SO_2), nitrogen oxides (NO_x), and volatile organic carbon (VOC) gases for five major source categories for the United States and Canada.

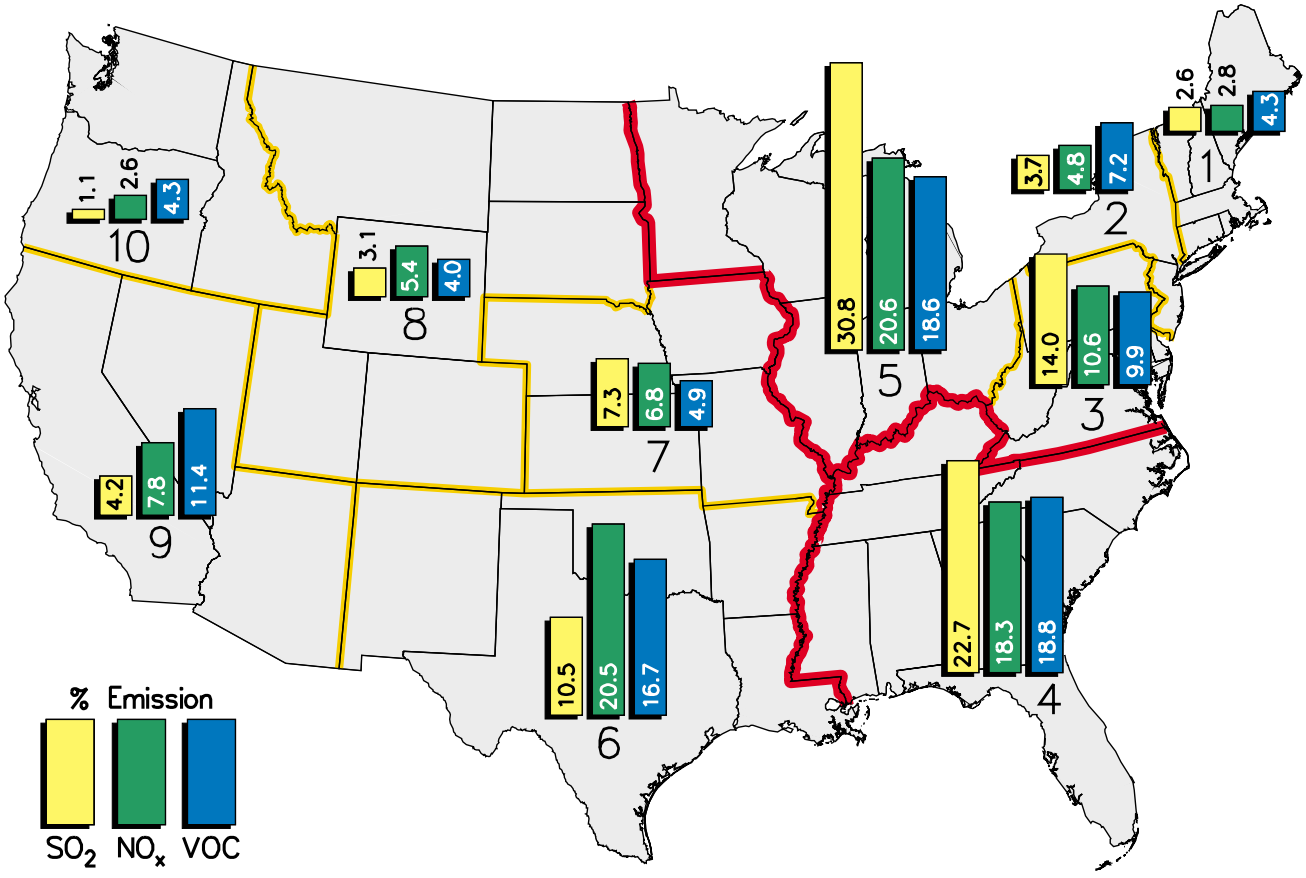

Fig. 7.2 Geographical distribution of sulfur dioxide (SO_2), nitrogen oxides (NO_x), and volatile organic carbon (VOC) gas emissions.

7.1 Back Trajectory Receptor Models

Two receptor modeling approaches that incorporate statistical treatments of air mass back trajectories serve to identify geographic regions with high emissions, and allow for apportionment estimates of secondary aerosols to general source areas and, therefore, in some cases, the source itself.

Back trajectory techniques have been applied quite successfully in all parts of the United States. A back trajectory is just a trace of where an air mass has been in some past-time increment. In the summary of back trajectory results presented here, a one layer model that relies solely on national weather service soundings was used. As such, it is not sensitive to terrain induced flow such as drainage of emissions down canyons and valleys. Therefore, this model tends to be more accurate when the atmosphere is well mixed in the vertical direction. These conditions are most often found during summer months. Furthermore, most trajectory analyses have focused on sulfur-related species, not because the analysis can not be carried out for other particle types, but because most sulfur particles are man-made and because they usually constitute a major fraction of the visibility reducing fine particle mass. Therefore, the following presentation will be directed toward presenting some of the information learned about the origins of fine particle sulfur.

Figures 7.3 through 7.11 are isopleth plots of the source contribution function (SCF) and, in some cases, conditional probabilities (CP) for "extreme" sulfur concentrations at Mount Rainier, Glacier, Grand Canyon, and Rocky Mountain National Parks, Chiricahua National Monument, and Big Bend and Shenandoah National Parks. Extreme refers to those concentrations that are greater than one standard deviation above the mean. The methodologies calculating these functions will be briefly reviewed here.

The geographic domain of interest is subdivided into one-by-one-degree grid cells. Then the number of back trajectory endpoints residing over each grid cell is counted for the sampling period and characteristic of interest. (A back trajectory endpoint is the geographic location of a back trajectory at some prespecified time interval.) Although aerosol samples with any characteristic could be used, the discussion here will be associated with aerosol samples that correspond to extreme sulfur concentrations. The spatial distribution of the number of endpoints in each grid cell is referred to as the residence time surface. If an SO_2 source area is responsible for high sulfate concentration at a receptor site, one might hypothesize that more trajectory endpoints will be found over that source area when sulfur concentrations are highest at the monitoring site. However, because all back trajectories originate at the receptor site, the number of endpoints will always increase as one moves toward the receptor location. This central tendency can be normalized out in a number of different ways.

The source contribution function surface reflects one method of normalization. It is calculated by dividing the residence time surface corresponding to extreme sulfur concentrations by the residence time surface corresponding to back trajectories departing from the receptor site in any direction with equal probability but with some average wind speed. Therefore, each isopleth line on the source contribution function contour plots in Figures 7.3 through 7.10 corresponds to those grid areas that are associated with equal probability of contributing extreme sulfur concentrations at the receptor site. The number associated with each SCF isopleth line is a relative probability that each grid area along the isopleth line will contribute to extreme sulfur contributions at the receptor site relative to any other contour line. For instance, grid areas along the line labeled 100 are 5 times as likely to contribute to high sulfur as along the contour line labeled 20. Since the contour lines are relative probabilities, they are dimensionless. The source contribution plots give an estimation of the location of those sources most likely to contribute to extreme sulfur concentration at a receptor site.

A second way of normalizing the residence time surface gives an indication not of the most likely origin of sources contributing to extreme sulfur concentrations, but rather the likelihood of an area to contribute to extreme sulfur concentrations given the condition that the air mass had actually passed over the source area. This conditional probability surface is obtained by dividing the residence time surface corresponding to extreme sulfur concentrations by the residence time surface for all sampling periods. This is referred to as the conditional probability surface. The numbers associated with each conditional probability contour in Figures 7.3 through 7.10 indicate the probability of air masses, having passed over a grid cell, to contribute to extreme sulfur concentrations at the receptor site.

It is possible for a region of the country to be associated with a low source contribution function, while at the same time having a high conditional probability. For instance, Figures 7.3a and 7.3b are the source contribution function and conditional probability surfaces for Mount Rainier National Park. Figure 7.3a shows that sources associated with extreme sulfur concentrations at Mount Rainier originate from a source region to the northwest. However, the front range of the Canadian Rocky Mountains (Alberta) has the highest probability of contributing to extreme sulfur concentration if the air mass actually passes over that region and arrives at Mount Rainier.

Figures 7.4a and 7.4b indicate the extreme sulfur source contribution and conditional probability surfaces for Glacier National Park. Most of the elevated sulfur days in Glacier are associated with source areas in eastern Washington and southwestern Idaho. More interesting, however, is the conditional probability surface which, like the conditional probability surface for Mount Rainier, identifies the front range of the Canadian Rocky Mountains as a source area associated with extreme sulfur at Glacier. Canadian sources north of the Dakotas, and possible sources in Minnesota, also contribute to extreme sulfate concentrations in Glacier.

The source contribution surfaces for Grand Canyon and Rocky Mountain National Parks are shown in Figures 7.5a and 7.6. Both parks show southern California, a source area hundreds of kilometers distant, to be the most probable source area associated with extreme sulfate concentrations at these parks. On the other hand, Figure 7.7, the source contribution function surface for Chiricahua National Monument, shows the nearby southern Arizona copper smelter region to be the most probable source of extreme sulfate, with southern California and an area along the Texas-

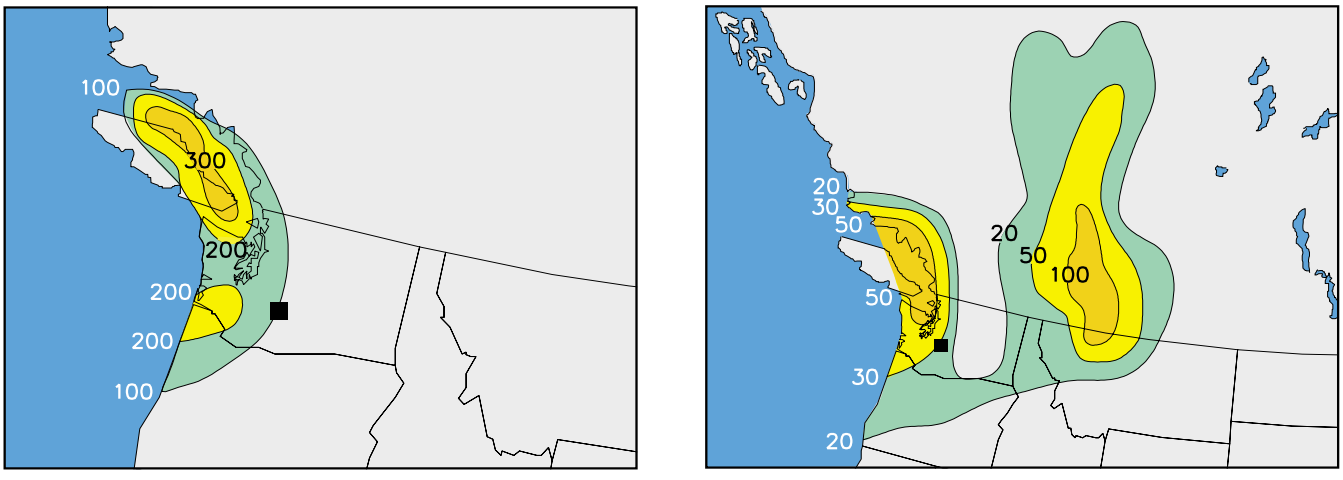

(a) *(b)*

Fig. 7.3 (a) Extreme fine sulfur concentration source contribution, Mount Rainier National Park. (b) Extreme fine sulfur concentration conditional probability, Mount Rainier National Park.

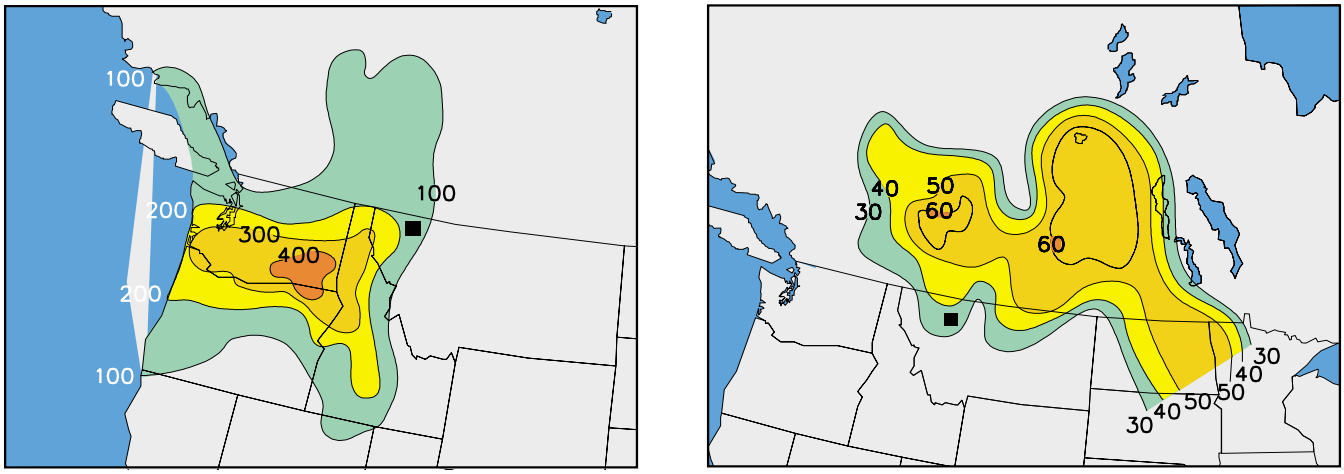

(a) *(b)*

Fig. 7.4 (a) Extreme fine sulfur concentration source contribution, Glacier National Park. (b) Extreme fine sulfur concentration probability, Glacier National Park.

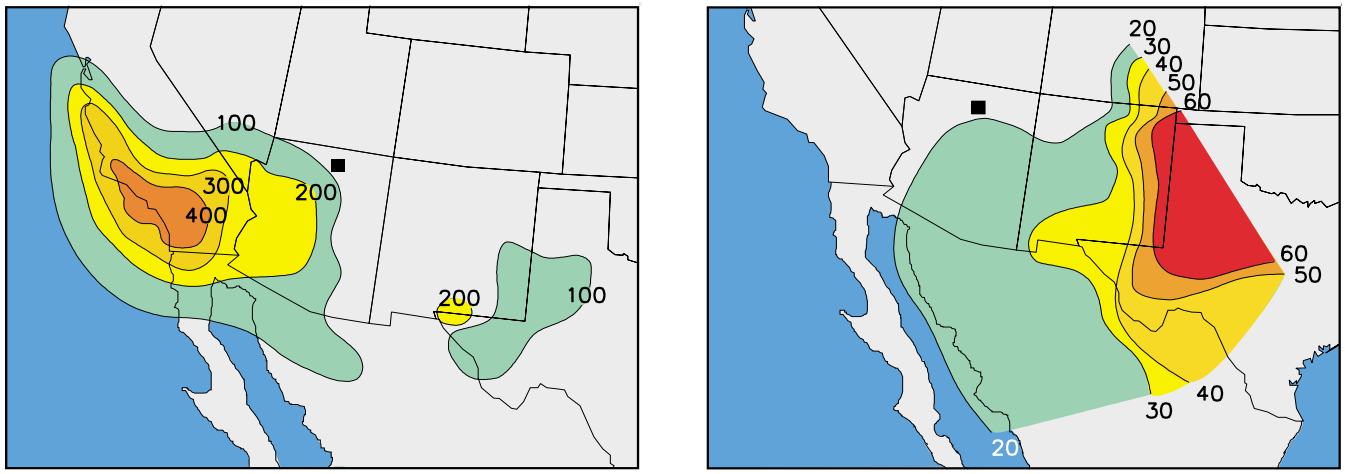

(a) *(b)*

Fig. 7.5 (a) Extreme fine sulfur concentration source contribution, Grand Canyon National Park. (b) Extreme fine sulfur concentration probability, Grand Canyon National Park.

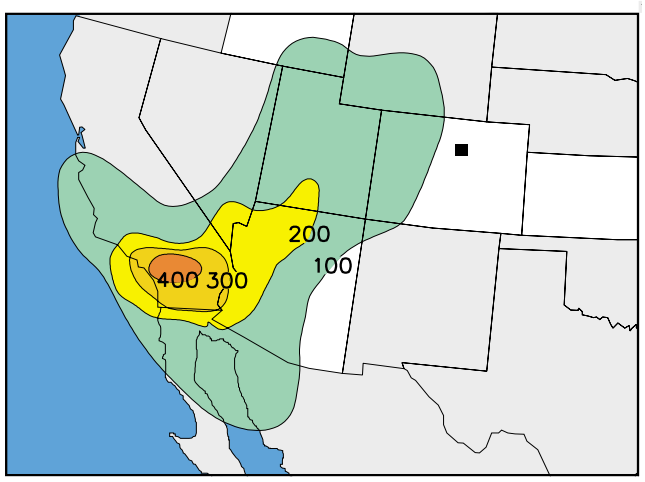

Fig. 7.6 Extreme fine sulfur concentration source contribution, Rocky Mountain National Park.

Mexico border being the second most probable sources of sulfates. The Big Bend National Park source contribution function surface (Figure 7.8) seems to confirm the sulfate source area along the Texas-Mexico border. This area has the highest probability of contributing extreme sulfur to Big Bend. The conditional probability surfaces for all four parks are similar. Figure 7.5b, the conditional probability surface for Grand Canyon National Park, shows that air masses arriving from the east have the greatest probability of being associated with extreme sulfur concentrations.

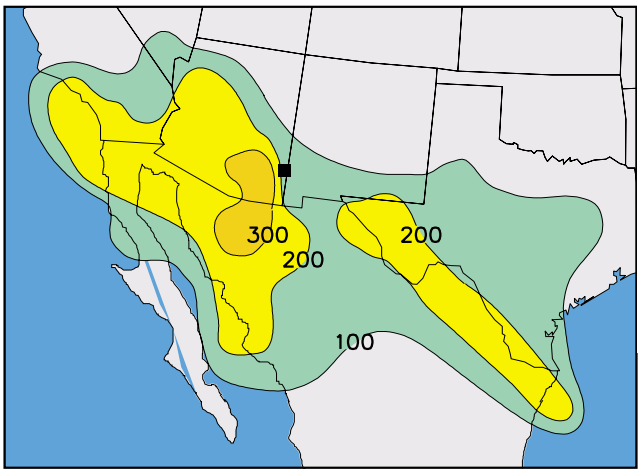

Fig. 7.7 Extreme fine sulfur concentration source contribution, Chiricahua National Monument.

Figure 7.9 shows that the air masses passing over the Ohio River Valley are most likely to contribute to extreme sulfur concentrations at Shenandoah National Park. The air masses passing over the source areas around Detroit and Chicago are the second most likely to contribute sulfur laden air to Shenandoah. The conditional probability surface for Shenandoah is similar to Figure 7.9. However, additional source areas show up along the Northeast coast. The source area in the Ohio River Valley has a large number of coal-fired power plants that emit sulfur dioxide.

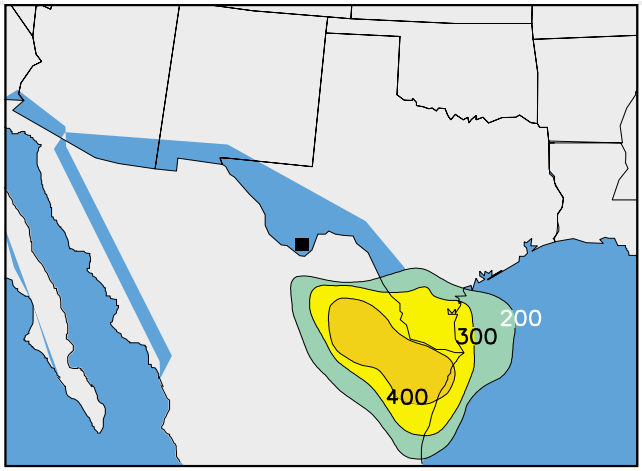

Fig. 7.8 Extreme fine sulfur concentration source contribution, Big Bend National Park.

A similar analysis can be carried out to show the origins of air masses that are associated with sulfur concentrations lower than one standard deviation below the mean. Figure 7.10a shows the conditional probability surface map for low sulfur concentrations for Grand Canyon National Park. Notice that only air masses arriving from the north are associated with low sulfur concentrations. In general, similar maps for other national parks show the Great Basin region associated with low sulfur concentrations. Figure 7.10b, a low sulfur conditional probability surface map for Mount Rainier, shows that air mass arriving from east of the Cascades but west of the

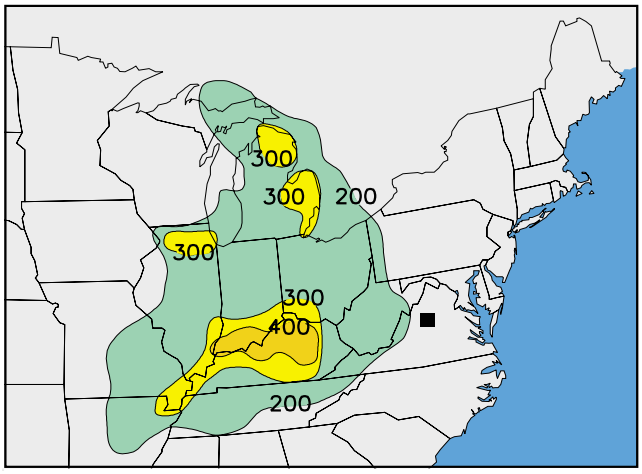

Fig. 7.9 Extreme fine sulfur concentration source contribution, Shenandoah National Park.

Rocky Mountains, and from northern California and southern Oregon, are associated with low sulfur concentrations.

Source contribution function and conditional probability surface analysis has been carried out for all National Park Service monitoring sites, and similar source areas show up for many areas, but with varying probabilities of impacting specific receptor sites. By comparing maps like those in Figures 7.3 through 7.10, it is possible to begin to understand the geographic extent to which sources affect various parts of the country.

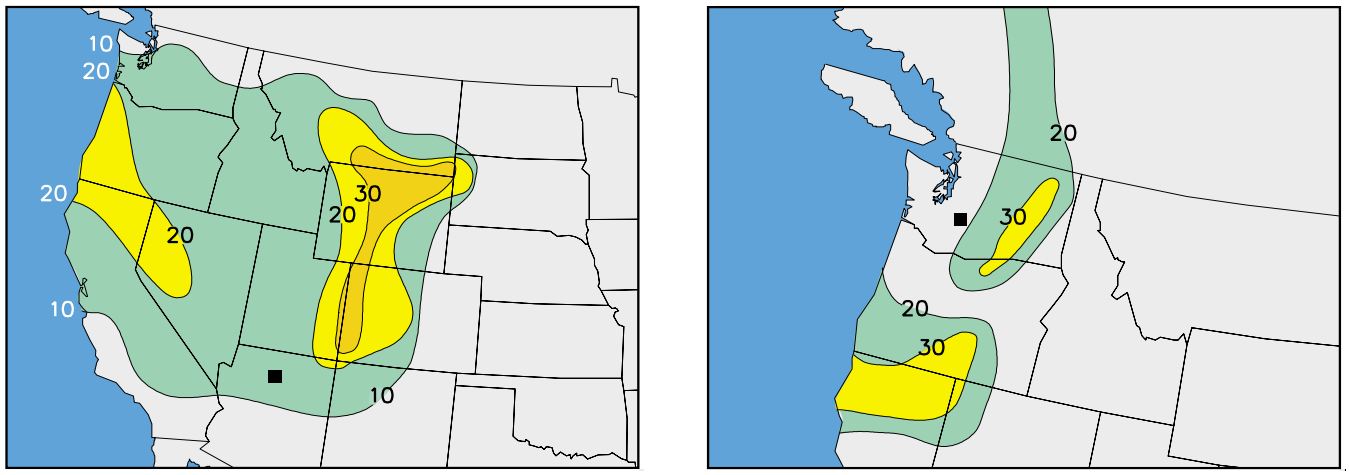

(a) *(b)*

Fig. 7.10 (a) Low fine sulfur concentration conditional probability, Grand Canyon National Park. (b) Low fine sulfur concentration conditional probability, Mount Rainier National Park.

However, comparison of a number of source contribution function surface figures is difficult and sometimes confusing. The source contribution function analysis can be modified to show the geographic extent of a single source area, rather than various sources impacting a single receptor site. To do this, the relative probability of a single source area at each of the receptor sites is contoured.

Figures 7.11a through 7.11e show the geographic extent to which emissions from four source areas contribute to high sulfate concentrations. The first area (Figure 7.11a), southern California, has its highest probability of impact in the Mohave Desert and Colorado Plateau, an area containing a number of national parks, such as Grand Canyon, Canyonlands, Arches, and Bryce Canyon. The graph also shows that southwestern California has a reasonably high probability of impacting areas as far north as Wind Cave National Park, South Dakota, Grand Teton National Park, Wyoming, and Craters of the Moon National Monument, Idaho. Figure 7.11b shows the extent to which copper smelter emissions contribute to elevated sulfate. The geographic area associated with the highest probability source contribution function extends from southern Arizona along the Arizona-New Mexico border, central Colorado, western Nebraska and southwestern South Dakota. Figure 7.11c shows that emissions from the industrial area near Monterrey, Mexico affect Big Bend and Guadalupe Mountains National Parks and as far north as Grand Canyon National Park. The source area associated with the uncontrolled Navajo Generating Station, a large, coal-fired power plant, contributes to extreme sulfate concentration throughout the central Rocky Mountains, southern Idaho, and Arizona (see Figure 7.11d). Finally, Figure 7.11e shows that sources around the Salt Lake City area have their largest impact on southern Idaho, but can be detected as far south as Grand Canyon.

7.2 Trajectory Apportionment Model

The previously described techniques identify source areas and the geographic extent to which these source areas contribute to extreme sulfur. These techniques do not allow for estimation of the fraction of sulfur contributed by each of the sources. However, a source receptor model utilizing trajectory endpoints in conjunction with known source areas approximates the relative contribution of different source areas to aerosol concentrations at receptor sites. The technique uses statistical models to relate the number of

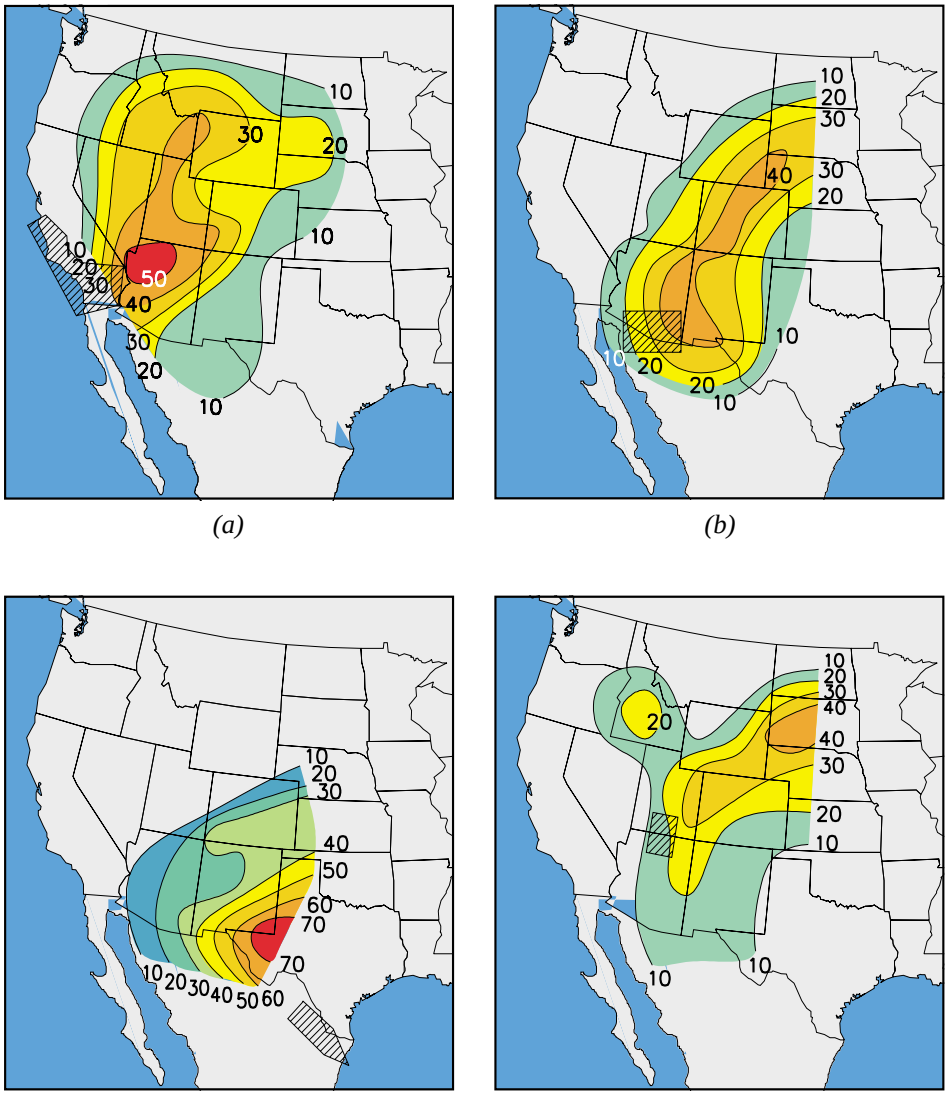

Fig. 7.11 Plots of constant source contribution function lines for (a) southern California, (b) southern Arizona copper smelter region, (c) Monterrey, Mexico region, (d) Navajo Generating Station, (e) northern Utah, Salt Lake City, and surrounding area.

back trajectory endpoints over source areas to sulfur concentrations at the receptor site as a function of time. The following discussion pertains to an analysis using data and emission inventories developed previous to 1991.

Figures 7.12a-f show relative contribution of various source areas to measured sulfur concentrations at a number of national parks. Relative source contributions were calculated for Mount Rainier, Grand Canyon, and Big Bend National Parks in the West, and at Acadia, Shenandoah, and Great Smoky Mountains National Parks in the East.

At Mount Rainier (see Figure 7.12a), sources on Vancouver Island, in western British Columbia, and in the Puget Sound area are estimated to contribute approximately 35% of the ambient sulfur, while sources in northern Washington are estimated to contribute 30% of ambient sulfur. The source regions north of Mount Rainier do not contain a single large source of SO_2, but a rather large number of smaller sources. These sources include industrial boilers, some mining and smelting activity, and pulp and

paper mill operations. The Pacific Power source region, which is estimated to contribute 34% of measured sulfur, includes the Centralia coal-fired power plant, which has SO_2 emissions in excess of 65,000 tons per year. Sources to the south of Mount Rainier are estimated to contribute less than 2% of ambient sulfur.

At Grand Canyon (see Figure 7.12b), sources in California contribute about 33% of measured sulfur at Grand Canyon, while southern Arizona accounts for 14%. California SO_2 sources consist of oil refining activities, electric generating facilities, and in Los Angeles, automobile and diesel emissions. The southern Arizona SO_2 sources are primarily associated with copper smelter activities. Other large sources of SO_2 contributing to sulfur at Grand Canyon (23%) are the Mohave, Reid Gardner, and Navajo Power Plants. Sources in Utah are estimated to contribute approximately 12% of measured sulfur, while other sources, including coal-fired power plants, some smelting activity in southeastern New Mexico, and the El Paso, Texas area, are estimated to contribute about 18%.

At Big Bend, (see Figure 7.12c), it is estimated that about 41% of the ambient sulfur is associated with emissions in the Monterrey, Mexico area, and about 29% from central Mexico. Thus, about 70% of the sulfur found at Big Bend has its origin in Mexico. It is not known what types of sources are responsible for the SO_2 emissions.

The source area contributing the most sulfur, 29%, to Acadia is the area around Sudbury, Canada (see Figure 7.12d). The nickel smelter operations at Sudbury emit approximately 700,000 tons of SO_2 per year during the time period this analysis was conducted. Coal-fired power plants in the New York-Philadelphia area are estimated to contribute approximately 15%, while power plants in northern New York contribute 24%. SO_2 sources in the Midwest, primarily Michigan, contribute approximately another 20% to the sulfur measured at Acadia.

About 30% of the sulfur measured at Shenandoah is from power plants in the Pittsburgh-Cleveland area (see Figure 7.12e). This source area contains the Environmental Protection Agency air quality control regions with the highest SO_2 annual average emission rates in the United States. Coal-fired power plants in that region emit over 3 million tons of SO_2 per year. The coal-fired power plants in the Columbus-Dayton-Cincinnati region contribute another 12% of sulfur at Shenandoah. Together, these two geographic areas, usually referred to as the Ohio River Valley, contribute 42% of the ambient sulfur at Shenandoah. Another dominant source area for Shenandoah, labeled as Piedmont-northern Tennessee, contributes 16% of ambient sulfur. These emissions are again associated with large coal-fired power plants. Coal-fired power plants in the Southeast contribute another 23% to the measured sulfur.

For Great Smoky Mountains (see Figure 7.12f), more than 35% of the sulfur is estimated to arrive from the Ohio River Valley region. Other dominant source regions are both areas containing large coal-fired power plants: Tennessee Valley Authority (western TVA and Piedmont) and Memphis regions contribute about 17%, while sources along the Gulf Coast's contribution to sulfur contribute more than 10%.

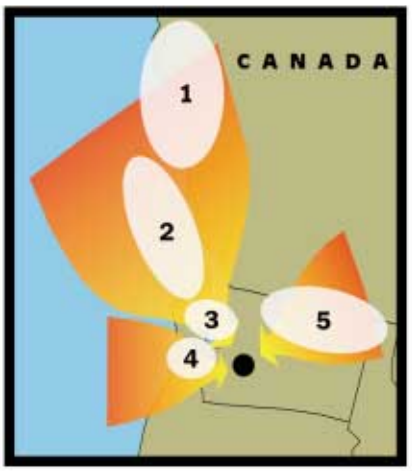

1. Western British Columbia: 5%
2. Vancouver Isle: 6%
3. Puget Sound: 24%
4. Westerly Transport: 34%
5. North Washington: 30%
6. Other Sources: 1%

(a)

1. San Joaquin: 6%
2. Southern California: 20%
3. Baja California: 7%
4. Near Canyon Sources: 23%
5. Northeasterly Transport: 12%
6. Southern Arizona: 14%
7. Other Sources: 18%

(b)

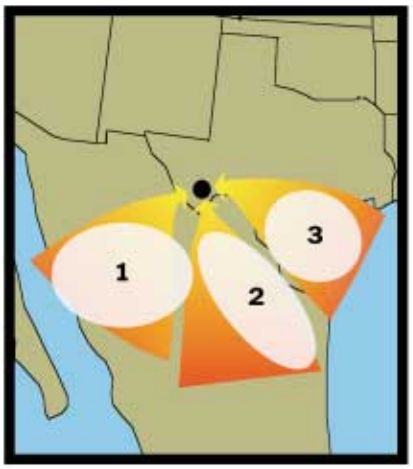

1. Central Mexico: 29%
2. Monterrey and further south: 41%
3. Houston and other Gulf Coast sources: 5%
4. Other Sources: 25%

(c)

1. Sudbury: 29%
2. Central Michigan: 9%
3. Chicago: 5%
4. Toledo: 5%
5. Northern New York: 24%
6. New York City & Philadelphia: 15%
7. Other Sources: 13%

(d)

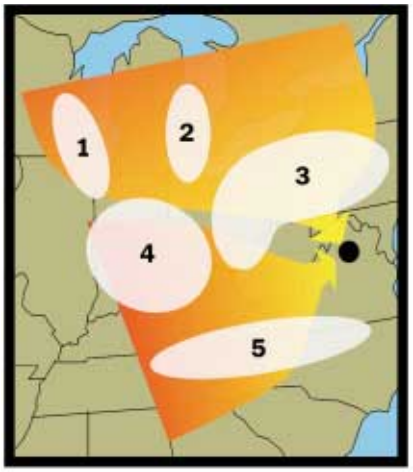

1. Chicago: 5%
2. Detroit & Toledo: 6%
3. Pittsburgh & Cleveland: 30%
4. Columbus, Dayton, & Cincinnati: 12%
5. Piedmont & N. Tennessee: 16%
6. Other Sources: 31%

(e)

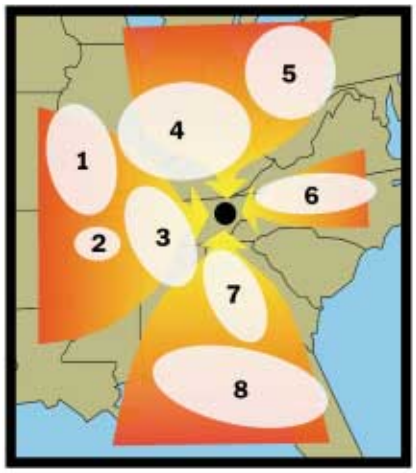

1. St. Louis Area: 6%
2. Memphis TVA: 8%
3. Western TVA: 9%
4. Columbus, Dayton, & Cincinnati: 28%
5. Pittsburgh & Cleveland: 9%
6. Piedmont & East Tennessee: 6%
7. Atlanta & Chattanooga: 7%
8. Florida: 6%
9. Other Sources: 21%

(f)

Fig. 7.12 Fraction of sulfate arriving at (a) Mount Rainier, (b) Grand Canyon, (c) Big Bend, (d) Acadia, (e) Shenandoah, and (f) Great Smoky Mountains National Parks, from various source regions.

SECTION 8

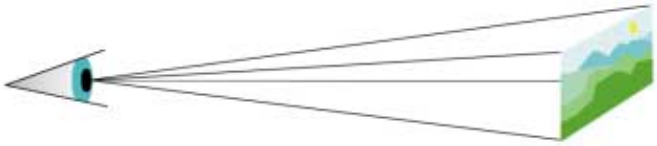

HUMAN PERCEPTION OF VISUAL AIR QUALITY

A major challenge in establishing visibility values is to develop ways of quantitatively measuring visibility impairment as perceived by the human eye. Quantification of visual impairment of a scenic resource requires two crucial components: 1) the establishment of the level of air pollution that is just noticeable, and 2) a determination of the functional relationship between air pollution and perceived visual air quality.

The first goal is important when it is necessary to quantitatively specify visible pollution under a given atmospheric condition. The second object is important when trying to assess the societal value of clear air, whether it be social, psychological, or economical. The first step in assessing value is to understand the relationship between perceived changes in visual air quality and an appropriate physical parameter, such as vista contrast or atmospheric extinction. For example, if a visitor is willing to pay $5.00 for a given decrease in atmospheric extinction (air pollution) at the Grand Canyon, but is unwilling to pay that same amount for a similar decrease at some other park, is it because a) that person values the scenic resource differently at the two parks, or b) the perceived change in visual air quality is different at the two parks? That is, at one park a given decrease in extinction can readily be seen, while at another that same decrease may go unnoticed.

Developing relationships between air pollution and visitor perception falls into two uniquely different categories. Air pollution can manifest itself either as layer or as uniform haze. Layered haze can be thought of as any confined layer of pollutants that results in a visible spectral discontinuity between that layer and its background (sky or landscape). Uniform haze exhibits itself as an overall reduction in air clarity. As discussed in Section 3, the classic example of a layered haze is a tight, vertically constrained, coherent plume (plume blight). However, as an atmosphere moves from a stable to unstable condition and a plume mixes with the surrounding atmosphere, the plume impact on visual air quality may manifest itself in an overall reduction in air clarity (uniform haze) rather than as a layer of haze.

The eye is much more sensitive to a sharp demarcation in brightness or color than it is to a gradual change in brightness or color, whether that change takes place in space or time. Layered haze falls into the first category, in that the layer of haze is observed at some specific time and against some background (sky or landscape element), while uniform haze falls into the second. Because changes in uniform haze usually take place over the course of hours or days, an evaluation of visual air quality change resulting from a uniform haze requires a person to “remember” what the scene looked like before a given change in air pollution took place. An evaluation of the impact a uniform haze has on visual air quality requires identification of those elements of the total vista that are deemed important to visitor experience. On the other hand, a layered haze, if visible, could constitute impairment regardless of background features.

It is also important to point out that judgments of visual air quality as a function of air pollution, whether manifest as layered or uniform haze, might be altered by variations in sun angle, cloud cover, or landscape features.

8.1 Perception Thresholds of Layered Haze (Plume Blight)

A first step to determining whether a plume with given size, shape, and contrast characteristics constitutes visibility impairment is to determine whether the plume can be detected. A Yes/No high threshold psychophysical procedure was used as the methodology to conduct laboratory experiments of plume perceptibility. The Yes/No method consists of randomly presenting subjects with stimuli, via computer generated photographic slides that show only the blue sky background, or show the background with the plume. The subjects' task is to indicate whether a plume could be seen in each of the presentations. Figure 8.1 depicts the physical layout of the testing room.

The projector was mounted on a platform 1.80 m high in a room adjacent to the back of the testing laboratory. It projected an image 0.87 m high x 1.31 m wide through an opening in the wall and onto a large screen mounted on the opposite wall 6.71 m away. Viewing chairs were located 4.80 m from the projected image and elevated on a platform 0.43 m high to allow subjects to view the images with a vertical offset and azimuth angle of approximately 0°. This configuration resulted in a projected image that subtended viewing angles of 10° vertically by 16° horizontally. The stimuli consisted of varying sizes of full length, oval, and circular plumes with Gaussian luminance distributions. In each case, the protocol for observer detection was the same for all experiments, the surround was kept at the same brightness, edge effects were dealt with uniformly, and stimuli representative of Gaussian plume brightness profiles were used.

Sixteen subjects participated in the full length plume experiment. The stimuli consisted of plumes with vertical angular sizes of 0.09, 0.18, 0.36, 0.72, 1.44, and 2.88° and a horizontal angular extent of 16.0°. Contrast values of 0.050, 0.040, 0.030, 0.020, 0.017, 0.015, 0.013, 0.011, and 0.005 were used for all sizes. Figure 8.2 shows the predicted probability of detection curves. As plume contrast increases the probability of detecting the plume increases. If a plume has a modulation contrast of greater than about 0.01, it will be detected nearly 100% of the time for all sizes. Furthermore, these curves show that the size of the plume is quite important! Plumes that subtend an angle of about 0.3° can be detected more easily than plumes that are larger or smaller. Results for the oval and circular plumes were similar.

Fig. 8.1 Configuration of the laboratory setup used to conduct the visual sensitivity experiment.

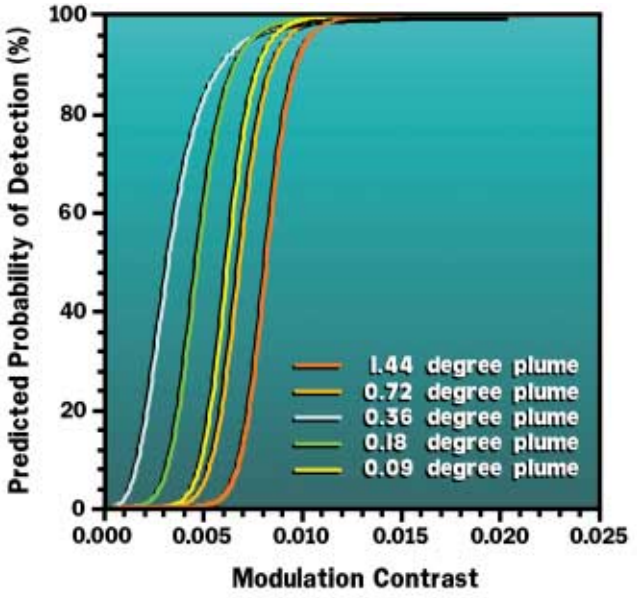

Fig. 8.2 Predicted probability of detection curves for one subject used in the full length plume study.

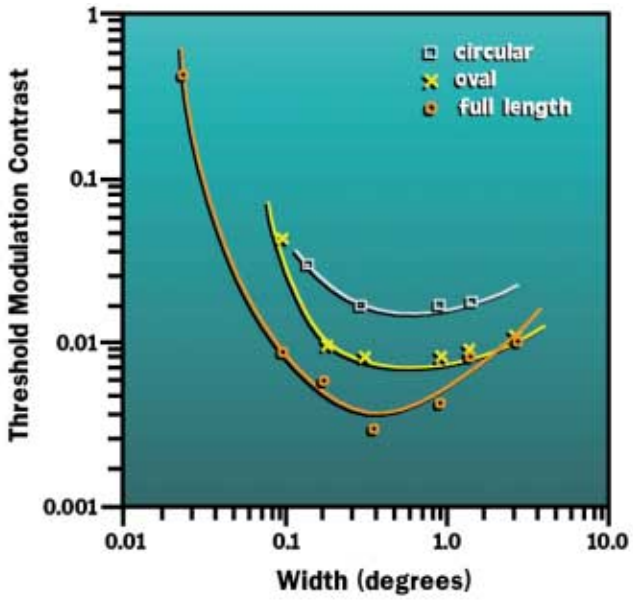

Fig. 8.3 Threshold modulation contrast plotted as a function of plume width in degrees for full length, oval, and circular plumes. The human observer is most sensitive to all plumes if they have a width of about 0.3°. Plumes larger or smaller than about 0.3° require increased contrast to be seen.

To more clearly see how the three shapes compared, the modulation contrast corresponding to 50% probability of detection for each shape is plotted against plume size in Figure 8.3. Notice that the general trend for all stimuli is the same, with plumes subtending about a 0.3° width being the easiest to detect. However, observers are most sensitive to full length plumes and least sensitive to circular stimuli, with the oval plumes being intermediate. The full length, oval, and circular plume contrast threshold data have been incorporated into a linear interpolation algorithm that allows plumes of any size to be estimated.

8.2 Perceived Visual Air Quality (PVAQ)

A good deal has been learned about the relationship between Perceived Visual Air Quality (PVAQ) and various visibility parameters for both layered and uniform haze. A number of studies have established relationships between PVAQ and various physical variables for vistas similar to those shown in the eight photographs of Figure 8.4. It would be ideal to find one variable that represents the same perceived change in air quality, whether the background atmosphere was clean or dirty, whether the vista was near or far, or whether the haze was layered or uniform.

To address these questions, a study was formulated that involved a visitor survey. Visitors to a number of national parks were asked to rate slides, on a scale of one (poor) to ten (good), that represented various levels of air quality. It was expected that sun angle, amount of snow cover, meteorological conditions, and other factors might affect ratings of visual air quality. Thus, a special effort was made to select slides that showed various air pollution levels under a number of atmospheric conditions. Specifically, a number of slides representing the best, worst, and intermediate levels of air quality were chosen to correspond to various cloud, snow cover, and sun angle conditions. These randomly ordered evaluation slides were preceded by ten preview slides

(a)

(b)

(c)

(d)

Fig. 8.4 Sample slides used to gauge public perception of visual air quality. Photographs (a) and (b) depict the 50 km distant La Sal Mountains as seen from Canyonlands National Park. Photograph (c) is of the 96 km distant Chuska Mountains as seen from Mesa Verde National Park. Photograph (d) is of a forest fire plume as seen from Grand Canyon National Park.

to orient the observers to the full range of visual air quality conditions.

Park visitors were approached and asked if they would like to participate in a study designed to evaluate visual air quality in national parks. If they concurred, the visitors were seated in a trailer and verbally instructed on how to rate the slides.

To determine the accuracy with which the observers used the rating scale, 15 identical control slides were mixed with evaluation slides. Calculations showed that if 50 ratings of the con-

(e)

(f)

(g)

trol slides were chosen at random from the total data set, the mean rating of different groups of 50 changed by less than 0.1 points, while the standard deviations varied by only 0.4. However, there is the possibility that, even though there may be some variability due to the observers' demographic backgrounds, a random selection would tend to average out the differences. Thus, an additional analysis involving the calculations of mean and standard deviations of the control slides as a function of demographic background determined that regardless of educational level, age, sex, or location of residence, individuals judged visual air quality essentially the same; means and standard deviations varied by as little as 0.3.

A most important result of these studies was the close agreement between on-site and slide ratings. Correlation between on-site and slide ratings was 0.94. In almost all cases, statistical tests indicated little significant

(h)

Fig. 8.4 (Continued). Photographs (e) and (f) are of Desert View (Grand Canyon National Park) as seen from Hopi Point. Photograph (g) is also taken from Hopi Point but in the opposite direction of Desert View. The distant mountain (96 km) is Mt. Trumbull. Photograph (h) is of the 50 km distant San Francisco Peaks as seen from Grand Canyon National Park.

difference between the window and slide ratings. These studies hence suggest that slides can serve as reasonable representations of actual scenes.

Notably, one simple relationship between vista contrast and PVAQ became apparent time and again. For example, one portion of the study used the photographs shown in Figures 8.5 and 8.6, i.e., two vistas under clear sky conditions but with various levels of air pollution. In Figure 8.5, a 50 km distant mountain range dominates the scenic vista, while in Figure 8.6, the distant mountain feature, which is the only scenic element that shows a visual effect from an increase in air pollution, takes up only 4% of the total scene. Yet when PVAQ, which is the average of the one-to-ten ratings assigned to each slide by the park visitors, is plotted against the contrast of the most distant scenic element, a straight line relationship results for either scene. This relationship is surprising for the second scene because the distant feature is quite small. A representative relationship of the change in PVAQ evoked by a given change in contrast is shown by the orange line in Figure 8.7.

Because visitors see a visual resource under a variety of atmospheric conditions it is important to determine the effect that cloud cover or changes in sun angle will have on the sensitivity of a vista to changes in contrast. Surprisingly, the answer is "None!" Figure 8.7 also shows how a PVAQ versus contrast curve changes when sun angle is changed or cloud cover is added. In both cases the overall ratings are higher but the slopes of the curves, representing the sensitivities, remain the same. The photographs of Figure 8.8 show the same two vistas under different sun angle conditions; the photographs of Figure 8.9 show the La Sal Mountains in the presence of cumulus clouds. When sun angle is changed, the foreground features are illuminated and their color enhanced. Changing either sun angle or cloud cover results in an increase in scenic beauty and thus an increase in the average PVAQ ratings. However, the sensitivity of the vista-to-contrast-change is

(a)

(b)

(c)

Fig. 8.5 The appearance of one Canyonlands National Park vista under various air quality levels. The distant (50 km) mountain range is the La Sal Mountains. Notice that the foreground features, because of the proximity to the observer and the bright color, show little change as air quality changes. Hatchett Peak goes from being very clear to almost disappearing. The sky-mountain contrast in (a) is -0.39, (b) is -0.26, and (c) is -0.23.

(a)

(b)

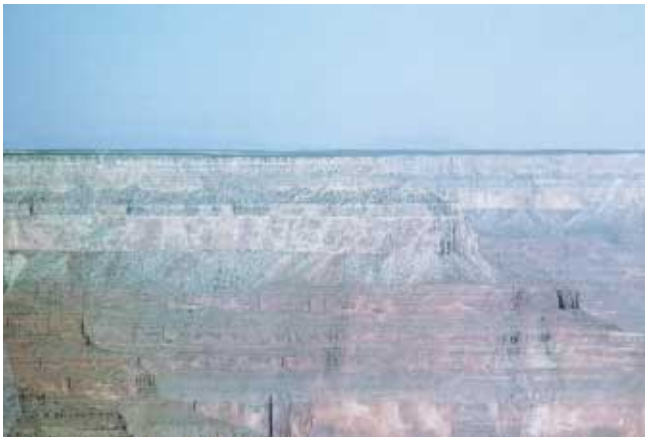

(c)

Fig. 8.6 Mt. Trumbull, 96 km distant, as seen from Grand Canyon National Park. Impairment is from a uniform haze. The sky-mountain contrasts for the three photographs, from best to worst, are (a) -0.32, (b) -0.29, and (c) -0.15.

not altered. This means that visitors to this type of vista would be equally sensitive to air pollution changes in the morning or afternoon, with or without clouds in the sky.

This linear relationship appeared consistent for all scenes as long as each scene had one specific scenic element that changed as a function of air pollution. Notice in the photographs of Figure 8.6 that the foreground features remain unchanged even though the visual air quality or contrast of the distant scene changes dramatically. The observers judging visual air quality appear to "key in" on the scenic element that is most sensitive to changes in air pollution. The visual sensitivity of

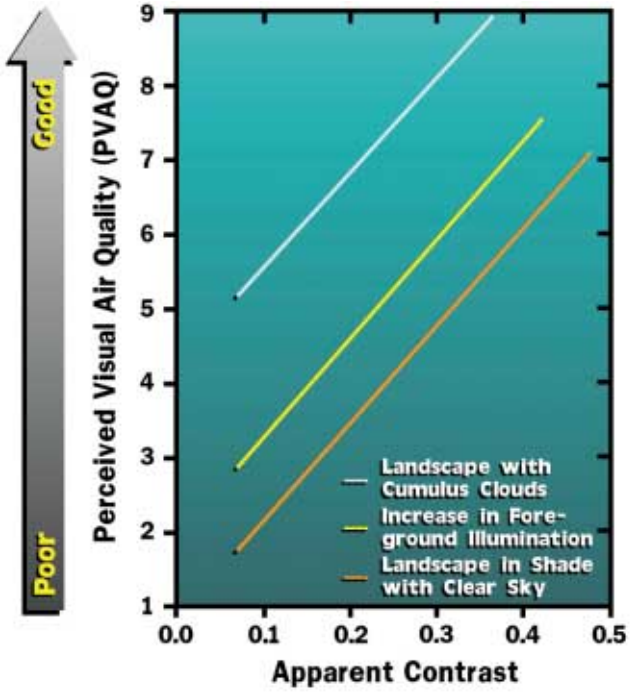

Fig. 8.7 Plot of judgments of perceived air quality (PVAQ) as a function of apparent vista contrast of most distant landscape feature for a typical scene. The orange line shows the linear relationship between these two variables where the scene is shaded from sunlight. The yellow line shows a similar relationship of the same vista but in direct sunlight. The blue line shows the relationship when cumulus clouds are present. Notice that the slopes of the PVAQ contrast lines do not change. The sensitivity of an observer to visibility haze is independent of sun angle and meteorological conditions.

(a)

(b)

Fig. 8.8 Mt. Trumbull as viewed from Hopi Point under two different lighting conditions. Foreground features change dramatically, but studies show that the sensitivity of the vista to air pollution impact remains unchanged.

(a)

(b)

Fig. 8.9 The effect of changes in sun angle as well as the visual effect of cumulus clouds in the La Sal Mountains.

an observer to increases in air pollution is represented by the slope of the PVAQ versus contrast curve in Figure 8.7.

An increase in vista color exists as the one common denominator between the effects that sun angle, meteorological conditions, and air pollution have on PVAQ. If vista color increases as a result of decreased air pollution, changing sun angle, or meteorological conditions, then the PVAQ increases. This does not mean that other perceptual clues, such as change in contrast detail or texture, should be ruled out as being important to PVAQ. However, there does not appear to be a systematic relationship between texture and PVAQ or contrast detail and PVAQ.

The effect of changing sun angle on color was further investigated using scenes similar to those shown in Figure 3.18. When the scene was in full shadow, the lowest PVAQ was evoked. As the sun rose in the sky, illuminating the vista and thus increasing its color, PVAQ also increased. This increase in PVAQ continued until the scene was fully illuminated (approximately noon) and then remained constant through the rest of the day (see Figure 8.10). These results support the idea of color change and PVAQ.

There does appear to be a simple linear relationship between PVAQ and other visibility parameters. One variable of particular interest is the particulate mass concentration, a direct measure of the amount of pollution in the atmosphere. The relationship between particulate mass concentration and PVAQ is shown in Figure 8.11. Notice the nonlinear nature of the relationship. A given change in mass concentration results in a much larger change in PVAQ when the air is clean than when it is dirty.

The effect of mass concentration on PVAQ is further illustrated by Figure 8.12. This graph shows the change in PVAQ resulting from a given increase in air pollution as a function of distance. First, a specified amount of air pollution increase has a much greater effect on PVAQ when the vista is seen in a clean atmosphere; second, there is an observer-target distance that is perceptually most sensitive to air pollution increases. In relatively clean areas, like the Grand Canyon, this distance is 60 to 100 km. In the East, where the atmosphere is already quite polluted, the most sensitive distance is closer to 10 km.

The above comments apply to vistas containing certain scenic elements that are substantially more sensitive to air pollution change than the rest of the scene. For more complicated scenes, it appears that the PVAQ varies as a function of the contrast change of each scenic element weighted in proportion to the area subtended by that element and to the inherent scenic beauty of each

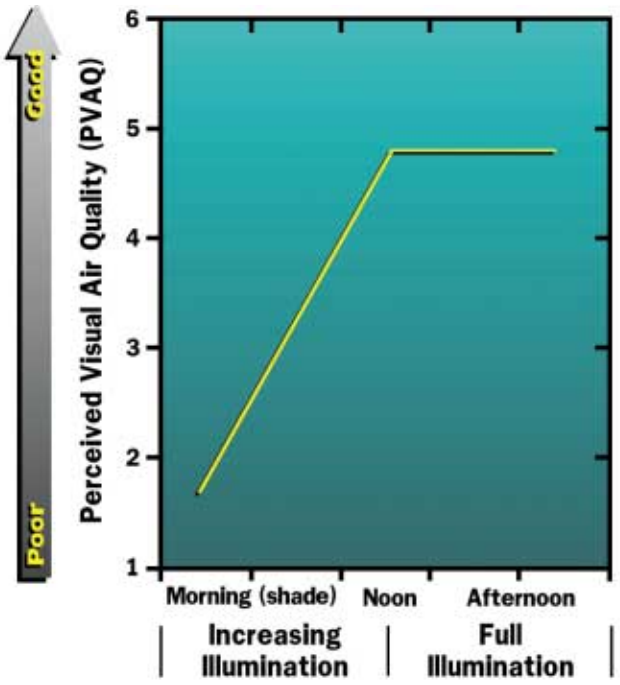

Fig. 8.10 Perceived visual air quality plotted as a function of sun angle. During early morning hours the vista is shaded from sunlight, and color saturation of the scene is low. As the sun rises in the sky the scene moves from shade into direct illumination and becomes saturated with color. Judgments of visual air quality increase over this time period until the scene is fully illuminated. It then remains constant during afternoon hours.

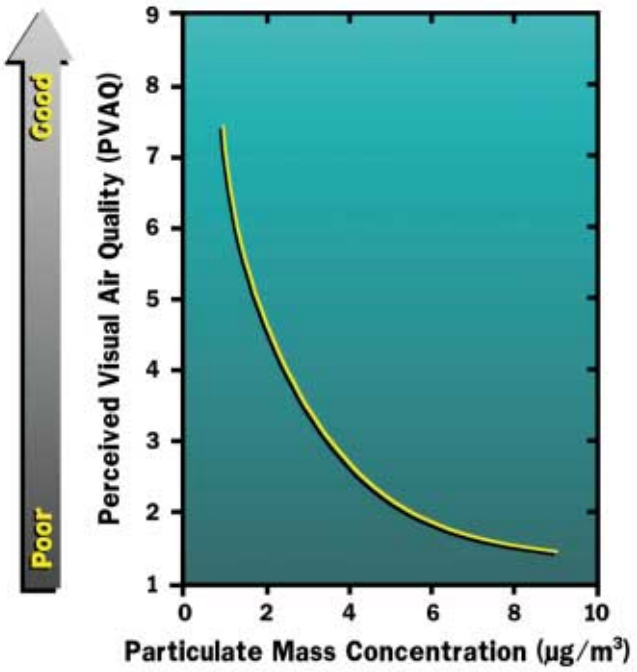

Fig. 8.11 In contrast to the very simple relationship between perceptions of visual air quality and vista contrast, perceived visual air quality plotted against particulate concentration shows a very nonlinear relationship.

scenic feature. However, in general these conclusions hold for these scenes as well.

Layered haze, whether it appears as a coherent plume or as a layer of pollutants trapped near the ground, is recognized by an abrupt change in color between itself and some background. Haze layers can be lighter or darker than the background sky, and under the right lighting conditions can also have a brown coloration. Figure 8.13 shows examples of three different haze layers. Figure 8.13a shows a white coherent plume over Navajo Mountain; Figure 8.13b shows a dark plume that just obscures the mountain top; and Figure 8.13c shows a trapped haze layer that obscures approximately half of Navajo Mountain.

Slides similar to those shown in Figure 8.13 were used in studies to determine individuals' perceptions of layered haze. Results of these studies are summarized in Figure 8.14; it should be kept in mind that a plume with a contrast of

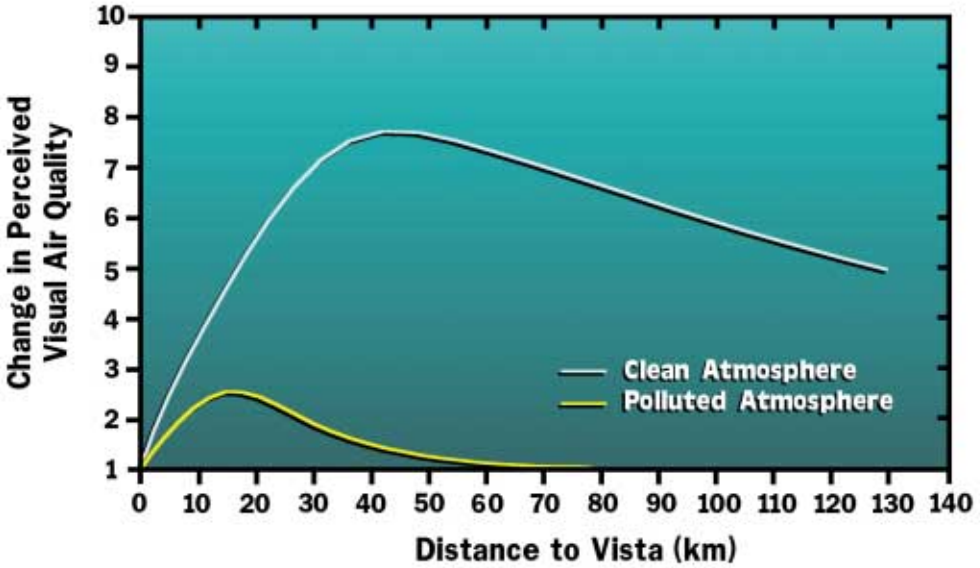

Fig. 8.12 Relationships between perceived visual air quality (PVAQ) and vista distance for different levels of air quality. The blue line shows the decrease in perceived visual air quality of hypothetical vista as a result of adding a small amount of particulate matter to a "clean" atmosphere as a function of distance to the vista. The yellow curve is similar in nature but shows perceived changes in air quality when the atmosphere is already "dirty." Most importantly, the graph shows that vistas viewed in a clean atmosphere are many more times sensitive to an incremental change in air pollution than when viewed under more impaired conditions, and secondly, there is a vista-observer distance that will result in a perceptual sensitivity that is greater than for any other distance.

(a)

(b)

(c)

Fig. 8.13 Three ways in which air pollutants can manifest themselves as layered haze. (a) Shows a white plume positioned over Navajo Mountain as seen from Bryce Canyon National Park, (b) shows a dark plume that just obscures the mountain top, and (c) is a dark haze layer that results from pollutants being trapped in a ground inversion layer.

0.02 to 0.05 is visible. The results indicate that plumes, when positioned in the sky in such a way as to not obscure the vista, have a minimal impact on PVAQ. However, dark plumes were rated lower or perceived to have a greater impact on visual air quality than light-colored plumes; as the plume, whether dark or light, obscured more and more of the vista, the ratings went down. A plume or haze layer with a sky-haze contrast of 0.3 is perceived to be worse if it obscures two thirds of the mountain than if it obscures only one third of the scenic element.

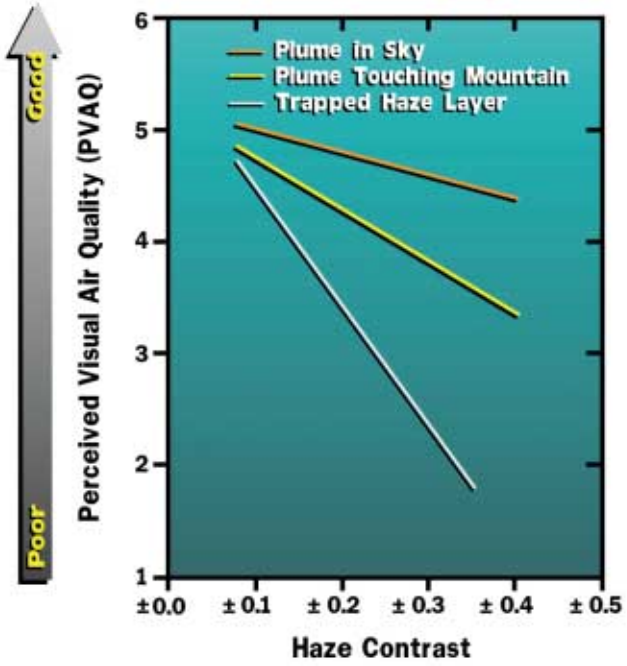

Fig. 8.14 Summarization of the results of the layered haze perception studies. The orange line shows the relationship between PVAQ and plume contrast for a white plume placed in the sky in such a way as to not touch any portion of the scenic vista. There is little change in PVAQ as plume contrast increases. The yellow line and blue lines suggest the relationship between PVAQ and layered haze contrast for a plume just obscuring the mountain top and for a haze layer obscuring the lower one half of the mountain, respectively. As haze obscures more of the mountain, the effect that a specific pollution level has on PVAQ increases. This is indicated by the increased slopes of the blue and yellow lines over that of the orange line.

The data presented in this document is a summation of the work of many scientists in the field. The current trends and particle contributions to visibility impairment were derived from the Interagency Monitoring of Protected Visual Environments (IMPROVE) program. IMPROVE is an interagency monitoring program funded and administered by the USDI National Park Service (NPS), USDA Forest Service (USFS), USDI Bureau of Land Management (BLM), USDI Fish and Wildlife Service (FWS), and the US Environmental Protection Agency (EPA). Other information presented in this document can be found in the National Acid and Precipitation Assessment Program (NAPAP) State of Science and Technology Report Number 24 (1990).

The assumptions, findings, conclusions, judgements, and views presented herein are those of the author and should not be interpreted as necessarily representing official National Park Service policies.

Acknowledgement

The author wishes to thank:

- Kristi Gebhart and Jim Sisler in helping with data analysis.
- The University of California at Davis and the Air Resource Specialists staffs for their diligent efforts in operating the IMPROVE monitoring network.
- Site operators for their efforts in site maintenance and operation.
- Rebecca Burke for editing and project coordination.
- Jeff Lemke for graphics, layout, and printing coordination.
- The many reviewers and their helpful comments.

GLOSSARY OF TERMS

absorption: a class of processes by which one material is taken up by another.

absorption coefficient: a measure of the ability of particles or gases to absorb photons; a number that is proportional to the number of photons removed from the sight path by absorption per unit length.

absorption cross section: the amount of light absorbed by a particle divided by its physical cross section.

aerosol: a dispersion of microscopic solid or liquid particles in a gaseous medium, such as smoke and fog.

air parcel: a volume of air that tends to be transported as a single entity.

anthropogenic: produced by human activities.

apportionment: to distribute or divide and assign proportionately.

attenuation: the diminuation of quantity. In the case of visibility, attenuation or extinction refers to the loss of image-forming light as it passes from an object to the observer.

back trajectory: a trace backwards in time showing where an air mass has been.

bimodal distribution: a plot of the frequency of occurrence of a variable versus the variable. A bimodal distribution exists if there are two maxima of the frequency of occurrence separated by a minimum. See mode.

budget: See light extinction budget.

coagulation: the process by which small particles collide with and adhere to one another to form larger particles.

condensation: the process by which molecules in the atmosphere collide and adhere to small particles.

condensation nuclei: the small nuclei or particles with which gaseous constituents in the atmosphere (e.g., water vapor) collide and adhere.

deciview: a unit of visibility proportional to the logarithm of the atmospheric extinction. Under many circumstances a change in one deciview will be perceived to be the same on clear and hazy days.

diffraction: modification of the behavior of a light wave resulting from limitations of its lateral extent by an obstacle. For example, the bending of light into the “shadow area” behind a particle.

diffusion: a process by which substances, heat, or other properties of a medium are transferred from regions of higher concentration to regions of lower concentration.

extinction: the attenuation of light due to scattering and absorption as it passes through a medium.

extinction coefficient: a measure of the ability of particles or gases to absorb and scatter photons from a beam of light; a number that is proportional to the number of photons removed from the sight path per unit length. See absorption.

extinction cross section: the amount of light scattered and absorbed by a particle divided by its physical cross section.

haze: an atmospheric aerosol of sufficient concentration to be visible. The particles are so small that they cannot be seen individually, but are still effective in visual range restriction. See visual range.

homogenous nucleation: process by which gases interact and combine with droplets made up of their own kind. For instance, the collision and subsequent adherence of water vapor to a water droplet is homogenous nucleation. See nucleation.

hydrocarbons: compounds containing only hydrogen and carbon. Examples: methane, benzene, decane, etc.

hygroscopic: readily absorbing moisture, as from the atmosphere.

IMPROVE: Interagency Monitoring of PROtected Visual Environments.

integrating nephelometer: an instrument that measures the amount of light scattered (scattering coefficient).

inversion: See temperature inversion.

isopleth: a line drawn on a map through all points having the same numerical value.

isotropic: a situation where a quantity (or its spatial derivatives) are independent of position or direction.

isotropic scattering: the process of scattering light equally in all directions.

LAC: See Light-Absorbing Carbon.

light-absorbing carbon: carbon particles in the atmosphere that absorb light. Black carbon.

light extinction budget: the percent of total atmospheric extinction attributed to each aerosol and gaseous component of the atmosphere.

long path measurement: an atmospheric measurement process that is made over distances in excess of a few hundred meters.

micron: a unit of length equal to one millionth of a meter; the unit of measure for wavelength.

mode: the maximum point in a plot of the frequency of occurrence of a variable versus the variable.

nitrogen dioxide: a gas (NO_2) consisting of one nitrogen and two oxygen atoms. It absorbs blue light and therefore has a reddish-brown color associated with it.

NO_2: See nitrogen dioxide.

nucleation: process by which a gas interacts and combines with droplets. See homogenous nucleation.

Perceived Visual Air Quality (PVAQ): an index that relates directly to how human observers perceive changes in visual air quality.

phase shift: a change in the periodicity of a waveform such as light.

photometry: instrumental methods, including analytical methods, employing measurement of light intensity. See telephotometer.

photon: a bundle of electromagnetic energy that exhibits both wave-like and particle-like characteristics.

plume blight: visual impairment of air quality that manifests itself as a coherent plume.

point source: a source of pollution that is point-like in nature. An example is the smoke stack of a coal-fired power plant or smelter. See source.

polar nephelometer: an instrument that measures the amount of light scattered in a specific direction. See integrating nephelometer.

precursor emissions: emissions from point or regional sources that transform into pollutants with varied chemical properties.

psychophysical: the branch of psychology that deals with the relationships between physical stimuli and resulting sensations and mental states.

PVAQ: See Perceived Visual Air Quality.

Rayleigh scattering: the scattering of light by particles much smaller than the wavelength of the light. In the ideal case, the process is one of a pure dipole interaction with the electric field of the light wave.

refraction: the change of direction of a ray of light in passing obliquely from one medium into another in which the speed of propagation differs.

relative humidity: the ratio of the partial pressure of water to the saturation vapor pressure, also called saturation ratio; often expressed as a percentage.

scattering (light): an interaction of a light wave with an object that causes the light to be redirected in its path. In elastic scattering, no energy is lost to the object.

scattering angle: the angle between the direction of propagation of the scattered and incident light (or transmitted light):

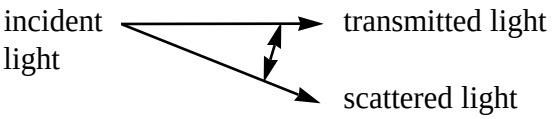

scattering coefficient: a measure of the ability of particles or gases to scatter photons out of a beam of light; a number that is proportional to the amount of photons scattered per unit length.

scattering cross section: the amount of light scattered by a particle divided by its physical cross section.

secondary aerosols: aerosol formed by the interaction of two or more gas molecules and/or primary aerosols.

SO_2: See sulfur dioxide.

source: in atmospheric chemistry, the place, places, group of sites, or areas where a substance is injected into the atmosphere. Can include point sources, elevated sources, area sources, regional sources, multiple sources, etc.

spectral: an adjective implying a separation of wavelengths of light or other waves into a spectrum or separated series of wavelengths.

stable air mass: an air mass which has little vertical mixing. See temperature inversion.

stagnant: referring to meteorological conditions that are not conducive to atmospheric mixing.

stagnation episodes: See stagnation periods.

stagnation periods: lengths of time during which little atmospheric mixing occurs over a geographical area, making the presence of layered hazes more likely. See temperature inversion.

sulfates: those aerosols which have origins in the gas-to-aerosol conversion of sulfur dioxide; of primary interest are sulfuric acid and ammonium sulfates.

sulfur dioxide: a gas (SO_2) consisting of one sulfur and two oxygen atoms. Of interest because sulfur dioxide converts to an aerosol that is a very efficient light scatterer. Also, it can convert into acid droplets consisting primarily of sulfuric acid.

sun angle: refers to the angle of the sun above the horizon of the earth.

telephotometer: an instrument that measures the brightness of a specific point in either the sky or vista.

temperature inversion: in meteorology, a departure from the normal decrease of temperature with increasing altitude such that the temperature is higher at a given height in the inversion layer than would be expected from the temperature below the layer. This warmer layer leads to increased stability and limited vertical mixing of air.

transmissometer: an instrument that measures the amount of light attenuation over a specified path length.

unstable air mass: an air mass that is vertically well mixed. See also stable air mass, temperature inversion.

visual range: the distance at which a large black object just disappears from view.

VOC: Volatile Organic Carbon - gaseous hydrocarbon.

wavelength: the distance, measured in the direction of propagation of a wave, between two successive points in the wave that are characterized by the same phase of oscillation.